

# Algebraic Number Starscapes

EDMUND HARRISS, KATHERINE E. STANGE, STEVE TRETTEL

**ABSTRACT.** We study the geometry of algebraic numbers in the complex plane, and their Diophantine approximation, aided by extensive computer visualization. Motivated by the resulting images, which we have called *algebraic starscapes*, we describe the geometry of the map from the coefficient space of polynomials to the root space, focussing on the quadratic and cubic cases. The geometry describes and explains the notable features of the illustrations, and motivates a geometric-minded recasting of fundamental results in the Diophantine approximation of the complex plane. Meanwhile, the images provide a case-study in the symbiosis of illustration and research, and an entry-point to geometry and number theory for a wider audience. In particular, the paper is written to provide an accessible introduction to the study of homogeneous geometry and Diophantine approximation.

We investigate the homogeneous geometry of root and coefficient spaces under the natural  $\mathrm{PSL}(2; \mathbb{C})$  action. Hyperbolic geometry and the discriminant play an important role in low degree. In particular, we rediscover the quadratic and cubic root formulas as isometries of  $\mathbb{H}^2$  and its unit tangent bundle, respectively. Utilizing this geometry, we determine when the map sending certain families of polynomials to their complex roots (our starscape images) are embeddings.

We reconsider the fundamental questions of the Diophantine approximation of complex numbers by algebraic numbers of bounded degree, from the geometric perspective developed. In the quadratic case (approximation by quadratic irrationals), we consider approximation in terms of *hyperbolic* distance between roots in the complex plane and the *discriminant* as a measure of arithmetic height on a polynomial. In particular, we determine the supremum on the exponent  $k$  for which an algebraic target  $\alpha$  has infinitely many approximations  $\beta$  whose hyperbolic distance from  $\alpha$  does not exceed  $\mathrm{acosh}(1 + 1/|\Delta_\beta|^k)$ . It turns out to fall into two cases, depending on whether  $\alpha$  lies on the image of a plane of rational slope in coefficient space (a *rational geodesic*). The result comes as an application of Schmidt's subspace theorem. Our results recover the quadratic case of results of Bugeaud and Evertse, and give some geometric explanation for the dichotomy they discovered [16]. Our statements go a little further in distinguishing approximability in terms of whether the target or approximations lie on rational geodesics.

The paper comes with accompanying software, and finishes with a wide variety of open problems.

---

*Date:* December 22, 2024.

2010 *Mathematics Subject Classification.* Primary: 11R04, 11R11, 11R16, 11J04, 11J68, 11J87, 53C30 Secondary: 11G50, 11H99 54E99 57M99.

This material is based upon work supported by the National Science Foundation under Grant No. DMS-1439786 and the Alfred P. Sloan Foundation award G-2019-11406 while the authors were in residence at the Institute for Computational and Experimental Research in Mathematics in Providence, RI, during the Illustrating Mathematics program. Katherine E. Stange is supported by NSF CAREER CNS-1652238.

## 1. INTRODUCTION

We begin (and indeed this research began) with the three images in Figure 1. Take a minute to look at them before continuing.

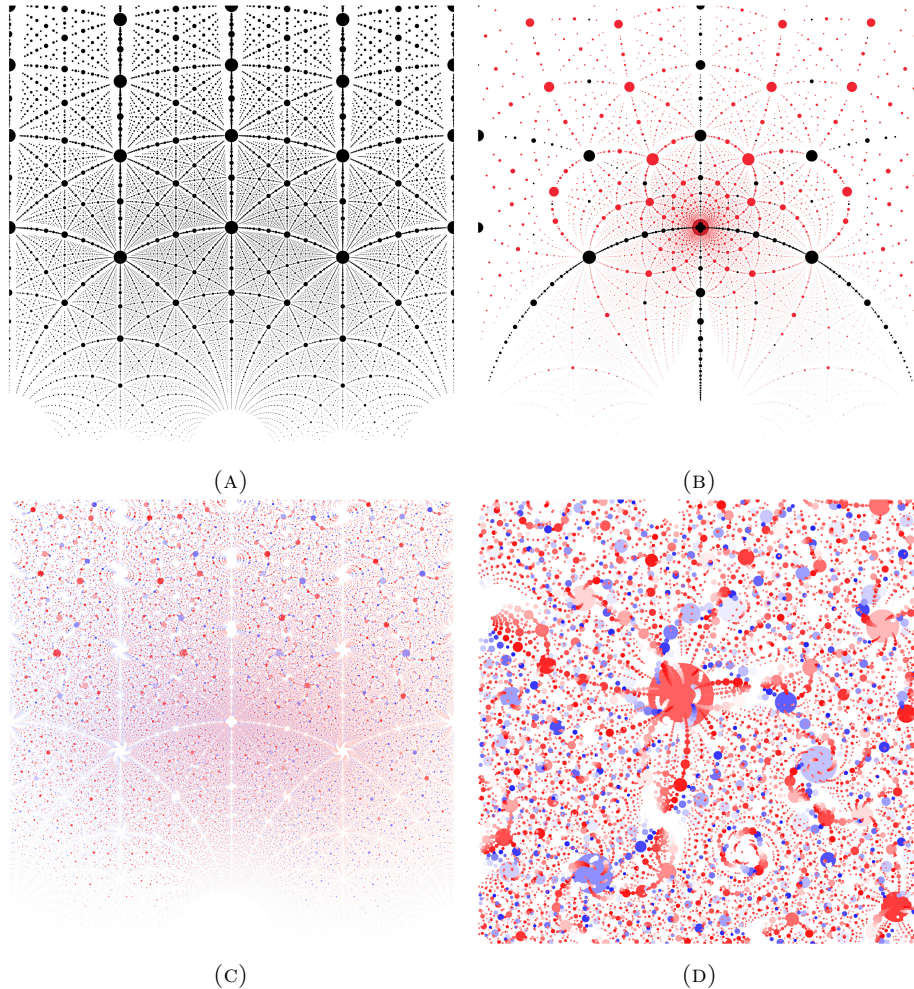


FIGURE 1. Complex algebraic numbers sized by the inverse of the discriminant of their minimal polynomial in the hyperbolic metric. All quadratics (1a). All roots (quadratic in black, cubic in red) of the polynomials  $ax^3 + cx^2 + bx + c = 0$  (1b). All cubics, coloured based on the value of the real root (1c) and the detail of the cubics around a root of  $x^3 + x + 1 = 0$ . The first three images, as many other figures here, are plotted from  $-1$  to  $1$  in the real axis and  $0$  to  $2$  in the imaginary axis.

On the top left (1a) you see complex quadratic algebraic numbers plotted and sized by discriminant in the hyperbolic metric, on the top left (1b) the complex roots of polynomials of the form  $ax^3 + cx^2 + bx + c = 0$ , and on the bottom all complex cubics coloured by their real conjugate (1c), with zoomed in detail around the complex root of  $x^3 + x + 1 = 0$  (1d). In each case the dot size is inversely proportional to the root discriminant (the discriminant to the root of the degree), and the points are plotted in the hyperbolic metric (meaning, the radius is hyperbolic in the upper half-plane model). This paper grew out of our excitement at the beauty

and detail present in these images and the search for mathematics that could be both seen and conjectured from their structure. In the first section we follow that visual investigation with a gallery of some of the images produced, and discussion of some of the structural aspects visible in the images. We develop those observations in the next two sections studying the geometry of the roots (in Section 3) and their number theory (in Sections 4 and 5).

The notion of plotting algebraic numbers is not new, and there are many beautiful mathematical visualisations made from them, many in the world of blogs and online mathematical discussions. A curation of those of which we are aware follows at the end of this introduction. Our images were studied initially from the perspective of their aesthetic, by asking, “What makes images that look interesting?” (without trying too hard to define *interesting*). However, they rapidly became both a tool to illuminate existing mathematics, including hyperbolic and projective geometry, representations of  $\mathrm{PSL}(2; \mathbb{C})$ , and Diophantine approximation, and also a source of new mathematics.

Diophantine approximation studies the relative placement of real and complex numbers with regards to algebraic numbers of bounded arithmetic complexity. Most of the classical story lives on the real line, but it has naturally been extended to the rest of the complex plane. The natural generalization concerns the euclidean distance in the plane, and various measures of arithmetic complexity taken from the real case [16, 31, 46, 51]. However, when one views algebraic starscapes such as those in Figure 1, it is immediately evident that geometry is playing a vivid role in the two dimensions of the complex plane; much more so than in the one dimension of the real line. This leads one to ask whether a geometric perspective on the placement of algebraic numbers can help explain Diophantine results. The answer is a definite yes. The beautiful necklaces in Figure 1 are the images of planes in the projective space of coefficients, transported to the complex plane by isometries preserving homogeneous geometries of  $\mathrm{PSL}(2; \mathbb{R})$ . From this perspective, it makes sense to approach Diophantine approximation with a sensitivity to the action of  $\mathrm{PSL}(2; \mathbb{Z})$ , and the underlying hyperbolic geometry. This leads to new conjectures on the approximation of complex numbers. The reader interested in novel Diophantine approximation results and proofs is directed to Section 5.

The images provide a portal to active mathematical research for those outside the subject. Mathematical beauty can be incredibly hard to communicate to people not indoctrinated into the details of the subject, yet these images have already appeared in an art exhibit in Iceland [26] and been used for engagement in a workshop with the Math Club for Battle Creek Area Math and Science Center in Michigan.

A note on our expository approach: we believe that the images presented here provide a motivated path into several topics in geometry and number theory. We have therefore attempted, especially in the earlier part of the paper, to keep the description as accessible as possible, introducing even well-known terminology as we build toward more sophisticated mathematics. We hope the paper might provide insight and interest to a motivated high school student and a mathematician in these research areas alike.

**Previous illustration.** The richest previous investigation of imagery grows out of the study of the roots of Littlewood polynomials [35, 41, 49], which are polynomials with coefficients  $\pm 1$ , and more generally polynomials with coefficients from a finite set. This produces the oldest images we have found, particularly in the work of Peter and Jonathan Borwein [7, 10, 11, 12, 43]. These collections of polynomials have the nice feature that all polynomials up to a certain degree can be considered. These polynomials also relate to the study of a mysterious object named Thurston’s master teapot [13].

In particular, a lot of interest was generated by the work of Dan Christiansen [17], shared and described by John Baez, including an incredibly intricate image created by Sam Derbyshire [5, 6, 38].

Many other people, some directly inspired by this, have also created, or discussed, the images, including Paul Nylander [40], Greg Egan [20], Andrej Bauer [8], Daniel Wiegrefe [55], Bernat Espigulé [22], Jwalin Bhatt [9], Jonathan Lidbeck [33], and Jordan Ellenberg [21].

Pictures not limiting coefficients so strongly, closer to those we present here, are rarer. The most notable are the images of Stephen Brooks used on Wikipedia [14], that were further developed and optimised by David Moore [4]. These images also inspired a Wolfram Demonstration from Enrique Zeleny [56]. Other interesting images we have found come from David Marciel [37] and Deviant Art user Fauxtographique [23]. There have also been discussions on Stack Exchange [24, 29], with the latter linking to further amazing images on the Flickr account of Stackexchange user “DumpsterDoofus” [45]. The ease of creating these images means that people quickly start making their own: for example, a twitter thread started by the first-named author [25] quickly prompted variations by Dan Anderson, Michael Pershan and Peter Farrell [1, 2, 42].

This list is extensive, but probably not exhaustive. We are interested in other versions of such patterns, especially earlier ones (before 2010, and even more before 2000) so please send us any you know of.

**Software and image generation.** We encourage the reader to explore along with us, throughout the paper, using the accompanying software, available as a Sage Mathematics Software [53] notebook, at [algebraicstarscapes.com](http://algebraicstarscapes.com).

In general the images here are produced by a rather simple three step process. We first generate a list of polynomials whose coefficients lie in a region about the origin (for example, a box or ball). These polynomials are then solved to give the collection of roots, with additional data (such as polynomial discriminant) attached to the roots, data which is eventually to be used for sizing. Finally, that list of data is converted into a collection of points and plotted. Most of the images drawn involve over 50,000 dots, but some get to over 250,000.

**Acknowledgements.** The authors are grateful to the Institute for Computational and Experimental Research in Mathematics in Providence, RI, and to the semester organizers, for the opportunity to be in residence for Fall 2019 at the Illustrating Mathematics program, where this work was initiated in the grand tradition of just being in the right place at the right time. The authors would also like to thank their respective home institutions for their help in making semester residency possible. Thanks are also due to the many participants in that program for helpful discussions, including Arthur Baragar and Joseph H. Silverman. Special thanks go to Pierre Arnoux and David Dumas for especially inspiring and detailed conversations as these ideas developed.

## 2. GALLERY

**2.1. In a galaxy far, far away.** The pictures shown in Figure 1 of the quadratics (1a) and the family of cubics (1b) have a striking self-similar curvilinear structure: the figures seem to be populated with beaded necklaces of discs subdividing the plane into smaller regions criss-crossed with similar, finer, necklaces. This general pattern seems to appear any time one works with a three dimensional linear family in coefficient space; more examples appear in Figure 2. As the degree increases, the curves and their relationships become more complicated, but the basic motif continues. We hope these images justify the term “algebraic starscapes.” When the family of polynomials is two-dimensional, we obtain a “linear starscape” (that is, a single beaded necklace threading through the plane; see Figure 26). When a family of polynomials is three-dimensional, we obtain “planar starscapes” such as those in Figure 2. One may continue this to higher dimension, but in four-dimensional families such as all cubics (Figure 1c), the collapse to the complex plane produces much more complicated, less immediately patternful, although nonetheless enticing, pictures.

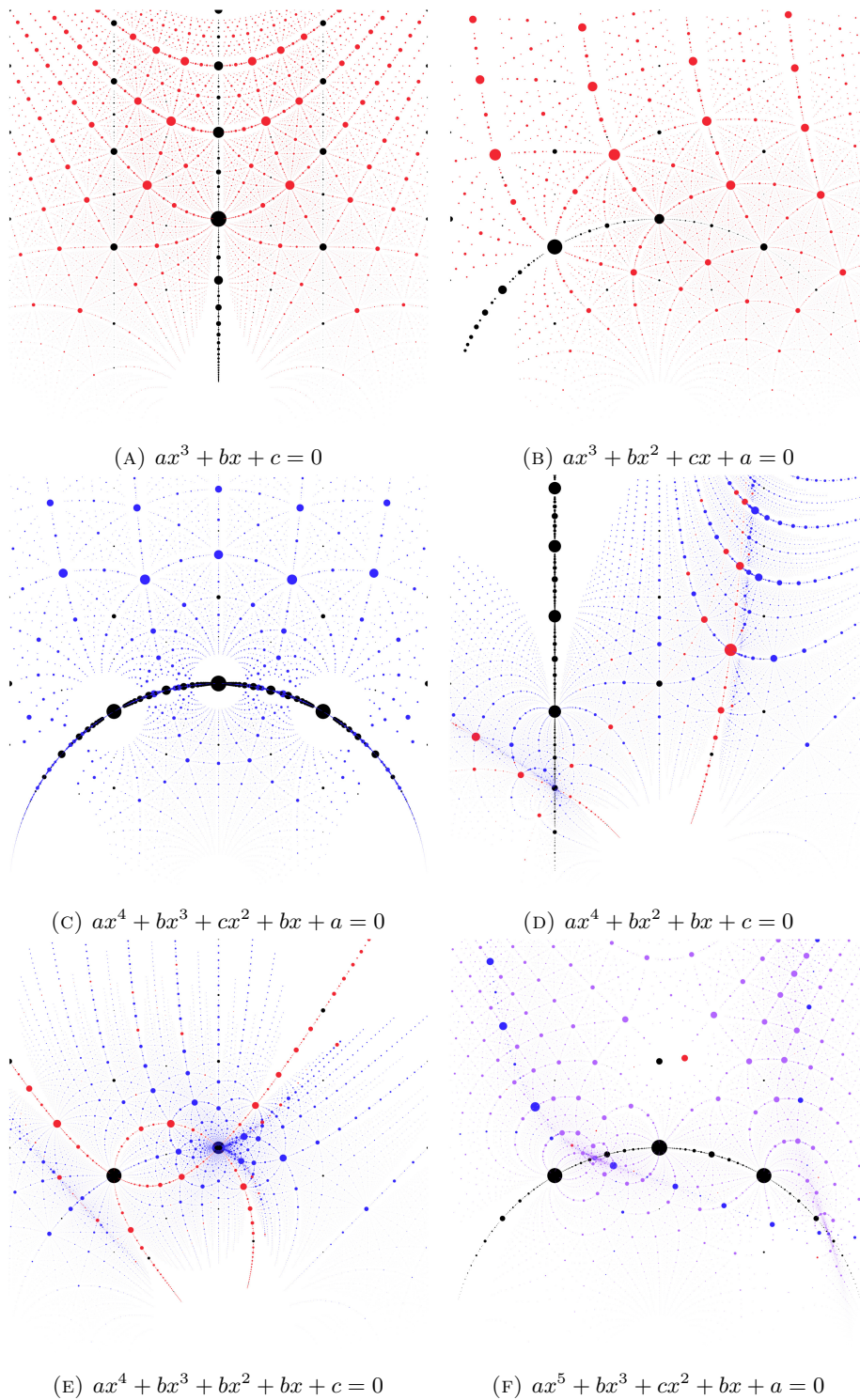


FIGURE 2. Complex algebraic numbers (roots of each polynomial family with  $a, b, c \in \mathbb{Z}$ ) sized by the root discriminant in the hyperbolic metric. Quadratic numbers are black, cubics red, quartics blue and quintics purple.

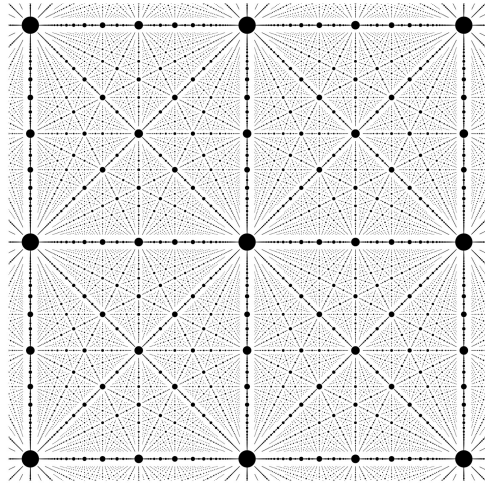


FIGURE 3. The points  $(b/a, c/a)$ , for  $a, b, c \in \mathbb{Z}$  with radius proportional to  $1/a$ . To see how this links to the view of a lattice for an observer, see Figure 17.

The simplest version of the basic motif that seems to pervade these images appears when looking at a lattice in perspective, as you can see in Figure 3. In this case the points only form straight lines. The one dimensional version of this effect is sometimes called the orchard illusion and can be experienced when driving past an orchard planted on a grid (Figure 4).

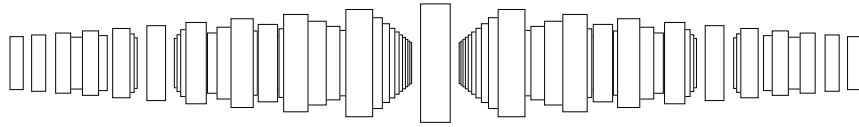


FIGURE 4. A sideways view of a grid of rectangles in perspective forming the orchard illusion.

In the quadratic case (Figure 1a) the lines might actually seem familiar to geometers as they are the straight lines (geodesics), not in euclidean geometry, but in the upper half plane model of the hyperbolic plane. In fact Figure 1a is a regular tiling of the upper half plane by a single tile, under the action of a group of symmetries preserving the hyperbolic distance. More precisely, the action is that of the *modular group*  $\mathrm{PSL}(2; \mathbb{Z})$  (Figure 5).

While the link to hyperbolic geometry and  $\mathrm{PSL}(2; \mathbb{Z})$  is especially strong in the quadratic case, it is more generally useful in understanding starscapes. From an aesthetic perspective, using the hyperbolic metric improves the look of the images close to the real line, as seen in Figure 6. There are more mathematical justifications for this approach described in later sections.

The observations we have described so far constitute a naïve visual approach to the images produced: we are simply asking what it is we are seeing. The underlying geometric explanation, especially for the quadratic and cubic cases, is developed in far more detail in Section 3, and the deeper connections to the study of Diophantine approximation in Sections 4 and 5.

**2.2. Mostly Harmless.** The images shown in Section 2.1 are compelling enough to encourage wider investigation. For example, one might move the families considered away from 0 to give affine subspaces of the coefficient space, as shown in Figure 7.

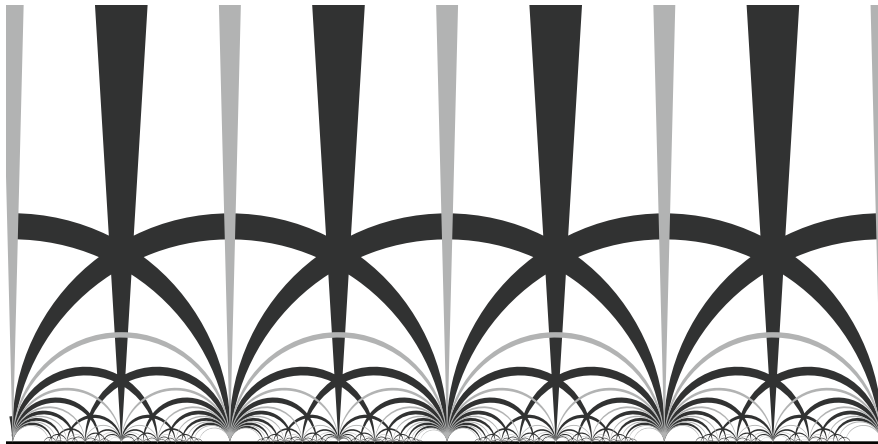


FIGURE 5. A tiling by infinite polygons on the hyperbolic plane (a partition of the hyperbolic plane by the action of  $\text{PSL}(2; \mathbb{Z})$ ). The curves seen here are some of those seen in Figure 1a.

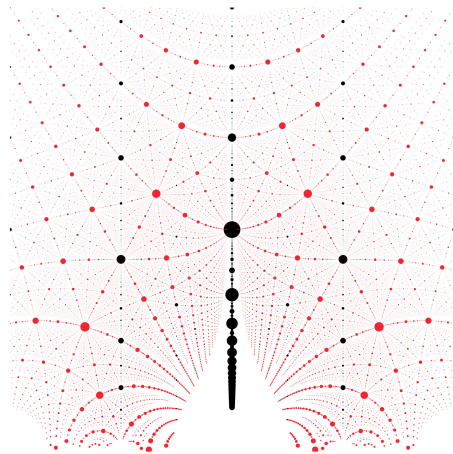


FIGURE 6. The depressed cubics, sized by the root discriminant, plotted in the euclidean metric (meaning, radii are interpreted as euclidean). Note how the plot is very dense at the bottom, but light at the top.

In these affine subspaces, a couple have particular interest: the algebraic integers (where the leading coefficient is 1) and the algebraic integer units (where the leading and constant coefficients are both 1). These are shown for the cubics and quartics in Figure 8.

Another approach is to consider real roots, or tuples of roots. For example, quadratics with real roots can be plotted in  $\mathbb{R} \times \mathbb{R}$  (Figure 9), though the lack of an ordering on the roots will cause each to appear twice.

A powerful property of the images of the quadratics with complex roots is that they show *all* the information about the roots, as the complex roots come as a complex conjugate pair (so that all the information is shown with just one of them). To extend this to the cubics requires an additional dimension. In this case the cubic polynomials with complex roots always have an additional real root.

To take into account this additional information, we could take a space in  $\mathbb{C} \times \mathbb{R}$  given by the upper half-plane for the complex root and the real line for the real root. Identifying this

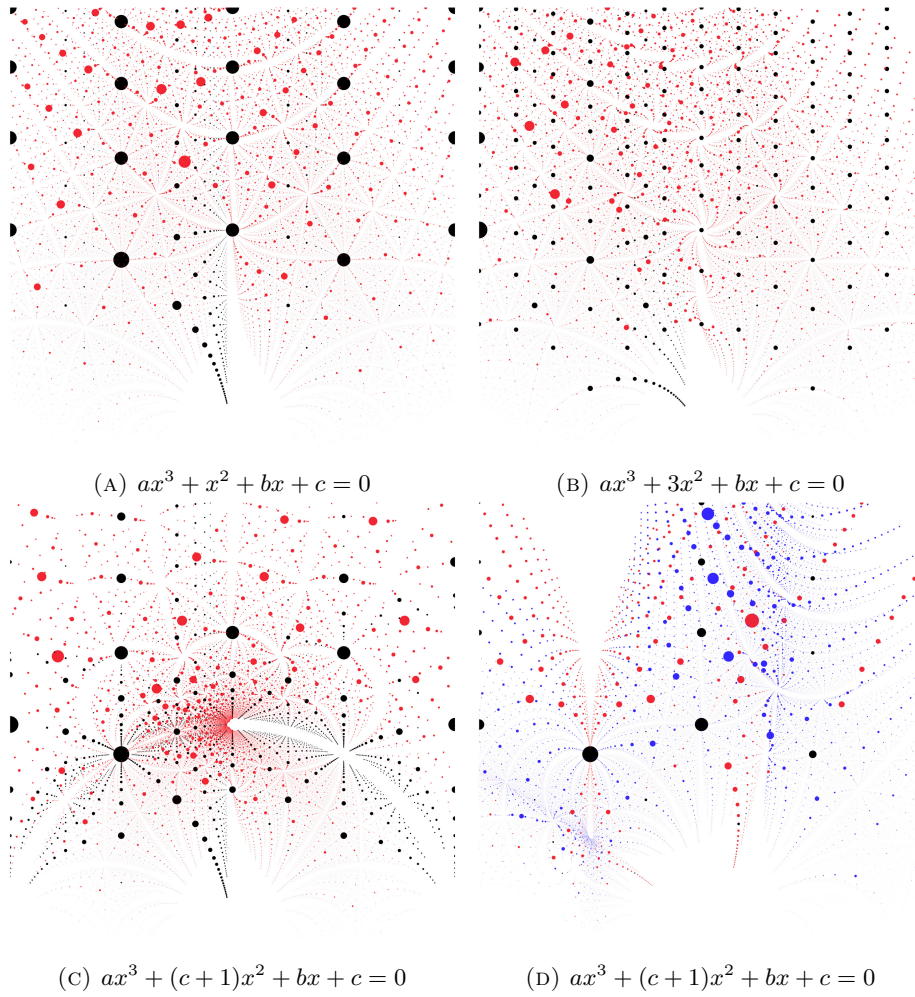


FIGURE 7. Roots on affine planes in coefficient space.

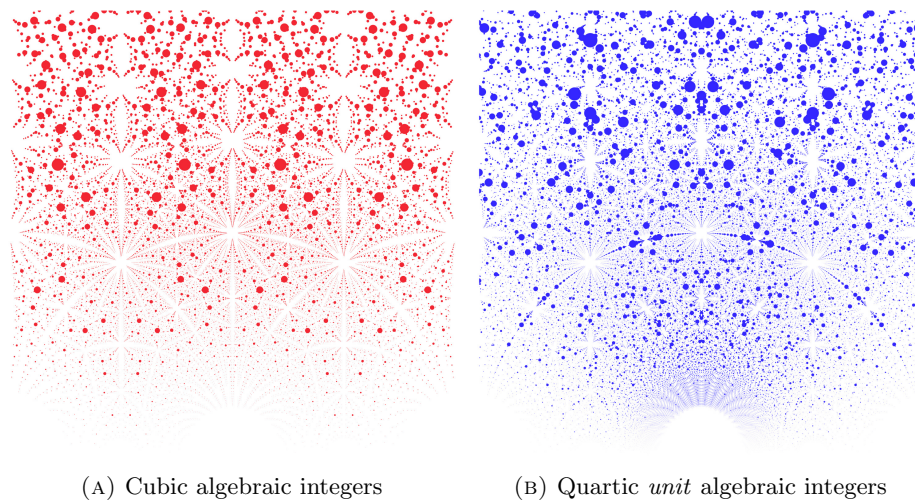


FIGURE 8. Algebraic integers and unit integers.

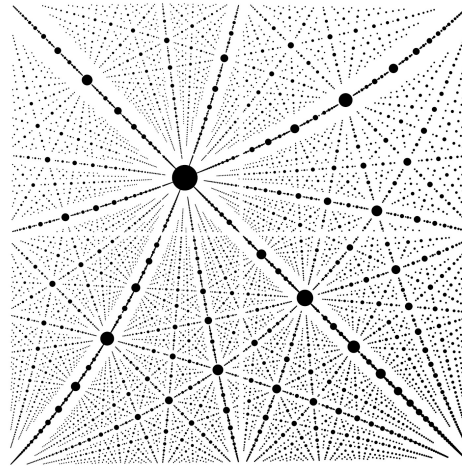


FIGURE 9. The real quadratics plotted against their algebraic conjugate, with one root (x-axis) between  $-1$  and  $0$  and the other between  $1$  and  $2$ . The large dot is the Golden ratio  $(\frac{1-\sqrt{5}}{2}, \frac{1+\sqrt{5}}{2})$ .

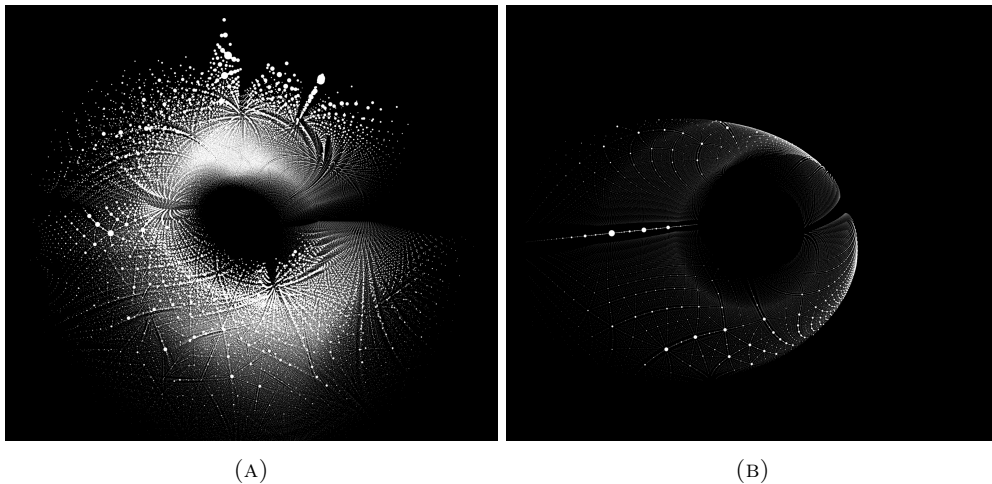


FIGURE 10. All cubic polynomials shown in the unit tangent bundle to  $\mathbb{H}^2$  (10a) and the roots of  $ax^3 + bx^2 + ax + c = 0$  (10b), forming a Möbius strip within it. Both are shown from the same angle so if you look carefully you can see the second image in the first. Images are screenshots from SL(View) by David Dumas [19].

real line with the ideal boundary of the upper half plane, we see in Section 3 that this space of cubics naturally identifies with the unit tangent bundle to the hyperbolic plane. Topologically a solid torus, the unit tangent bundle embeds in  $\mathbb{R}^3$ , providing a useful visualization. The integer cubics (again sized by the root discriminant) are shown again in Figure 10 using this approach.

The cubic families we have considered nicely embed into this picture as 2d surfaces. The polynomials  $ax^3 + bx^2 + ax + c = 0$  having a complex root even create a Möbius strip (Figure 10b). Both of these images are even more powerful when you can manipulate them yourself

in 3d, and we encourage you to check out David Dumas’ beautiful software SL(View) that we used to make these images ourselves [19]; see [algebraicstarscapes.com](http://algebraicstarscapes.com) for the datasets.

There are many other spaces to explore that have the potential to reveal many aspects of the structure of algebraic numbers and illustrate various geometric ideas. Using the colour of the dots has the potential to give pictures with up to 6 dimensions of information (3 spatial and 3 colour (red, green and blue, for example)). As an example, more of the structure of Figure 2d is revealed when real roots are used to colour points, as shown in Figure 11.

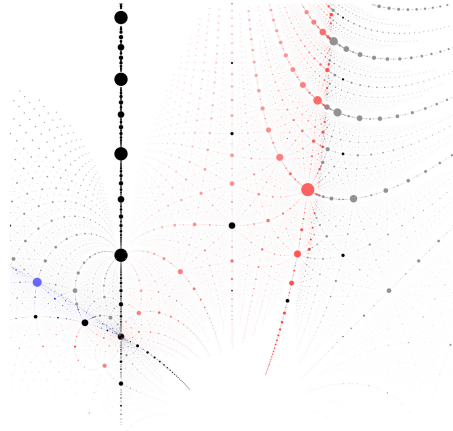


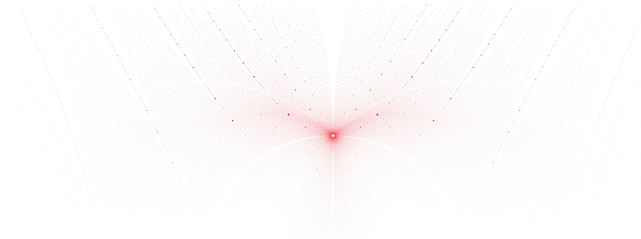
FIGURE 11. The starscape shown in Figure 2d coloured by a real root (simply the first given by Sage), red for negative and blue for positive, each fading to white as the absolute value increases. Quadratic Points are black and points with no real conjugate are shown in gray.

The challenge is to produce images that are attractive, informative or, ideally, both. From our explorations so far we have found that chasing the first is a surprisingly reliable (though not guaranteed) path to the second.

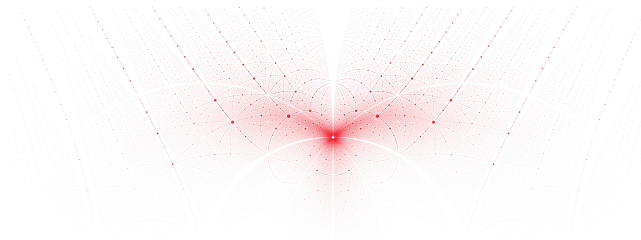
**2.3. A celestial dance.** In all our images so far, there is a feeling that larger dots repel each other, like binary stars locked in a mutual orbit, unable to approach. We also see remarkable spiraling trajectories of shrinking dots surrounding large ones, like the arms of small galaxies, as in Figure 1d. We have been using the root discriminant as the way to size the dots: this provides a rough measure of the “complexity” of an algebraic number. The notion of needing increasingly complicated algebraic numbers to successively better and better approximate a target is a classic idea in number theory, and is explored in the field of *Diophantine approximation*.

The paradigm is that as the polynomial gets more complicated, the dots representing its roots are drawn smaller. There are many notions of complexity one might use to size the points. Ideas of “complicated” are generally tied to the coefficients (as in the discriminant); Figure 12 shows some classic metrics on the coefficients. In Figure 13a we show the Weil height (or Mahler measure), a more sophisticated way to show complexity. These are all discussed in more detail in Section 4. Compare with the discriminant in Figure 13b.

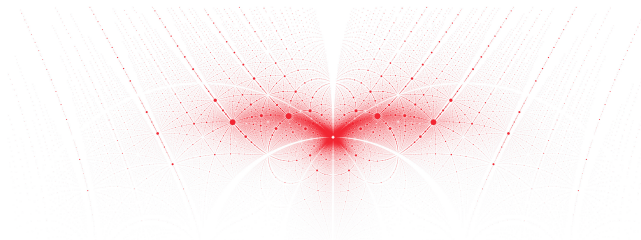
From a geometric perspective, we’ve seen that this type of repulsion effect can arise from a lattice in projection, with the dots appearing smaller in some sense proportional to their distance. If we consider the lattice of points  $(p, q)$  for  $p, q \in \mathbb{Z}$ , we can map to a line by taking  $\frac{p}{q}$  and get the rational numbers, as in Figure 16 and its result, Figure 15. In this setup, the points are sized inversely to their denominators. But as it turns out, the traditional measure of arithmetic complexity of a rational number is in fact, simply its denominator! The geometric



(A) The 1-Norm on the coefficients (sum of absolute value).



(B) The standard euclidean norm on the coefficients.

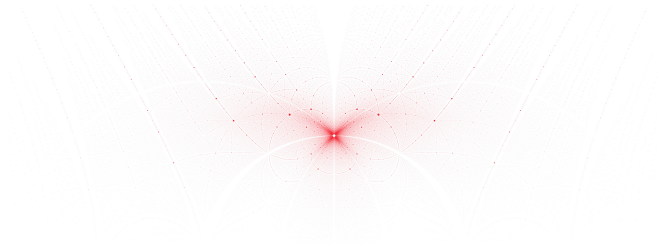


(C) The  $\infty$ -Norm giving the largest absolute coefficient.

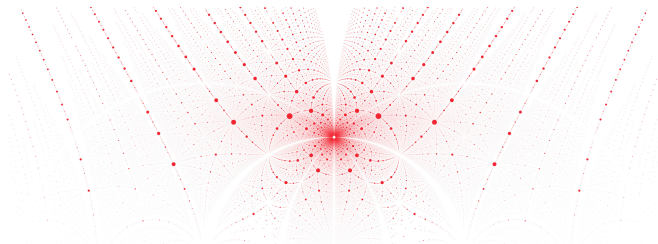
FIGURE 12. Complex roots of polynomials of the form  $ax^3 + bx^2 + cx + a = 0$ , using different dot sizing from the geometry of the coefficients, given by the inverse of the given quantity. All points with  $a, b, c$  between  $-40$  and  $40$  are plotted, in the region between  $-2.5$  and  $2.5$  on the real axis and  $0$  and  $2$  on the imaginary axis, for a total of  $231710$  roots.

aligns with the arithmetic. This is the most elementary example of the relationship between geometry and arithmetic that plays out throughout the paper.

A natural arithmetic question is to ask how well a real number can be approximated by rationals. The first answer to this, of course, is that the rational numbers are dense, so you can get approximations as close as you wish. On the other hand, one might consider  $\frac{22}{7}$  to be a surprisingly good approximation for  $\pi$ , given the simplicity of the numerator and denominator. After all,  $|\pi - \frac{22}{7}| < 0.0013$ . To quantify this, it's convenient to imagine a cost (the complexity) of a rational number, with higher denominators considered more expensive. We can then ask which approximations are particularly good value for money.



(A) The Weil Height, or Mahler measure.



(B) The root discriminant as used more generally in the paper.

FIGURE 13. Companion to Figure 12, showing two sizings based based on the polynomial and number theory of the roots.

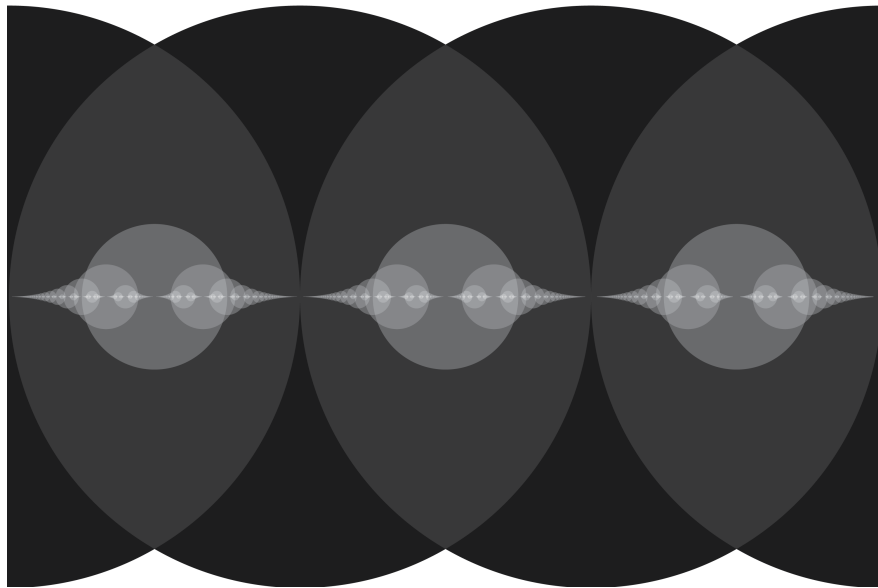


FIGURE 14. Disks centred at rational numbers  $\frac{p}{q}$  between 0 and 3 with radius  $\frac{1}{q^2}$ , illustrating Dirichlet's theorem.

To illustrate such approximations, we could surround each rational number with a disk, where more expensive points have smaller disks; then we could call an approximation to  $\alpha \in \mathbb{R}$  *good* if the corresponding disk covers  $\alpha$ . This notion is, of course, very dependent on the disk sizing. It turns out a sizing of  $\frac{1}{q^2}$  is a sort of cusp in behaviour, as demonstrated by the following theorem, illustrated in Figure 14.

**Theorem 2.1** (Dirichlet’s Approximation Theorem). *For any  $\alpha \in \mathbb{R}$ ,  $\alpha$  is irrational if and only if there exist infinitely many distinct  $p/q \in \mathbb{Q}$  such that*

$$|\alpha - p/q| < 1/q^2.$$

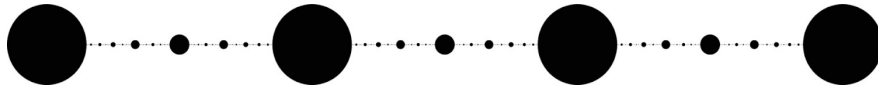


FIGURE 15. Disks centred at rational numbers  $\frac{p}{q}$  between 0 and 3 with radius  $\frac{3}{20q^2}$ .

This gives good approximations to irrational numbers (the  $p/q$  that satisfy Theorem 2.1) and also shows that the rational numbers cannot be easily approximated by other rationals, demonstrating the idea that the points are repelling each other. By scaling the points down, the repulsion rather than the notion of approximation becomes clearer, and we have an image close to a one dimensional version of the starscapes (Figure 15).

These ideas and pictures lie at the heart of Diophantine approximation. Linking geometry and number theory, they provide many of the key ideas that can be extended to the algebraic numbers. It is therefore with geometry that we will start the next section, moving from a study of images to the mathematical ideas expressed in them. In later sections, we will return to Diophantine approximation, motivated by the geometry to recast and reprove some variations on and extensions of standard results.

### 3. THE GEOMETRY

The gallery images show some structures in the lattice of polynomials over the integers, viewed in two dimensions by drawing their roots in the complex plane. Because polynomials are basic and important objects across mathematics, it should perhaps be no surprise (although it was one to the authors!) that their geometric story involves many familiar characters: from projective geometry and discrete groups, to hyperbolic space, the representation theory of  $SL_2(\mathbb{C})$  and symmetric powers of the sphere. A recurring theme:

*Patterns in the distribution of algebraic numbers are shadows of the geometry of their lattice of minimal polynomials.*

Understanding this involves transferring geometric information about a polynomial’s coefficients to information about its roots. Central to this story is the roots map  $\mathcal{R}$  sending the coefficients of a complex polynomial to its multi-set of roots. This provides a two-way bridge between the space of polynomial solutions and their coefficients, relating the structures in these images directly to structures already present in their sets of minimal polynomials. Making use of this bridge requires understanding what kind of information (topological, representation-theoretic, geometric) survives the trip. We summarize three main themes here:

- The fundamental theorem of algebra implies that the roots map is a *homeomorphism* between the spaces of roots and coefficients over  $\mathbb{C}$ . Thus topological properties of collections of algebraic numbers are equivalent to topological properties of their corresponding sets of minimal polynomials.

- For  $\mathbb{F} \in \{\mathbb{R}, \mathbb{C}\}$ , the roots map  $\mathcal{R}$  is equivariant with respect to natural  $\mathrm{PSL}(2; \mathbb{F})$  actions on the spaces of roots and coefficients. This equips each of these with a notion of geometry preserved by  $\mathcal{R}$ . Thus, geometric properties of the space of minimal polynomials determine geometric properties of the algebraic numbers.
- In small degree, this action has finitely many orbits, decomposing the space of polynomials into a union of homogeneous geometries for  $\mathrm{PSL}(2; \mathbb{F})$ .

By ‘geometric’ throughout, we mean in the sense of homogeneous geometry, following Felix Klein. In a vast generalization of euclidean geometry, Klein proposed in his 1872 Erlangen Programm that a geometry is *defined as a space  $X$ , together with the transitive action of a group  $G$* . This group action is interpreted as the allowable, or ‘rigid’ motions of this geometry, its transitivity implies the geometry is *homogeneous* or behaves the same at every point<sup>1</sup>.

In the sections that follow, we give a detailed analysis of the roots map in low degree, and introduce the necessary geometric objects as they arise. In particular, we use the geometry of homogeneous spaces for  $\mathrm{PSL}(2; \mathbb{R})$  to give an interpretation of the quadratic and cubic formulas in terms of familiar geometric spaces:

- The space of real quadratics with complex roots identifies with the hyperbolic plane. Restricted to this subset, the roots map (the quadratic formula) is an isometry between the projective model (in coefficient space) and upper half plane model (in root space).
- The space of real cubics with complex roots is topologically a solid torus, and identifies with the unit tangent bundle to the hyperbolic plane. The roots map is an isometry between the models of this geometry constructed from coefficients and roots, respectively.
- Viewing the space of these cubics as the unit tangent bundle to  $\mathbb{H}^2$  gives a geometric factorization of the cubic formula. Computing the complex and real roots amounts to a projection onto the base and fiber (with respect to a fixed trivialization) respectively.

As the algebro-geometric study of polynomials of low degree spans centuries, these are almost certainly not new, but we do not know of a reference. We prove them in this section (Theorems 3.3, 3.10, 3.14, 3.22 and 3.23) for the benefit of the reader. These geometric interpretations provide both insight into the gallery images and new perspectives on results from number theory. We summarize some of these insights here.

- The starscapes are naturally interpreted through hyperbolic geometry. Inversion in the unit circle and translation along a horocycle through  $\infty$  preserve integer polynomials, explaining the evident  $\mathrm{SL}(2; \mathbb{Z})$  symmetry in figures such as Figure 1a and Figure 1c.
- The roots map is an isometry, so we can measure distances between quadratic numbers explicitly using the discriminant quadratic form on their minimal polynomials, which we will use in Section 5.
- The identification of cubics with complex conjugate roots with the unit tangent bundle to  $\mathbb{H}^2$  suggests new ways of visualizing cubic numbers: as subsets of the solid torus (Figures 10a, 29b, 31) and as vector fields in  $\mathbb{C}$  (Figure 30).
- Under this identification, two parameter families of cubics embed in  $\mathbb{C}$  via the roots map when everywhere transverse to the fibers of the unit tangent bundle. This provides a condition on precisely when the projection onto the complex root is not a homeomorphism: compare and contrast Figures 7c and 33b.

3.0.1. *Notation.* We briefly collect here some useful notation and conventions used throughout. A *complex polynomial of one variable* is a function  $f: \mathbb{C} \rightarrow \mathbb{C}$  of the form  $f(x) = a_n x^n + \dots + a_1 x + a_0$  for  $a_0, \dots, a_n \in \mathbb{C}$ . Throughout this section we focus instead on *complex binary forms in two variables*, which are polynomials in  $x, y$  where each term has constant total degree,

<sup>1</sup>From this perspective the euclidean plane is  $\mathbb{R}^2$  equipped with the group of rotations and translations. Projective geometry, hyperbolic geometry, and de Sitter space are other common examples, which we will encounter throughout our journey.

i.e. of the form  $a_n x^n + a_{n-1} x^{n-1} y + \dots + a_1 x y^{n-1} + a_0 y^n$  for  $a_0, \dots, a_n \in \mathbb{C}$ . These generalize the single variable case (setting  $y = 1$  returns its single variable counterpart) with several advantages. Chiefly, binary forms of degree  $n$  naturally include all single variate polynomials of lower degree<sup>2</sup>, providing spaces to study all algebraic numbers of bounded degree.

For a fixed degree  $n$ , we let  $\text{Coefs}_n$  be the space of all coefficients of all degree  $n$  binary forms, and  $\text{Roots}_n$  be the space of all multi-sets of their roots (we drop the subscript when no confusion results). For binary forms, it is convenient to allow roots to lie in the extended complex plane  $\mathbb{CP}^1 = \mathbb{C} \cup \{\infty\}$ . In this way, every polynomial of degree  $n$  has exactly  $n$  roots (with multiplicity)<sup>3</sup>. The roots map  $\mathcal{R}_n: \text{Coefs}_n \rightarrow \text{Roots}_n$  returns all roots of a polynomial as a function of its coefficients. As the roots of a polynomial are unchanged by rescaling all coefficients by a constant, we abuse notation and also write  $\mathcal{R}_n$  for the roots map on scaling classes  $\mathcal{R}_n: \mathbb{P}\text{Coefs}_n \rightarrow \text{Roots}_n$ . Similarly, we write  $\Delta_n: \text{Coefs} \rightarrow \text{Roots}$  for the discriminant, dropping  $n$  when unambiguous.

Often, we will identify a certain subset of polynomials with some geometric or topological space  $X$ . Depending on our perspective, we may find it useful to think of these as either being built out of the polynomial's coefficients or its roots. To keep these two conceptually distinct, we will often decorate  $X$  accordingly, writing  $X_{\text{Coefs}} \subset \text{Coefs}$  and  $X_{\text{Roots}} \subset \text{Roots}$ . Some of the important spaces that arise in this way (and will be defined in the following sections) are the projective spaces  $\mathbb{RP}^1, \mathbb{CP}^1$ , their generalizations  $\mathbb{RP}^n, \mathbb{CP}^n$ , the symmetric powers of the sphere  $\text{SP}^n(\mathbb{CP}^1)$ , and the hyperbolic plane  $\mathbb{H}^2$ .

**3.1. Projective Geometry and Rational Numbers.** An analysis of the rational numbers  $\mathbb{Q}$  provides a gentle introduction to the recurring themes of this section, and an excellent first introduction to projective geometry. Secretly of course, this is just the story of linear polynomials over  $\mathbb{Z}$  and their roots. The simplicity of the roots map  $\mathcal{R}(ax - b) = b/a$  allows us to suppress much of this formalism and focus on examples of our main idea: *complex patterns that reveal themselves when viewed as shadows of some higher dimensional structure.*

After introducing projective geometry, we provide two examples of this. We give the geometric explanation for the otherwise strange mediant addition law  $\frac{p}{q} \oplus \frac{r}{s} = \frac{p+r}{q+s}$  used the construction of Farey sequences, and enumeration of the rationals via the Stern-Brocot tree. Then, working over  $\mathbb{C}$ , we discover hidden hypercubes in the field of fractions of Gaussian integers.

**3.1.1. Projective Space.** Recall that every rational number  $r$  is the quotient of two integers  $r = p/q$ , so it is natural to expect our analysis of  $\mathbb{Q}$  to be deeply intertwined with the lattice  $\mathbb{Z} \oplus \mathbb{Z}$ . However, to actually build  $\mathbb{Q}$  from  $\mathbb{Z}^2$ , there are two minor complications to be resolved: (1) a pair  $(p, q) \in \mathbb{Z}^2$  does not uniquely determine a rational number, as  $\frac{p}{q} = \frac{np}{nq}$ , and (2) not all pairs  $(p, q) \in \mathbb{Z}^2$  determine rational numbers, as division by zero is undefined. Both of these issues evaporate upon the realization that as *ratios* of integers, we should not model rationals by *points in  $\mathbb{Z}^2$*  but rather as *slopes*. This is more memorably stated as follows:

*The rational numbers  $\mathbb{Q}$  are what the integer lattice  $\mathbb{Z}^2$  looks like if you stand at the origin  $(0, 0)$  and look around (Figure 16).*

Formally, considering objects up to scaling is called *projectivization*, and scaling classes of pairs of integers form the *rational projective line* or  $\mathbb{QP}^1$ :

$$\mathbb{QP}^1 = \{(p, q) \neq \vec{0} \mid p, q \in \mathbb{Z}\} / (p, q) \sim (np, nq).$$

<sup>2</sup>For example the linear polynomial  $2x + 3$  can be thought of as the homogeneous linear polynomial  $2x + 3y$ , or the homogeneous quadratic  $2xy + 3y^2$ , or the homogeneous cubic  $2xy^2 + 3y^3$ , etc.

<sup>3</sup>Again taking the univariate polynomial  $2x + 3$  as an example, thought of as a linear homogeneous equation this has a single root. But thought of as a quadratic, such linear equations have an additional root "at infinity".

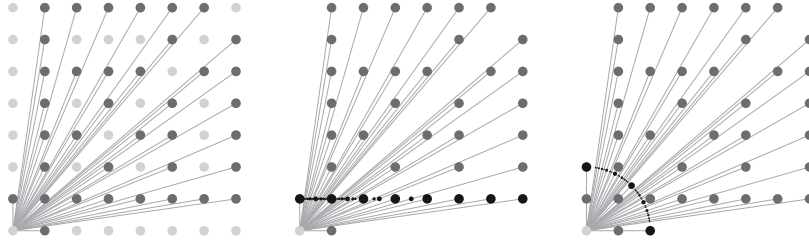


FIGURE 16. The rational numbers as the projection of integer lattice (left) onto an affine patch (middle) and visual sphere (right). The darker point on the left represent the first point on each rational slope, as viewed from the origin (lower left dot).

The points of  $\mathbb{Q}\mathbb{P}^1$  are denoted  $[p : q]$ . Note that by definition these points are unchanged by a global scaling of their coordinates, resolving issue (1) above: for example  $[p : q] = [2p : 2q] = [\frac{p}{2} : \frac{q}{2}]$ . Thus, one may recover the usual perspective of the rational numbers as points on a line from this, by imagining a screen (called an *affine patch*) placed a unit distance in front of one's eyes. The rational number  $[p : q]$  projects onto this screen to  $[\frac{p}{q} : 1]$  (Figure 16, middle).

This definition automatically resolves point (2) as well, and gives a rigorous interpretation for  $1/0$  as the projective point  $[1 : 0] \in \mathbb{Q}\mathbb{P}^1$  associated to the horizontal axis in the plane. This line does not intersect the affine patch  $\{[x : 1] \mid x \in \mathbb{Q}\}$ , so it is not a rational number but a *point at infinity*, often denoted  $[0 : 1] = \infty$ . The rational projective line fixes the asymmetry of  $\mathbb{Q}$ 's relation to  $\mathbb{Z} \times \mathbb{Z}$  by adding a single point:  $\mathbb{Q}\mathbb{P}^1 = \mathbb{Q} \cup \{\infty\}$ . There are many contexts in which scaling classes are the right objects to consider, and this construction generalizes far beyond the rational numbers.

**Definition 3.1.** Let  $\mathbb{F}$  be a field, and  $n \in \mathbb{N}$ . Then  $n$ -dimensional projective space over  $\mathbb{F}$ , denoted  $\mathbb{F}\mathbb{P}^n$ , is given by scaling classes of the nonzero elements of  $\mathbb{F}^{n+1}$  up to elements of  $\mathbb{F}^\times$ :

$$\mathbb{F}\mathbb{P}^n = \{\mathbf{x} = (x_1, \dots, x_{n+1}) \neq \vec{0} \mid x_i \in \mathbb{F}\} / (\mathbf{x} = a\mathbf{x}, a \in \mathbb{F}^\times).$$

An equivalence class in  $\mathbb{F}\mathbb{P}^n$  is denoted  $[\mathbf{x}] = [x_1 : x_2 : \dots : x_{n+1}]$ . Given  $X \subset \mathbb{F}^{n+1} \setminus \vec{0}$ , we write  $\mathbb{P}X = \{[x] \mid x \in X\} \subset \mathbb{F}\mathbb{P}^n$  for the scaling classes of all elements in  $X$ . An *affine patch* of  $\mathbb{F}\mathbb{P}^n$  is a subset homeomorphic to  $\mathbb{F}^n$  equivalent to  $\{[x_1 : x_2 : \dots : x_n : 1]\}$  under some change of coordinates.

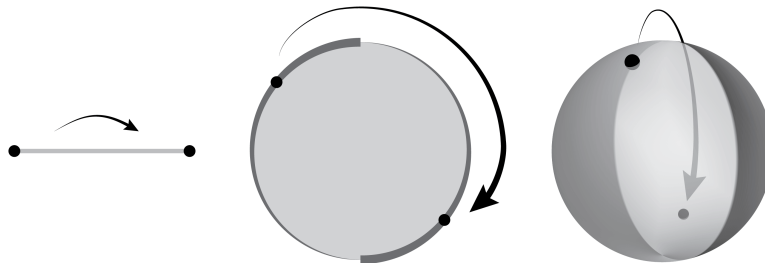


FIGURE 17. Real projective space can be constructed from a solid ball by identifying its boundary via the antipodal map. Here we see this in dimensions 1, 2 and 3.

*Remark 3.2.* For any field  $\mathbb{F}$ , we may see that  $\mathbb{F}\mathbb{P}^1 \cong \mathbb{F} \cup \{[1 : 0]\} = \mathbb{F} \cup \{\infty\}$  by the same argument as for  $\mathbb{Q}$ . In fact,  $\mathbb{F}\mathbb{P}^1$  is the *one point compactification of  $\mathbb{F}$* , so  $\mathbb{R}\mathbb{P}^1$  is a circle and  $\mathbb{C}\mathbb{P}^1$  is a sphere.

For us, a main advantage of this perspective<sup>4</sup> is to aid in switching back and forth between thinking about objects in  $\mathbb{F}\mathbb{P}^n$  and objects in the higher dimensional space  $\mathbb{F}^{n+1}$ . We give two simple, but surprisingly beautiful applications of this below.

3.1.2.  $\mathbb{Q}\mathbb{P}^1$  and the Stern-Brocot Tree. A means of representing the lowest-terms representative of each rational number by an infinite binary tree was discovered independently by Stern and Brocot in the mid 1800s. This tree is depicted in Figure 18. The construction of the tree is inductive, where the elements of the  $n^{\text{th}}$  row are produced from those in prior rows by taking *mediants*. The *mediant of two fractions  $\frac{p}{q}$  and  $\frac{r}{s}$*  in lowest terms is the fraction  $\frac{p+r}{q+s}$ , which appears to be a rather algebraically unnatural construction<sup>5</sup>. Taking mediants is a common step in such enumeration sequences (including the Farey sequence, a source of much beautiful mathematics on  $\mathbb{Q}\mathbb{P}^1$ ), but is best understood not as an *algebraic operation* on  $\mathbb{Q}$  but rather as a *geometric operation* on  $\mathbb{Q}\mathbb{P}^1$ . Indeed, before projectivizing, the points  $(p, q)$  and  $(r, s)$  are vectors in  $\mathbb{R}^2$ , and here the mediant operation is simply *vector addition!* This is completely natural geometrically on  $\mathbb{Q}\mathbb{P}^1$ : given two points, lift to their representatives in  $\mathbb{Z}^2$  which are closest to the origin. These two vectors determine two sides of a parallelogram, whose main diagonal connects you directly to the mediant.

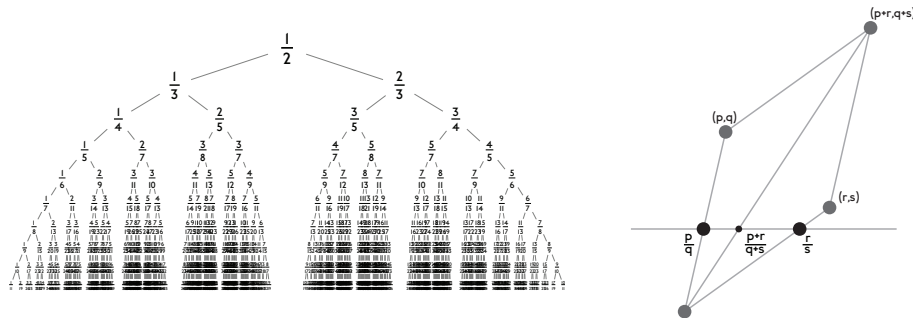


FIGURE 18. The Stern-Brocot Tree enumerating the rationals, and a geometric description of the mediant of two fractions, essential to its construction.

3.1.3.  $\mathbb{Q}\mathbb{P}^1$  and Hidden Hypercubes. A second example of gaining a totally new perspective through “de-projectivizing” and rephrasing things in a higher dimension involves the Gaussian integers and complex projective space. A *Gaussian integer* is a complex number of the form  $a + bi$  where  $a, b \in \mathbb{Z}$ . Much as the rational numbers  $\mathbb{Q}$  are the set of quotients of integers, we may analogously define the field of fractions of the Gaussian integers,  $\mathbb{Q}(i)$ .

$$\mathbb{Q}(i) = \left\{ \frac{a + bi}{c + di} \mid a, b, c, d \in \mathbb{Z} \right\}$$

<sup>4</sup>In addition to managing to rigorously make sense of  $1/0$  of course!

<sup>5</sup>However, it is certainly a visually natural thing to try given our representation of rationals as quotients - indeed probably the most common mistake when first learning arithmetic is to add rationals by taking their mediant!

The set  $\mathbb{Q}(i)$  of such ratios is dense in  $\mathbb{C}$  and displays incredible structure. Figure 19 shows the points of  $\mathbb{Q}(i) \subset \mathbb{C}$  sized inversely proportional to the squared magnitude of their denominator, as in Figure 15.

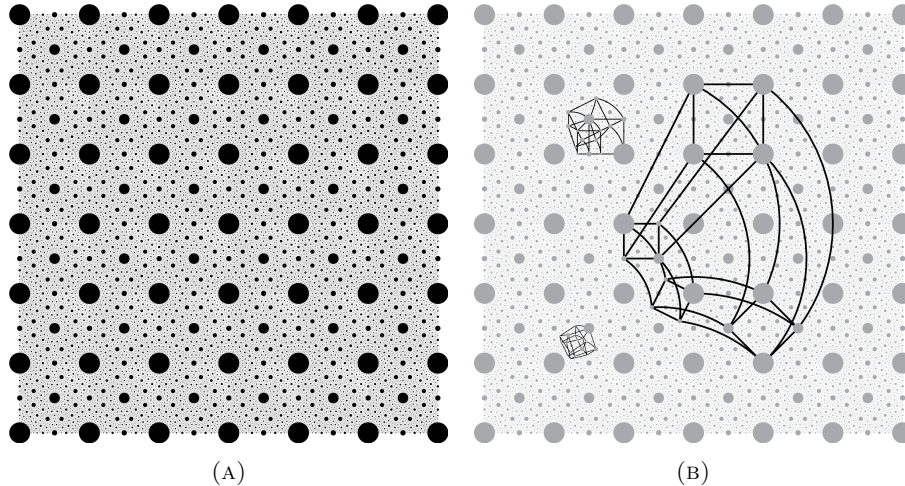


FIGURE 19. Ratios of Gaussian integers  $\frac{a+bi}{c+di}$  (19a) and the hidden hypercubes (19b), arising from the tiling  $(\mathbb{Z} + i\mathbb{Z})^2 \subset \mathbb{C}^2$ .

To deal with the possibility that  $c = d = 0$  it is perhaps easiest to include  $1/0 = \infty$  and view these points as elements of the complex projective line  $\mathbb{CP}^1$ . But this small change, from  $\mathbb{C}$  to  $\mathbb{C} \cup \{\infty\} = \mathbb{CP}^1$  suggests an alternative view of  $\mathbb{Q}(i)$ . Rescaling the points in  $\mathbb{CP}^1$  representing  $\mathbb{Q}(i)$  by clearing denominators, we see

$$\mathbb{Q}(i) = \left\{ \left[ \frac{a+bi}{c+di} : 1 \right] \right\} = \left\{ [a+bi : c+di] \right\} = \mathbb{P}(\mathbb{Z} + i\mathbb{Z})^2$$

That is,  $\mathbb{Q}(i)$  is just the projection of the standard cubical lattice  $\mathbb{Z}^4 \subset \mathbb{R}^4$  (thought of as  $\mathbb{C}^2$ ) under the projectivization map rescaling along complex lines through the origin. Even though this projectivization drops two real dimensions, ghosts of  $\mathbb{Q}(i)$ 's origin as a tiling of  $\mathbb{R}^4$  by hypercubes are still visible once you know about this hidden symmetry. Figure 19b highlights some of these.

3.1.4. *The Roots Map.* We briefly record the solution to linear equations  $ax+by$  in our standard notation, for later use when discussing cubics. Over  $\mathbb{C}$ , the space of coefficients identifies naturally with  $\mathbb{C}^2 = \{(a, b) \mid a, b \in \mathbb{C}\}$ , and so up to scaling we have  $\mathbb{PCoefs} = \mathbb{CP}^1$ . The space of their roots is also  $\mathbb{CP}^1$ , thought of as the extended complex plane; as  $ax + by$  has solution  $[-b : a] = [-b/a : 1]$  when  $a \neq 0$  and otherwise  $\infty = [1 : 0]$ . Thus the roots map here is a linear isomorphism of  $\mathbb{CP}^1$  with itself:

$$\mathcal{R}_1 : \mathbb{CP}_{\text{Coefs}}^1 \rightarrow \mathbb{CP}_{\text{Roots}}^1 \quad [a : b] \mapsto [-b : a]$$

This gives a natural identification between the spaces of roots and (projectivized) coefficients, allowing us to simplify the stories above. In the following sections,  $\mathcal{R}$  will continue to be a homeomorphism  $\mathbb{PCoefs} \rightarrow \text{Roots}$ , and topologically the mapping from a polynomial's coefficients to its solutions is still equivalent to projectivization. However,  $\mathcal{R}$  is no longer such a simple isomorphism, and much of the work involved in accurately transferring information from coefficients to roots involves a careful analysis of  $\mathcal{R}$  and the symmetries it preserves.

**3.2. Hyperbolic Geometry and Quadratic Numbers.** Some of the striking images in the gallery involve *quadratic numbers*, or solutions in  $\mathbb{C}$  to degree-two polynomials with integer coefficients  $ax^2 + bx + c$ . The suggestively “hyperbolic” nature of these (Figure 1a) is no accident; and the goal of this section is to make this connection explicit. In particular, we prove the following.

**Theorem 3.3.** *Let  $\mathbb{H}_{\text{Coefs}}^2$  be the projectivized set of coefficients of real quadratics with complex roots and  $\mathbb{H}_{\text{Roots}}^2$  be the set of their root-sets, equipped with the following metrics:*

- $\mathbb{H}_{\text{Coefs}}^2 = \{[a : b : c] \mid b^2 < 4ac\}$  is given the projectively invariant metric it inherits as a convex subset of  $\mathbb{RP}^2$ ,
- $\mathbb{H}_{\text{Roots}}^2 = \{\{x \pm iy\} \mid x, y \in \mathbb{R}, y > 0\}$  is given the Möbius-transformation invariant metric from identification with the upper half plane  $\subset \mathbb{CP}^1$ .

*Both of these spaces are isometric to the hyperbolic plane. Furthermore, the quadratic formula, given as the map  $[a : b : c] \mapsto \left\{ \frac{-b \pm i\sqrt{4ac - b^2}}{2a} \right\}$  is an isometry between these two metrics.*

In short, the proof follows from the equivariance of the roots map on real quadratics with respect to a  $\text{PSL}(2; \mathbb{R})$  action on each side. In this section we take a narrative approach, and show how natural symmetry considerations might lead one to notice this in the first place. This is good preparation for the cubic case, and additionally avoids unenlightening calculation.

The existence of irreducible quadratics over  $\mathbb{R}$  makes the complex numbers essential to our discussion. As such, we begin with a discussion of binary forms over  $\mathbb{C}$ . This has several advantages<sup>6</sup>, and after getting comfortable here we will restrict back to real coefficients to prove Theorem 3.3.

**3.2.1. Complex Quadratics.** In this section we precisely define the space of coefficients, space of roots, and the map  $\mathcal{R}: \text{Coefs} \rightarrow \text{Roots}$  for complex homogeneous quadratics. This lays the foundation for a bridge between properties of quadratic numbers and properties of their minimal polynomials, by the following observation.

**Observation 3.4.** *The roots map  $\mathcal{R}: \text{Coefs} \rightarrow \text{Roots}$  is a homeomorphism from the space of complex homogeneous quadratics to the multi-sets of their roots in  $\mathbb{CP}^1$ .*

The polynomial  $f = ax^2 + bxy + cy^2$  is determined by its coefficients  $a, b, c \in \mathbb{C}$ , so  $\text{Coefs} \cong \mathbb{C}^3$ . We denote the scaling class of a quadratic  $f = ax^2 + bxy + cy^2$  by  $[f]$ , with coefficients  $[a : b : c] \in \mathbb{P}\text{Coefs} = \mathbb{P}(\mathbb{C}^3) = \mathbb{CP}^2$  in the complex projective plane. The roots map  $\mathcal{R}$  is just the quadratic formula; taking the polynomial with coefficients  $[a : b : c]$  with  $a \neq 0$  to its solutions  $\left[ \frac{-b \pm \sqrt{b^2 - 4ac}}{2a} : 1 \right]$ , or  $[-b \pm \sqrt{b^2 - 4ac} : 2a] \in \mathbb{CP}^1$  after clearing denominators<sup>7</sup>. The space of roots comes with no natural ordering. Thus,  $\text{Roots}$  does not identify with the space of *ordered pairs*  $\mathbb{CP}^1 \times \mathbb{CP}^1$  of points in the extended complex plane, but rather the set of *unordered pairs in  $\mathbb{CP}^1$* . This space is called the *second symmetric power of  $\mathbb{CP}^1$* , and we write  $\text{Roots} = \text{SP}^2(\mathbb{CP}^1)$ . An explicit construction of this space results from the quotient of  $\mathbb{CP}^1 \times \mathbb{CP}^1$  by the action of  $\mathbb{Z}_2$  swapping coordinates.

*Remark 3.5.* It may be helpful to pause here to gain some intuition from the lowest-dimensional example of a nontrivial symmetric power. The second symmetric power of a circle  $\text{SP}^2(\mathbb{S}^1)$  is the quotient of a torus  $\mathbb{S}^1 \times \mathbb{S}^1$  by the involution  $(x, y) \mapsto (y, x)$ . This fixes the diagonal  $(x, x)$ , and the quotient is a Möbius strip with these points as the boundary curve (Figure 20).

<sup>6</sup>As  $\mathbb{C}$  is algebraically closed, the space of roots is easy to describe, defining the roots map does not require passing to a field extension, and the  $\text{PSL}(2; \mathbb{C})$  symmetry can be exhibited at its most natural level of generality.

<sup>7</sup>It is quick to check that as  $r \rightarrow \infty$  the coefficients of the polynomial  $(x - ry)(ax + by)$  converge projectively to  $[0 : a : b]$  and the roots to  $\{[1 : 0], [-b : a]\} = \{\infty, -b/a\}$ . Thus the quadratic formula extends continuously to linear equations interpreted as ‘quadratics with roots at infinity’ as noted in Section 3.1.

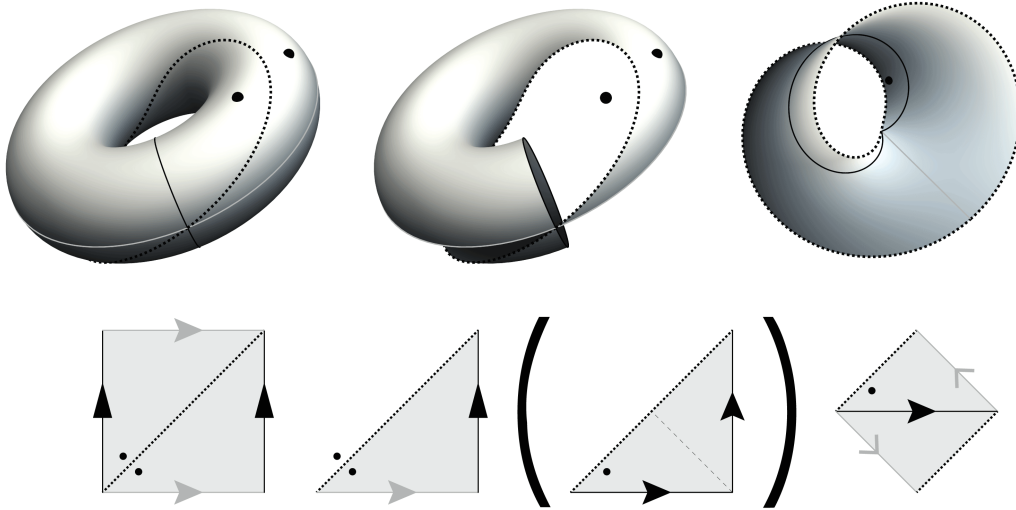


FIGURE 20. The space  $\text{SP}^2(\mathbb{R}\mathbb{P}^1)$  of unordered pairs of points on the circle  $\mathbb{R}\mathbb{P}^1 \cong \mathbb{S}^1$  is homeomorphic to a Möbius band. The space of quadratic polynomials parameterized by their roots is  $\text{SP}^2(\mathbb{C}\mathbb{P}^1)$ , with analogous construction over the complex numbers.

Not only do every pair of points in  $\mathbb{C}\mathbb{P}^1$  determine a scaling class of quadratics, but as a consequence of the fundamental theorem of algebra, every scaling class has two roots (with multiplicity) determining it. Together with the continuity of  $\mathcal{R}$ , this implies that the roots map is a homeomorphism<sup>8</sup> from  $\text{Coefs} = \mathbb{C}\mathbb{P}^2$  to  $\text{Roots} = \text{SP}^2(\mathbb{C}\mathbb{P}^1)$ . Thus topological properties of (projectivized) collections of quadratic polynomials completely determine the topology of their collection of roots. To strengthen this connection, we next focus on natural symmetries of the space of polynomials which are preserved by the roots map.

3.2.2.  $\text{PSL}(2; \mathbb{C})$  *Symmetry*. From both the roots and coefficients perspectives, quadratics are intimately tied to complex projective spaces. But these spaces are only half the story. To work geometrically, we must also describe their groups of allowable motions. As projective space  $\mathbb{C}\mathbb{P}^n$  is just scaling classes of vectors in  $\mathbb{C}^{n+1}$ , the most natural group of symmetries is the linear group  $\text{GL}(n+1; \mathbb{C})$  acting on these scaling classes via  $A \cdot [v] = [Av]$  for  $A \in \text{GL}(n; \mathbb{C})$ ,  $[v] \in \mathbb{C}\mathbb{P}^n$ . For simplicity, we may consider these matrices up to constant multiples as well, and take the *projective special linear group*  $\text{PSL}(n+1; \mathbb{C}) = \{[A] \mid \det A = 1\}$  as the symmetries of  $\mathbb{C}\mathbb{P}^n$ . For points in  $\mathbb{C}\mathbb{P}^1$  thought of as  $\mathbb{C} \cup \{\infty\}$ , these are known as *Möbius transformations*: the transformation corresponding to  $\begin{pmatrix} p & q \\ r & s \end{pmatrix}$  acts on  $z \in \mathbb{C}$  as

$$\begin{pmatrix} p & q \\ r & s \end{pmatrix} \cdot z = \begin{bmatrix} p & q \\ r & s \end{bmatrix} \cdot [z : 1] = \left[ \begin{pmatrix} p & q \\ r & s \end{pmatrix} \begin{pmatrix} z \\ 1 \end{pmatrix} \right] = \left[ \begin{pmatrix} pz + q \\ rz + s \end{pmatrix} \right] = \left[ \frac{pz + q}{rz + s} : 1 \right] = \frac{pz + q}{rz + s}.$$

Thus,  $\mathbb{P}\text{Coefs} \cong \mathbb{C}\mathbb{P}^2$  naturally has the symmetries of  $\text{PSL}(3; \mathbb{C})$ . As  $\text{Roots} = \mathbb{C}\mathbb{P}^1 \times \mathbb{C}\mathbb{P}^1 / \mathbb{Z}_2$  is built from the complex projective line, the natural symmetries of the space of roots are  $\text{PSL}(2; \mathbb{C})$ , inherited from  $\mathbb{C}\mathbb{P}^1$  via  $[A] \cdot \{[z], [w]\} = \{[A \cdot z], [A \cdot w]\}$ . Initially these two notions of geometry are completely independent, constructed from our models of  $\text{Roots}$  and  $\text{Coefs}$  respectively. However, given that  $\mathcal{R}: \text{Coefs} \rightarrow \text{Roots}$  is a homeomorphism, we may use it to

<sup>8</sup>This is an important argument in its own right, for it shows topologically the symmetric power  $\text{SP}^2(\mathbb{S}^2)$  is the complex projective plane in disguise. In particular, it is a closed manifold. Compare this with Remark 3.5 where  $\text{SP}^2(\mathbb{S}^1)$  is a manifold with boundary. This generalizes to arbitrary degree  $n$ , and the roots map provides a homeomorphism  $\mathcal{R}_n: \mathbb{C}\mathbb{P}^n \xrightarrow{\sim} \text{SP}^n(\mathbb{C}\mathbb{P}^1)$ .

compare the symmetries on one side to the other. The main observation of this section is that these two actions are actually *compatible*<sup>9</sup> with each other.

**Observation 3.6.** *Moving the space of roots by a (projective) linear transformation is represented on the space of coefficients by a (projective) linear transformation as well. That is, conjugation of this action by  $\mathcal{R}$  embeds  $\mathrm{PSL}(2; \mathbb{C})$  into  $\mathrm{PSL}(3; \mathbb{C})$ .*

One may then directly convert any knowledge about this representation into geometric statements binding the spaces of roots and coefficients yet closer together. This  $\mathrm{PSL}(2; \mathbb{C})$  on the space of coefficients has a natural description: conjugation by the roots map simply declares that  $[A] \in \mathrm{PSL}(2; \mathbb{C})$  send the polynomial with roots  $\{[z], [w]\}$  to the polynomial with roots  $\{[Az], [Aw]\}$ . Writing this out explicitly, let  $A = \begin{pmatrix} p & q \\ r & s \end{pmatrix} \in \mathrm{PSL}(2; \mathbb{C})$  and  $f$  be a homogeneous quadratic with coefficients  $[f] = [a : b : c]$ . Then  $[A].[f] = [f \circ A^{-1}]$ , which gives the following.

$$f \left( \begin{bmatrix} s & -q \\ -r & p \end{bmatrix} \begin{bmatrix} x \\ y \end{bmatrix} \right) = f \left( \begin{bmatrix} sx - qy \\ py - rx \end{bmatrix} \right) = a(sx - qy)^2 + b(sx - qy)(py - rx) + c(py - rx)^2$$

Expanding and collecting like terms in  $x^i y^j$  shows that the new coefficient vector is a *linear transformation* of  $[a : b : c]$  involving  $p, q, r, s$ , which confirms Observation 3.6. Specifically, the coefficients of  $[A].[f]$  satisfy

$$\begin{bmatrix} p & q \\ r & s \end{bmatrix} . [a : b : c] = \left[ \begin{pmatrix} s^2 & -rs & r^2 \\ -2qs & qr + ps & -2pr \\ q^2 & -pq & p^2 \end{pmatrix} \begin{pmatrix} a \\ b \\ c \end{pmatrix} \right] \quad (1)$$

This  $3 \times 3$  matrix is the *representation* of  $\begin{pmatrix} p & q \\ r & s \end{pmatrix}$  acting on  $\mathrm{Coefs} = \mathbb{CP}^2$ . Let  $\rho: \mathrm{PSL}(2; \mathbb{C}) \rightarrow \mathrm{PSL}(3; \mathbb{C})$  denote this representation. By construction, for each  $A \in \mathrm{PSL}(2; \mathbb{C})$  we have  $f(A.[x : y]) = (\rho(A).f)([x : y])$ . This implies the roots map is  *$\rho$ -equivariant*, satisfying the following important identity:

$$\mathcal{R}(\rho(A).f) = \mathcal{R}(f \circ A^{-1}) = A.\mathcal{R}(f). \quad (2)$$

In principle, this formula for the action lets us completely compute anything we desire about the relationship between the spaces of roots and coefficients (including the quadratic formula itself, Corollary 3.10). The sort of qualitative understanding useful to interpret patterns in the gallery images emerges from looking at the geometry of these spaces after restricting back to real coefficients. This  $\mathrm{PSL}(2; \mathbb{C})$  action divides the space of quadratics into two components or orbits: those with a double root, and (the generic case) those with distinct roots. Because the action of  $\mathrm{PSL}(2; \mathbb{C})$  is transitive on each of these components, they can be interpreted as homogeneous geometries in the sense of Klein. This allows us to use geometric properties to understand the behavior of the roots map.

**3.2.3. Real Quadratics.** The spaces of real quadratics naturally inherit their topology and geometry as subsets of the corresponding spaces over  $\mathbb{C}$ . This reduces the space of coefficients from  $\mathbb{C}^3$  to  $\mathbb{R}^3$ , so we work with the projective plane  $\mathbb{P}\mathrm{Coefs} = \mathbb{RP}^2$ , and its symmetries  $\mathrm{PSL}(3; \mathbb{R})$ . The space of roots is more complicated to describe due to the fact that real quadratics may have complex roots. However, as the roots map is a homeomorphism over  $\mathbb{C}$ , we can immediately determine its topology:  $\mathrm{Roots} = \mathcal{R}(\mathbb{P}\mathrm{Coefs}) = \mathcal{R}(\mathbb{RP}^2) \cong \mathbb{RP}^2$ . We will denote these two models of projective space as  $\mathbb{RP}_{\mathrm{Coefs}}^2, \mathbb{RP}_{\mathrm{Roots}}^2$  in what follows.

$$\begin{aligned} \mathbb{RP}_{\mathrm{Coefs}}^2 &= \{[a : b : c] \mid (a, b, c) \in \mathbb{R}^3 \setminus \mathbf{0}\} \subset \mathbb{CP}^3 \\ \mathbb{RP}_{\mathrm{Roots}}^2 &= \{\{x, y\} \mid x, y \in \mathbb{RP}^1\} \cup \{\{x \pm iy\} \mid x, y \in \mathbb{R}, y > 0\} \subset \mathrm{SP}^2(\mathbb{CP}^1) \end{aligned}$$

<sup>9</sup>This picture may already be familiar from representation theory: the action of  $\mathrm{PSL}(V)$  on a 2-dimensional complex vector space  $V$  induces actions on symmetric powers of  $V$ , which are the irreducible representations of  $\mathrm{PSL}(V)$ . Projectivizing this picture under an identification  $V = \mathbb{C}^2$  yields the result we exhibit here.

The natural symmetry group on the roots restricts to  $\mathrm{PSL}(2; \mathbb{R})$ , and equation (1) confirms that the representation faithfully translates this to a subgroup of  $\mathrm{PSL}(3; \mathbb{R})$  on the coefficients. Thus  $\mathcal{R}: \mathbb{RP}_{\mathrm{Coefs}}^2 \rightarrow \mathbb{RP}_{\mathrm{Roots}}^2$  remains equivariant with respect to the  $\mathrm{PSL}(2; \mathbb{R})$  symmetries on each side. Recall that over  $\mathbb{C}$ , this action divided the space of quadratics into two orbits. Any two polynomials with distinct roots are related to one another by a symmetry transformation, as are any two with a double root; but  $\mathrm{PSL}(2; \mathbb{C})$  cannot convert one type into the other. Over  $\mathbb{R}$  the story gets more interesting, as the generic case (polynomials with distinct roots) splits.

**Observation 3.7.** *The  $\mathrm{PSL}(2; \mathbb{R})$  action divides the space of real quadratics into three orbits<sup>10</sup>: (1) quadratics with a double real root, (2) quadratics with distinct real roots, and (3) quadratics with complex conjugate roots.*

The orbit (1) is homeomorphic to a circle<sup>11</sup> as any point  $[p : q] \in \mathbb{RP}^1$  determines a quadratic  $f = (px - qy)^2$  with double root at  $[p : q]$ . The orbit (2) of quadratics with distinct roots identifies with the space of unordered pairs of points of  $\mathbb{RP}^1$ , which we saw in remark 3.5 to be the Möbius band. We are mainly interested in orbit (3), which consists of unordered pairs of *complex conjugates* in  $\mathbb{C} \setminus \mathbb{R}$ . Each such pair contains a unique point  $x + iy$  with  $y > 0$ , so we identify this with the upper half plane in  $\mathbb{C}$ . As the  $\mathrm{PSL}(2; \mathbb{R})$  action on each is transitive on each orbit, all three of these pieces inherit the structure of a homogeneous geometry, listed below.

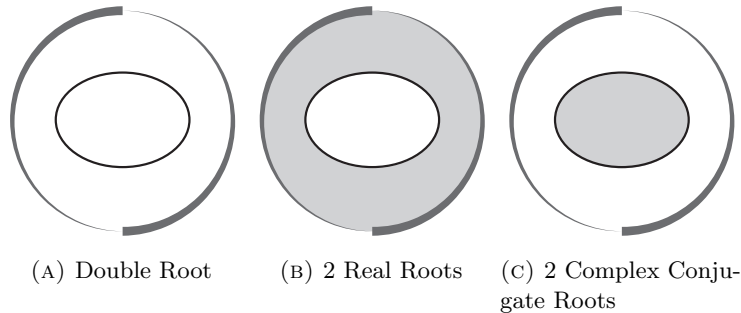


FIGURE 21. The four  $\mathrm{PSL}(1; \mathbb{R})$  orbits on the  $\mathbb{RP}^2$  of real quadratics, as subsets of  $\mathbb{RP}^2$ . As in Figure 17, the topology of each component is recovered by identifying points on the boundary circle via the antipodal map.

**Observation 3.8.** *The  $\mathrm{PSL}(2; \mathbb{R})$  action on the projective plane of real quadratics divides it into three disjoint homogeneous geometries.*

- (1) *The geometry of quadratics with a double root is the familiar geometry of the real projective line.*
- (2) *The geometry of quadratics with distinct real roots is that of de Sitter space, a two dimensional Lorentzian geometry<sup>12</sup>.*
- (3) *The geometry of quadratics with complex conjugate roots is a disk equipped with a  $\mathrm{PSL}(2; \mathbb{R})$  action - that is, the hyperbolic plane.*

<sup>10</sup>On  $\mathbb{RP}_{\mathrm{Coefs}}^2$ , the orbit of quadratics with double root is exactly the discriminant locus; its complement is the union of the other two orbits.

<sup>11</sup>In fact, from here, elementary topology completes the story as all separating circles divide  $\mathbb{RP}^2$  into a Möbius strip and a disk, giving the topological type of (2) and (3) respectively.

<sup>12</sup>Lorentzian geometry is the flavor of geometry useful to describe space-time in relativity theory. De Sitter 2-space describes a world with one space and one time dimension of positive curvature.

3.2.4. *Hyperbolic Geometry and the Roots Map.* It is the real quadratics with complex roots which are responsible for the beautiful images in the gallery such as Figure 1a, so we study the  $\mathrm{PSL}(2; \mathbb{R})$  geometry<sup>13</sup>. An abstract understanding of hyperbolic space is insufficient for our goals, which rely on an explicit understanding of the geometry of the roots map  $\mathcal{R}$ . Thus we need to consider both the model  $\mathbb{H}_{\mathrm{Coefs}}^2$  of hyperbolic geometry given by the coefficients of these polynomials, and model  $\mathbb{H}_{\mathrm{Roots}}^2$  formed by their roots.

We begin with  $\mathbb{H}_{\mathrm{Roots}}^2$ . Identifying this space with the upper half plane  $\{x + iy \mid y > 0\} \subset \mathbb{C}$ , the Riemannian metric<sup>14</sup> for hyperbolic geometry is  $ds^2 = (dx^2 + dy^2)/y^2$ , which follows directly from the  $\mathrm{PSL}(2; \mathbb{R})$  action, translating the standard metric  $dx^2 + dy^2$  at  $i$  around by the group action. The shortest paths, or geodesics, between two points are given by arcs of semicircles whose center lies on the boundary  $y = 0$ , together with vertical lines (circles of infinite radius). From this, an explicit formula for the distance between two points  $x_1 + iy_1$  and  $x_2 + iy_2$  in  $\mathbb{H}_{\mathrm{Roots}}^2$  can be calculated:

$$d_{\mathrm{Roots}}(x_1 + iy_1, x_2 + iy_2) = 2 \ln \left( \frac{\sqrt{(x_2 - x_1)^2 + (y_2 - y_1)^2} + \sqrt{(x_2 - x_1)^2 + (y_2 + y_1)^2}}{2\sqrt{y_1 y_2}} \right). \quad (3)$$

Next, we turn to  $\mathbb{H}_{\mathrm{Coefs}}^2$ . Here the basic geometry is likely familiar from the study of conic sections, often studied in high school mathematics. Generic real quadratics have either two real roots or a pair of complex conjugate roots, as determined by the discriminant  $\Delta(ax^2 + bx + c) = b^2 - 4ac$  being positive or negative, respectively. In fact, this and more can be explicitly recovered from studying the  $\mathrm{PSL}(2; \mathbb{R})$  action given by the representation  $\rho$  on  $\mathbb{RP}_{\mathrm{Coefs}}^2$ . We focus here on the polynomials with complex roots; similar reasoning applies in the other case. As  $\mathrm{PSL}(2; \mathbb{R})$  acts transitively on  $\mathbb{H}_{\mathrm{Roots}}^2$ , we may recover the entire space as the orbit of any point. Using the defining property  $\mathcal{R}(\mathbb{H}_{\mathrm{Coefs}}^2) = \mathbb{H}_{\mathrm{Roots}}^2$  and equation (2), we see that

$$\mathbb{H}_{\mathrm{Roots}}^2 = \mathrm{PSL}(2; \mathbb{R}) \cdot \{\pm i\} \implies \mathbb{H}_{\mathrm{Coefs}}^2 = \rho(\mathrm{PSL}(2; \mathbb{R})) \cdot [1 : 0 : 1], \quad (4)$$

as  $[1 : 0 : 1]$  are the coefficients of  $x^2 + 1$ , with roots  $\{\pm i\}$ . Computing this orbit, we see that it is actually a hyperboloid of two sheets in  $\mathbb{R}^3$ , which is the  $-1$  level set of the discriminant  $\Delta(a, b, c) = b^2 - 4ac$ . The entire action of  $\mathrm{PSL}(2; \mathbb{R})$  on  $\mathbb{R}^3$  via the representation  $\rho$  preserves the quadratic form  $\Delta$ , and the inner product  $\langle (a_1, b_1, c_1), (a_2, b_2, c_2) \rangle = b_1 b_2 - 2a_1 c_2 - 2a_2 c_1$  for which  $\Delta(v) = \langle v, v \rangle$ . Thus the symmetries of  $\mathbb{H}_{\mathrm{Coefs}}^2$  are contained in the *special orthogonal group*<sup>15</sup> of this form<sup>16</sup>  $\mathrm{SO}(\Delta)$ . The hyperbolic space  $\mathbb{H}_{\mathrm{Coefs}}^2$  is the projectivization of the negative cone of  $\Delta$ ; or  $\mathbb{H}_{\mathrm{Coefs}}^2 = \{[a : b : c] \mid 4ac > b^2\}$ . In fact, as the discriminant is preserved by the entire  $\mathrm{PSL}(2; \mathbb{R})$  action<sup>17</sup>.

Topologically  $\mathbb{H}_{\mathrm{Coefs}}^2$  is a disk, but depending on the affine patch of  $\mathbb{RP}^2$  that we choose it may take different forms. Indeed, the patch  $[1 : b : c]$  corresponding to taking the monic representatives of quadratics represents  $\mathbb{H}_{\mathrm{Coefs}}^2$  as the interior of a paraboloid, with one point on its boundary at infinity:  $\mathbb{H}_{\mathrm{Coefs}}^2 = \{[1 : b : c] \mid 4c > b^2\}$ .

<sup>13</sup>Hyperbolic geometry, commonly denoted  $\mathbb{H}^2$ , is the unique two dimensional geometry with constant negative curvature, and was the first non euclidean geometry discovered. Negative curvature implies that  $\mathbb{H}^2$  violates Euclid's fifth postulate with an infinitude of parallel lines to a given line through any point not on it. For an introductory treatment of the hyperbolic plane, see [3].

<sup>14</sup>A Riemannian metric is a choice of inner product for each tangent space, which allows one to measure the length of vectors, and hence the arc length of curves.

<sup>15</sup>The special orthogonal group of a quadratic form  $q$  is the group of all determinant-1 matrices whose action leaves  $q$  invariant:  $\mathrm{SO}(q) = \{A \in \mathrm{SL}(n; \mathbb{R}) \mid q(v, w) = q(Av, Aw)\}$ .

<sup>16</sup> $\rho$  is actually an isomorphism onto the identity component and  $\mathrm{PSL}(2; \mathbb{R}) \cong \mathrm{SO}_0(\Delta)$ .

<sup>17</sup>A similar description can be given for the two other geometries of quadratic polynomials. The  $\mathbb{RP}^1$  of polynomials with double roots is the zero set of  $\Delta$ , or the projectivization of the light cone  $b^2 = 4ac$ . The de Sitter space of polynomials with distinct real roots corresponds to points on which  $\Delta$  is positive.

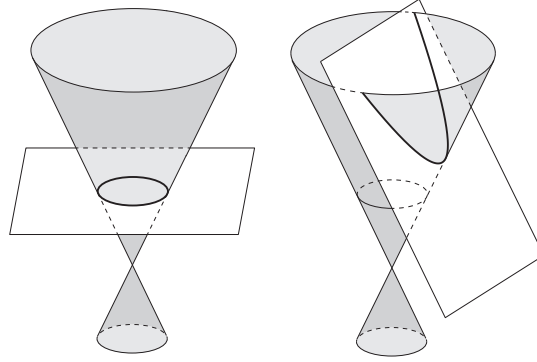


FIGURE 22. The cone determined by the discriminant in  $\mathbb{R}^3$ , together with two affine patches giving the usual Klein model (left) and a parabola model (right) of  $\mathbb{H}^2$ .

As  $\mathbb{H}_{\text{Coefs}}^2$  is a convex set in  $\mathbb{RP}^2$ , it can be endowed with a natural metric invariant under projective transformations<sup>18</sup>. As the discriminant carries all the geometry associated with the  $\text{PSL}(2; \mathbb{R})$  symmetries, there is a nice description of this metric in terms of  $\Delta$ . The geodesics in this metric are straight line segments in any affine patch containing  $\mathbb{H}_{\text{Coefs}}^2$ , and the distance between two points  $f_1 = [a_1 : b_1 : c_1]$  and  $f_2 = [a_2 : b_2 : c_2]$  is given by

$$d_{\text{Coefs}}(f_1, f_2) = \text{acosh} \left( \frac{-\langle f_1, f_2 \rangle}{\sqrt{\Delta(f_1)\Delta(f_2)}} \right) = \text{acosh} \left( \frac{2a_1c_2 + 2a_2c_1 - b_1b_2}{\sqrt{(4a_1c_1 - b_1^2)(4a_2c_2 - b_2^2)}} \right) \quad (5)$$

Bringing this all together, we have seen the natural  $\text{PSL}(2; \mathbb{R})$  actions on both the spaces of roots and coefficients endows the space of real quadratics with complex conjugate roots with the homogeneous geometry of the hyperbolic plane. The roots map is a homeomorphism (Observation 3.4), which is equivariant with respect to the action of the isometry groups on each side (the definition of  $\rho$  in Equation 1). Thus,  $\mathcal{R}: \mathbb{H}_{\text{Coefs}}^2 \rightarrow \mathbb{H}_{\text{Roots}}^2$  is an isomorphism of geometries. In particular, it preserves the metric, which proves the main theorem of this section.

**Theorem 3.9.** *Let  $\mathbb{H}_{\text{Coefs}}^2 = \{[a : b : c] \in \mathbb{RP}^2 \mid 4ac > b^2\}$  be equipped with the projectively invariant metric it inherits as a convex subset of  $\mathbb{RP}^2$ , and  $\mathbb{H}_{\text{Roots}}^2 = \{x \pm iy \mid x, y \in \mathbb{R}, y > 0\}$  be equipped with the curvature -1 metric arising from its identification with the upper half plane. Then the restricted roots map  $\mathcal{R}: \mathbb{H}_{\text{Coefs}}^2 \rightarrow \mathbb{H}_{\text{Roots}}^2$  is an isometry.*

We may use this to derive the quadratic formula from hyperbolic geometry. Fix any quadratic  $f$  (say,  $x^2 + 1$ ) with complex root  $r$  (here  $i$ ) in the upper half plane, and let  $A \in \text{PSL}(2; \mathbb{R})$ . By equivariance, the polynomial with root  $A.r$  is  $\rho(A).f$  for  $\rho: \text{PSL}(2; \mathbb{R}) \rightarrow \text{PSL}(3; \mathbb{R})$  the irreducible representation (Equation 1). Writing this out, we see the polynomial with roots  $x \pm iy = \begin{pmatrix} y & x \\ 0 & 1 \end{pmatrix} \cdot \{\pm i\}$  has coefficients  $\rho\left(\begin{pmatrix} y & x \\ 0 & 1 \end{pmatrix}\right) \cdot [1 : 0 : 1] = [1 : -2x : x^2 + y^2]$ . This is an explicit formula for the inverse of the roots map,  $\mathcal{R}^{-1}: \mathbb{H}_{\text{Roots}}^2 \rightarrow \mathbb{H}_{\text{Coefs}}^2$ , sending the roots  $\{x \pm iy\}$  to the polynomial with (projectivized) coefficients  $[1 : -2x : x^2 + y^2]$ . Inverting the relation  $[1 : -2x : x^2 + y^2] = [a : b : c]$  gives  $x = -b/2a$  and  $y = \sqrt{c/a - x^2}$ , or

$$x + iy = \frac{-b}{2a} + i \frac{\sqrt{4ac - b^2}}{2a}.$$

Theorem 3.9 allows us to compute any geometric quantity of interest using either the roots or coefficients. This simplifies certain calculations. In particular, if  $\alpha, \beta \in \mathbb{C}$  are complex roots of

<sup>18</sup>This is called the Hilbert metric.

the real quadratics  $f_\alpha, f_\beta$  respectively we may avoid using equation (3) to compute  $d_{\text{Roots}}(\alpha, \beta)$ , and instead compute  $d_{\text{Coefs}}(f_\alpha, f_\beta)$  using equation (5). This is used for the results in Section 5.

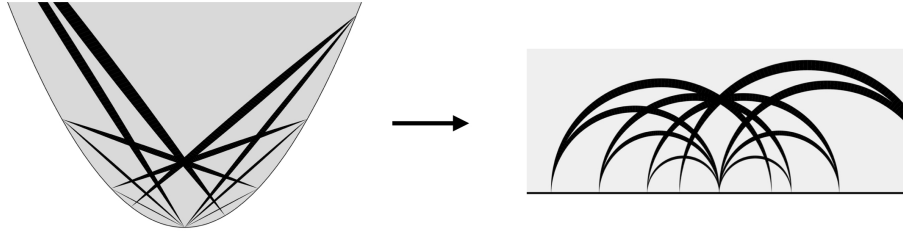


FIGURE 23. Isometry from the projective model  $\{[a : b : c] \mid 4ac > b^2\}$  and the upper half plane model of the hyperbolic plane, given by the quadratic formula.

**Corollary 3.10.** *After the projective change of coordinates  $\mathbb{RP}^2 \rightarrow \mathbb{RP}^2$  given by  $[a : b : c] = [\frac{w+u}{2} : v : \frac{w-u}{2}]$ , the quadratic formula is precisely the usual isometry from the Klein disk model of  $\mathbb{H}^2$  to the upper half plane model,*

$$[u : v : 1] \mapsto \frac{-v \pm i\sqrt{1 - u^2 - v^2}}{1 + u}.$$

Qualitatively, this provides a complete understanding of the roots map<sup>19</sup>: affine lines in the space of coefficients are geodesics in the projective model of  $\mathbb{H}^2$ , and so the roots of such a 1-parameter family of polynomials form a geodesic in the upper half plane model: generalized circles orthogonal to  $\mathbb{R} \subset \mathbb{C}$ .

There is also a very nice geometric interpretation of the roots map for quadratics with two real roots. We do not give many details here, as these quadratics do not occur in the starscape images. Nonetheless, we cannot resist telling the beginning of the story.

**Observation 3.11.** *The roots map for quadratics with a double root is the continuous extension of  $\mathcal{R}: \mathbb{H}_{\text{Coefs}}^2 \rightarrow \mathbb{H}_{\text{Roots}}^2$  to the ideal boundary of the hyperbolic plane. For polynomials of positive discriminant, the roots map decomposes geometrically as follows:*

- (1) *Send the polynomial with coefficient vector  $v = [a : b : c]$ , thought of as a point in the Möbius band  $\mathbb{RP}^2 \setminus \mathbb{H}_{\text{Coefs}}^2$ , to the set  $\{w_1, w_2\} \in \partial_\infty \mathbb{H}^2$ , where the line through  $v$  and  $w_i$  is tangent to the ideal boundary.*
- (2) *Follow by applying to each  $w_i$  the homeomorphism  $\partial_\infty \mathbb{H}_{\text{Coefs}}^2 \rightarrow \partial_\infty \mathbb{H}_{\text{Roots}}^2$  sending the projectivized lightcone to the extended real line in  $\mathbb{CP}^1$ . The resulting two points are the roots of  $f(x) = ax^2 + bx + c$ .*

Using the transitivity of the  $\text{PSL}(2; \mathbb{R})$  action (via  $\rho$ ) on the space of quadratics with positive discriminant, it is enough to check this assertion at a single point. The polynomial  $f(x) = (x+1)(x-1)$  has coefficients  $v = [1 : 0 : -1]$  and roots  $\{1, -1\} \in \mathbb{R}$ . These roots are identified with the polynomials  $(x \pm 1)^2$  on the lightcone, so  $w_i = [1 : \pm 2 : 1]$ , and the lines through  $v$  and  $w_i$  are easily verified to be tangent to the discriminant locus, as claimed.

<sup>19</sup>As particular examples, the 1-parameter families of quadratics with coefficients  $[1 : 0 : t]$ , and  $[1 : t : 1]$  project under the roots map to the vertical geodesic and unit circle through  $i \in \mathbb{C}$  respectively.

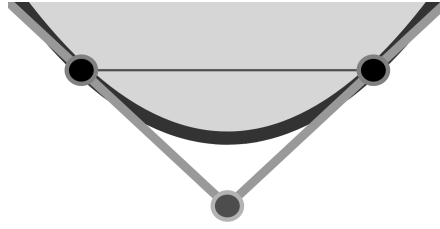


FIGURE 24. The roots map for quadratics with two real roots associates a point exterior to the hyperbolic plane in  $\mathbb{RP}^2_{\text{Coefs}}$  to its two points of tangency with  $\partial_\infty \mathbb{H}^2_{\text{Coefs}}$ .

3.2.5. *Applications to quadratic algebraic numbers.* We now can apply this to the original case of interest: quadratic algebraic numbers and integer quadratic polynomials. The integer polynomials form a  $\mathbb{Z}^3$  lattice in the space  $\mathbb{R}^3$  of coefficients, and its image in  $\mathbb{RP}^2$  can be interpreted as what it would look like to see the integer lattice from the origin (much like we saw for  $\mathbb{QP}^1$  and  $\mathbb{Z}^2$  in Figure 16). The quadratics of interest line inside of the cone cut out by the discriminant, with planes through the origin projecting to lines in the disk  $\mathbb{H}^2_{\text{Coefs}}$ . And, with the roots map an isometry onto the upper half plane model, we know the image of these geodesics are also geodesics - here represented by circles orthogonal to the boundary. This explains the small scale patterns visible everywhere in the picture of the integer quadratic numbers - they are just the perspective view of a cubic lattice, distorted by the isometry taking the Klein model to the upper half plane model.

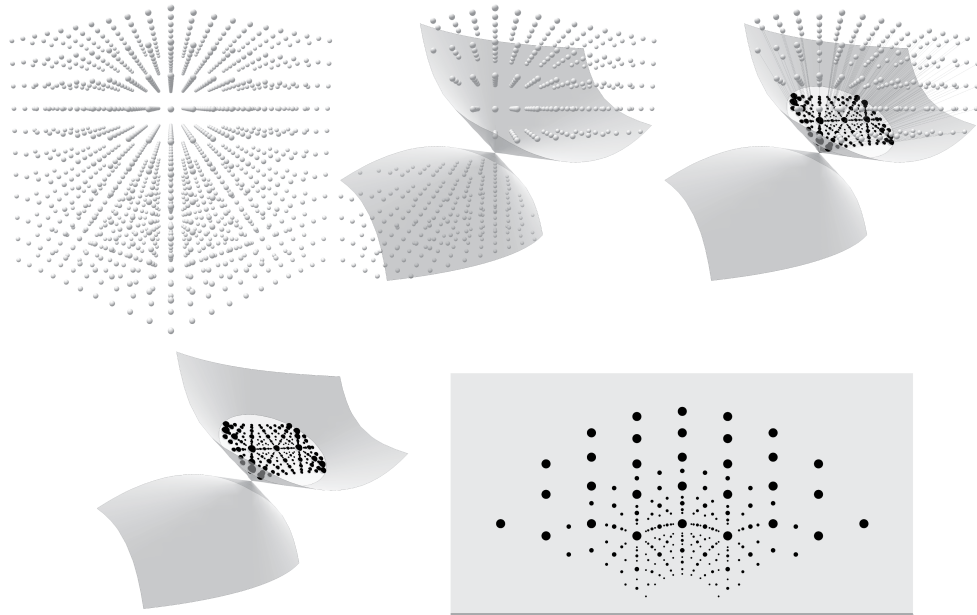


FIGURE 25. The lattice of integer quadratic polynomials, and its image under the roots map, decomposed as a sequence of geometric steps.

The natural  $\mathrm{PSL}(2; \mathbb{C})$  action on roots and coefficients does not preserve the  $\mathbb{Z}^3$  lattice. The subgroup which does is exactly  $\mathrm{PSL}(2; \mathbb{Z})$  (as the intersection of  $\rho(\mathrm{PSL}(2; \mathbb{C}))$  with  $\mathrm{PSL}(3; \mathbb{Z})$ ), and it will play an important role in Sections 4 and 5.

The two-dimensional sublattices of  $\mathbb{Z}^2$  will play a special role in what is to come. The planes such a sublattice can span are exactly planes with rational normal vector. These project to lines in  $\mathbb{H}_{\mathrm{Coefs}}^2$  which we will call *rational geodesics*. These are the dominant features in Figure 1a. There are a few important facts to collect about rational geodesics; these are just immediate consequences of the geometry.

- Observation 3.12.**
- (1) For  $z \in \mathbb{C}$ , its corresponding point  $\{z, \bar{z}\}$  in root space pulls back to  $[1 : -z - \bar{z} : z\bar{z}]$ , and so  $z$  lies on a rational geodesic if and only if  $1, z + \bar{z}$  and  $z\bar{z}$  are  $\mathbb{Q}$ -linearly dependent.
  - (2) Any two quadratic irrationalities  $z, w \in \mathbb{C}$  share a unique rational geodesic, since any two points in  $\mathbb{RP}^2$  determine a unique line. Any quadratic irrationality lies on infinitely many rational geodesics, and any two rational geodesics intersect at a quadratic irrationality.
  - (3) The images of rational geodesics under the roots map are exactly the hyperbolic geodesics of the upper half plane given by the upper half circles centred on a rational number, with rational radius-squared.
  - (4) The  $\mathrm{PSL}(2; \mathbb{Z})$  orbit of any rational geodesic consists of all hyperbolic upper half plane geodesics whose limit points  $\{x, y\} \subset \mathbb{R}$  form a non-rational conjugate pair of points in a real quadratic field  $K$ . In this way the orbits of  $\mathrm{PSL}(2; \mathbb{Z})$  are identified with the ideal classes of real quadratic fields  $K$ .

The last point is a consequence of the observation that  $\mathrm{PSL}(2; \mathbb{Z})$  (and in fact  $\mathrm{PSL}(2; \mathbb{R})$ ) acts on the limit points of geodesics in the usual way, by Möbius transformations on  $\mathbb{CP}^1$ .

The geometric description of the roots map for quadratics with two real roots (Observation 3.11) has a nice interpretation for geodesics. Realizing such a geodesic  $\gamma$  as the intersection of a plane  $\mathcal{S}$  with the cone of positive discriminant, denote the normal to  $\mathcal{S}$  by  $n$  and the endpoints of  $\gamma$  by  $x, y$  on the ideal boundary of  $\mathbb{H}_{\mathrm{Coefs}}^2$  (the projectivized lightcone of the discriminant). Recalling an often-useful fact about the projective model of the  $\mathbb{H}^2$ , the tangent planes to  $\partial_\infty \mathbb{H}_{\mathrm{Coefs}}^2$  at  $x, y$  intersect along  $n$ . By Observation 3.11, the map sending  $n$  to its two points of tangency with  $\partial_\infty \mathbb{H}^2$ , followed by the isometry from the projective to upper half plane model of  $\mathbb{H}^2$  is none other than the roots map on quadratics of positive discriminant. Thus, if we think of a geodesic as determined by its normal vector  $n = (n_2, n_1, n_0)$  (often computationally an attractive thing to do), we may directly recover the geodesic from  $n$  as its endpoints are precisely the roots of  $n_2x^2 + n_1x + n_0 = 0$ . This is visible in Figure 24.

**3.3. Beyond Discworld: The Geometry of Cubics.** Similarly to the quadratic case, we begin with space of all complex binary forms together with the  $\mathrm{PSL}(2; \mathbb{C})$  action arising from precomposition with Möbius transformations. Cubics are the last degree<sup>20</sup> where this action is enough to equip the various open subsets of generic cubics (components of the complement of the discriminant locus) with the structure of homogeneous geometries. Because  $\mathrm{PSL}(2; \mathbb{R})$  is so tightly linked to  $\mathbb{H}^2$ , the hyperbolic plane remains a prominent actor in this story. Indeed, restricting to real cubics with negative discriminant, the complex root determines a point in  $\mathbb{H}^2$  and the real root a direction - identifying this geometry as the unit tangent bundle to the hyperbolic plane. Both the spaces of coefficients and roots form models of this geometry, related by the roots map, resulting in an analogous theorem to Theorem 3.3.

<sup>20</sup>This action has finitely many orbits as  $\mathrm{PSL}(2; \mathbb{C})$  acts simply transitively on ordered triples of distinct elements of  $\mathbb{CP}^1$ . Thus, some of these orbits are open. In higher degree, there are a continuum of orbits, which are parameterized by the moduli of  $n$  possibly indistinct points in  $\mathbb{CP}^1$  up to projective transformations (see also Remark 3.16).

**Theorem 3.13.** *Let  $\text{UTH}_{\text{Coefs}}^2$  be the set of real quadratics with exactly one real root,  $\text{UTH}^2 = \{[a : b : c : d] \mid \Delta_3(a, b, c, d) < 0\}$ , and  $\text{UTH}_{\text{Roots}}^2 = \{\{r, z, \bar{z}\} \mid r \in \mathbb{RP}^1, z \in \mathbb{C} \setminus \mathbb{R}\}$  be the set of their root-sets. Equipped with their natural  $\text{PSL}(2; \mathbb{R})$  actions, each of these is isomorphic to the unit tangent bundle to the hyperbolic plane. The roots map  $\mathcal{R}: \text{UTH}_{\text{Coefs}}^2 \rightarrow \text{UTH}_{\text{Roots}}^2$  is equivariant with respect to these  $\text{PSL}(2; \mathbb{R})$  actions, and thus an isometry.*

Utilizing this geometry both on the spaces of roots and coefficients provides a geometric description of the cubic formula. We state the full version in Theorem 3.23.

**Theorem 3.14.** *The roots map  $\mathcal{R}_{\mathbb{C}}: \mathbb{PCoefs} \rightarrow \mathbb{C}$  returning the complex root of a cubic with real coefficients factors as the projection onto the base of the fiber bundle  $\text{UTH}_{\text{Coefs}}^2 \rightarrow \mathbb{H}_{\text{Coefs}}^2$  under the identification above, followed by the isometry  $\mathcal{R}_2: \mathbb{H}_{\text{Coefs}}^2 \rightarrow \mathbb{H}_{\text{Roots}}^2$  from the projective model to the upper half plane of Theorem 3.9.*

$$\begin{array}{ccccc}
 & & & & \mathcal{R}_{\mathbb{C}} \\
 & & & & \curvearrowright \\
 \mathbb{PCoefs} & \xrightarrow{\cong} & \text{UTH}_{\text{Coefs}}^2 & & \\
 & & \downarrow \pi & & \\
 & & \mathbb{H}_{\text{Coefs}}^2 & \xrightarrow{\mathcal{R}_2} & \mathbb{H}_{\text{Roots}}^2 & \hookrightarrow & \mathbb{C}
 \end{array}$$

Because the space of projectivized cubics with complex roots is three dimensional, there are many interesting 1 and 2 dimensional families, producing linear and planar starscapes respectively. Some such linear starscapes are highlighted in the planar starscapes below (Figure 26). We use the geometry of the unit tangent bundle to study these 1 and 2 dimensional families of cubics, and in particular give a simple condition for when a starscape embeds in the complex plane under the projection onto the complex root (Figure 26a) and when it is singular, collapsing some curve to a point (Figure 26b).

**Corollary 3.15.** *Let  $\mathcal{S} \subset \text{UTH}_{\text{Coefs}}^2$  be a one or two dimensional affine plane of real cubics in the space of projectivized coefficients, and  $\mathcal{R}|_{\mathcal{S}}: \mathcal{S} \rightarrow \mathbb{C}$  the projection onto the complex root. Then  $\mathcal{R}|_{\mathcal{S}}$  is an embedding if and only if  $\mathcal{S}$  is everywhere transverse to the fibers of the unit tangent bundle.*

For this failure of embedding to actually be *visible* in a cubic starscape, it must occur at some cubic or quadratic number, and accounting for this gives the more refined statement of Corollary 3.26. Quadratics are too low-degree for any interesting analogs of this behavior to occur<sup>21</sup>, but it persists in higher degree (Figure 2), making cubics an important testing ground. We fill in the details of this picture below.

**3.3.1. General Complex and Real Coefficients.** A homogeneous cubic in two variables has the form  $ax^3 + bx^2y + cxy^2 + dy^3$ , so the sets of coefficients of all such cubics naturally identifies with  $\mathbb{C}^4$ . As previously, we are mostly concerned with cubics only up to a global scaling, and so take the space of projectivized coefficients  $\mathbb{PCoefs} = \mathbb{CP}^3$ , together with the natural action of  $\text{PSL}(4; \mathbb{C})$  as our starting point.

From the perspective of their solutions, cubics may be identified with unordered triples of (possibly coincident) points in the extended complex plane, so  $\text{Roots} = \text{SP}^3(\mathbb{CP}^1)$  is the third symmetric power of the sphere. The symmetric power admits a natural action of  $\text{PSL}(2; \mathbb{C})$  coming directly from its usual action on  $\mathbb{CP}^1$  by Möbius transformations. More precisely, the action of  $A = \begin{pmatrix} p & q \\ r & s \end{pmatrix}$  on the triple of points  $\{z_1, z_2, z_3\}$  is

<sup>21</sup>For quadratics, the roots map is a homeomorphism on the entire space: there are no 2-dimensional subfamilies, and all 1-dimensional curves are geodesics.

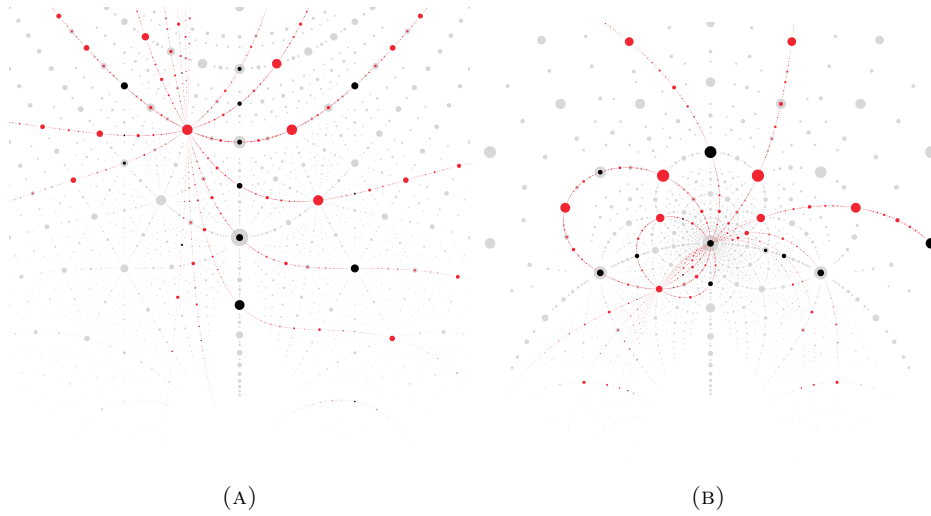


FIGURE 26. Some linear starscapes. In (26a) some of the lines through the root of  $x^3 - 2x^2 + 1$  are plotted in the depressed cubic starscape (also shown in Figure 2a). In (26b) some of the lines through the root of  $x^3 - x^2 - 1$  are plotted in the starscape for the family  $ax^3 + cx^2 + bx + c$  (also shown in Figure 1b). In the latter, these lines all also pass through  $i$ , which is the projection of a fibre  $(dx + e)(x^2 + 1) = dx^3 + ex^2 + dx + e$ . This can be seen in a different way in Figure 30a.

$$A.\{z_1, z_2, z_3\} = \left\{ \frac{pz_1 + q}{rz_1 + s}, \frac{pz_2 + q}{rz_2 + s}, \frac{pz_3 + q}{rz_3 + s} \right\}. \quad (6)$$

Again, the roots map  $\mathcal{R}: \mathbb{P}\text{Coefs} \rightarrow \text{Roots}$  realizes a homeomorphism from  $\mathbb{P}\text{Coefs} = \mathbb{C}\mathbb{P}^3$  to  $\text{Roots} = \text{SP}^3(\mathbb{C}\mathbb{P}^1)$ . Conjugating the  $\text{PSL}(2; \mathbb{C})$  action on  $\text{Roots}$  by  $\mathcal{R}$  gives an action on  $\mathbb{P}\text{Coefs}$ , which is compatible with its natural  $\text{PSL}(4; \mathbb{C})$  action: it is the projectivization of the irreducible representation  $\text{SL}(2; \mathbb{C}) \rightarrow \text{SL}(4; \mathbb{C})$ . As in Section 3.2.2, the explicit formula for this representation is defined by  $\rho(A).f(x) = f(A^{-1}.x)$ :

$$\begin{pmatrix} p & q \\ r & s \end{pmatrix} \xrightarrow{\rho} \begin{pmatrix} s^3 & -rs^2 & r^2s & -r^3 \\ -3qs^2 & 2qrs + ps^2 & -qr^2 - 2prs & 3pr^2 \\ 3q^2s & -q^2r - 2pqs & 2pqr + p^2s & -3p^2r \\ q^3 & pq^2 & -p^2q & p^3 \end{pmatrix} \quad (7)$$

This  $\text{PSL}(2; \mathbb{C})$  action divides the space of cubic polynomials into three components: cubics with three distinct roots, cubics with a pair of coincident roots, and cubics with a triple root. As each component is an orbit of the action,  $\text{PSL}(2; \mathbb{C})$  acts transitively on each.

*Remark 3.16.* Here the (real) dimension of the space of homogeneous cubics is 6, which coincides with the dimension of  $\text{PSL}(2; \mathbb{C})$ . Thus, cubics are the last dimension on which this  $\text{PSL}(2; \mathbb{C})$  action remains transitive on the open subset of generic cubics, giving it the structure of a  $\text{PSL}(2; \mathbb{C})$  homogeneous space.

Restricting to real cubics replaces the space of coefficients  $\mathbb{C}\mathbb{P}^3$  with  $\mathbb{R}\mathbb{P}^3$ , and its image under the roots map is an embedding of real projective 3-space in  $\text{SP}^3(\mathbb{C}\mathbb{P}^1)$ . The restricted  $\text{PSL}(2; \mathbb{R})$  action divides  $\mathbb{R}\mathbb{P}^3$  into four components. The discriminant locus  $\Delta^0 := \mathbb{P}\Delta^{-1}(0)$  consists of the

union of the orbits with triple and double roots, and is homeomorphic to a torus<sup>22</sup>. Over  $\mathbb{R}$  the generic case splits into polynomials with three distinct real roots  $\Delta^+$  (positive discriminant) and those with a complex conjugate pair of complex roots  $\Delta^-$  (negative discriminant). We see below each of  $\Delta^\pm$  are individually homeomorphic to a solid torus, forming the standard Heegaard decomposition of  $\mathbb{RP}^3$ .

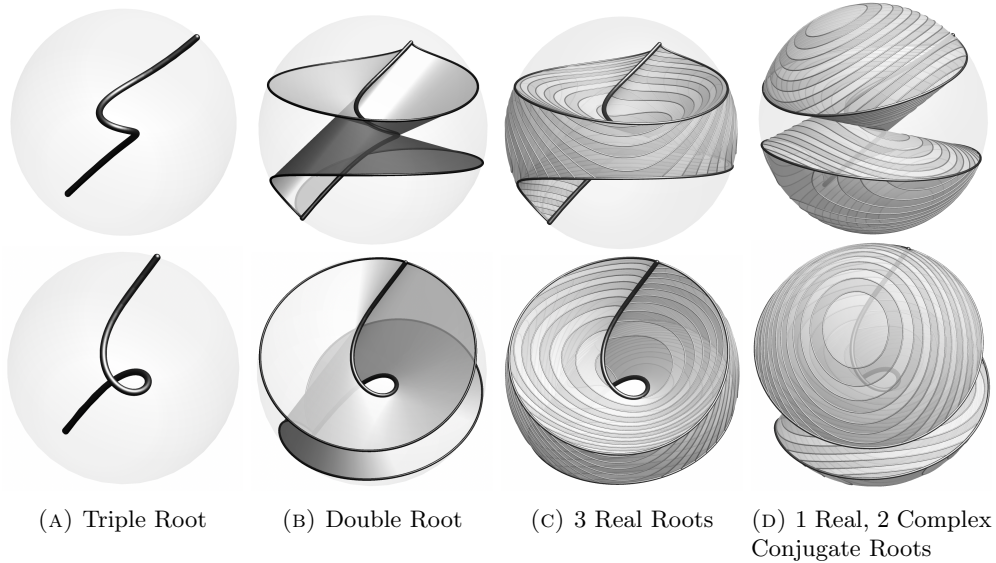


FIGURE 27. The four  $\mathrm{PSL}(2; \mathbb{R})$  orbits on the  $\mathbb{RP}^3$  of real cubics, as subsets of  $\mathbb{RP}^3$ . As in Figure 17, the topology of each component is recovered by identifying points on the boundary sphere via the antipodal map.

The action of  $\mathrm{PSL}(2; \mathbb{R})$  is transitive on all four components, so we may consider each as a homogeneous geometry. Like in the complex case, via dimension count we see that  $\dim \Delta^+ = \dim \Delta^- = \dim \mathrm{PSL}(2; \mathbb{R})$ , so this action has at most a discrete stabilizer. For  $\Delta^+$ , this stabilizer is the symmetric group on three elements<sup>23</sup>, as  $\mathrm{PSL}(2; \mathbb{R})$  acts simply transitively on the space of ordered distinct triples in  $\mathbb{RP}^1$ . For  $\Delta^-$  however, this action is free. In the following section we look in detail at this geometry both from the coefficients and roots perspectives.

3.3.2. *Cubics and the Unit Tangent bundle to  $\mathbb{H}^2$* . Each cubic in  $\Delta^-$  has a real root and complex conjugate pair of complex roots. The image under  $\mathcal{R}$  in  $\mathrm{SP}^3(\mathbb{CP}^1)$  is easily described, as

$$\mathcal{R}(\Delta^-) = \{ \{r, z, \bar{z}\} \mid r \in \mathbb{RP}^1, z = x + iy \text{ for } x, y \in \mathbb{R}, y > 0 \}.$$

This is exactly an embedding of the product of  $\mathbb{RP}^1$  and the upper half plane in  $\mathrm{SP}^3(\mathbb{CP}^1)$ , so this describes the homeomorphism of  $\Delta^-$  with a solid torus, as observed in Figure 27d. As  $z$  is a point in the upper half plane being acted on by  $\mathrm{PSL}(2; \mathbb{R})$  it is tempting to think of it as a point of  $\mathbb{H}^2$ . From this perspective, the real root  $r \in \mathbb{RP}^1$  lies on the ideal boundary of the upper half plane model of  $\mathbb{H}^2$ , so we may think of it as specifying a *direction*. We make this precise in the following proposition, which is the first half of Theorem 3.14 highlighted in the introduction to this section.

<sup>22</sup>Note this torus is not smoothly embedded in the space of coefficients, and is singular along the  $\mathbb{RP}^1$ 's worth of cubics with a triple root.

<sup>23</sup>Thus the space of cubics with three distinct roots is an infinite volume three dimensional orbifold with a geometric structure modeled on  $\widetilde{SL}_2(\mathbb{R})$

**Proposition 3.17.** *The space of roots of cubics in  $\Delta^-$  naturally identifies with the unit tangent bundle to the hyperbolic plane  $\text{UT}\mathbb{H}^2$ .*

*Proof.* The space  $\mathcal{R}(\Delta^-)$  is given by pairs  $\{z, \bar{z}, r\}$  for  $z \in \mathbb{H}^2, r \in \partial_\infty \mathbb{H}^2$  as noted above. The unit tangent bundle  $\text{UT}\mathbb{H}^2$  is the collection of all unit vectors based at all points of the hyperbolic plane,  $\text{UT}\mathbb{H}^2 = \{v \in T_z \mathbb{H}^2 \mid z \in \mathbb{H}^2, \|v\| = 1\}$ . We may specify a homeomorphism  $\Phi: \mathcal{R}(\Delta^-) \rightarrow \text{UT}\mathbb{H}^2$  geometrically, as follows. To each triple  $\{r, z, \bar{z}\}$ , we associate the unit tangent vector  $v \in T_z \mathbb{H}^2$  such that  $v$  is the initial tangent vector to the geodesic ray  $\gamma$  starting at  $z$  and limiting to the ideal point  $r = \gamma(+\infty)$ .

To see this is an isomorphism of geometries, we must further show the natural actions of  $\text{PSL}(2; \mathbb{R})$  are preserved by  $\Phi$ . That is, we need that  $A.\Phi(\{z, \bar{z}, r\}) = \Phi(A.\{z, \bar{z}, r\})$  for all  $A \in \text{PSL}(2; \mathbb{R})$  and all points of  $\mathcal{R}(\Delta^-)$ . The action on  $\mathcal{R}(\Delta^-)$  is given by equation (6), where  $A$  acts on both  $z, r$  by the same Möbius transformation of  $\mathbb{C}\mathbb{P}^1$ . The action on  $\text{UT}\mathbb{H}^2$  is given by the differential of its action on  $\mathbb{H}^2$  by isometries. The compatibility of these actions follows immediately from the fact that geodesics (and thus their endpoints at infinity) are determined by their initial conditions. That is,  $\Phi(\{A.z, A.\bar{z}, A.r\})$  is the tangent vector based at  $A.z$  pointing in the direction of  $A.r$ , which is the image of the tangent vector  $\Phi(\{z, \bar{z}, r\})$  under  $A$ , by existence and uniqueness of solutions to the geodesic equation.  $\square$

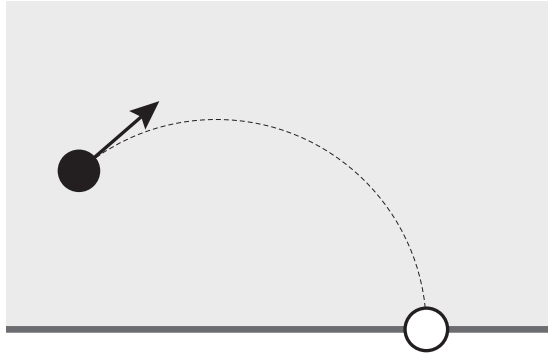


FIGURE 28. Cubic on upper halfplane (black point) and the real conjugate (white point), showing the geodesic between them and the direction from the complex root looking along the geodesic to the real root.

From now on, we will denote this collection of polynomials as  $\mathcal{R}(\Delta^-) = \text{UT}\mathbb{H}^2_{\text{Roots}}$ , to emphasize this geometric structure. This provides a nice way of thinking about the space of roots, avoiding the complicated space  $\text{SP}^3(\mathbb{C}\mathbb{P}^1)$  in which it was originally defined.

The upper half plane model of  $\mathbb{H}^2$  is a subset of  $\mathbb{C}\mathbb{P}^1$ , so the map  $\Phi$  in Proposition 3.17 above explicitly identifies  $\mathcal{R}(\Delta^-)$  with a subset of  $\text{UTC}\mathbb{P}^1$ . But, as  $\mathbb{C}\mathbb{P}^1$  is topologically the 2-sphere (Remark 3.2),  $\text{UTC}\mathbb{P}^1$  is just the unit tangent bundle of the sphere<sup>24</sup>, which is topologically  $\mathbb{R}\mathbb{P}^3$ . As the space of coefficients is naturally a subset of  $\mathbb{R}\mathbb{P}^3$ , this provides a uniform means of drawing both spaces, see Figures 29a and 31.

To make use of this geometry in our analysis of cubics, we recall some facts about the hyperbolic plane's tangent bundle. First, the circle of unit tangent vectors at each point provides a foliation by circles: every point of  $\text{UT}\mathbb{H}^2$  is the unit tangent vector to *some unique point* of  $\mathbb{H}^2$  and thus lies on a unique one of these circles. But we may also define a collection of sections of  $\mathbb{H}^2 \rightarrow \text{UT}\mathbb{H}^2$  of the unit tangent bundle such that every point lies on exactly one such

<sup>24</sup>One shows the isometries of  $\mathbb{S}^2$  act freely and transitively on the unit tangent bundle, which then provides a diffeomorphism from  $\text{Isom}(\mathbb{S}^2) = \text{SO}(3)$  and  $\text{UT}\mathbb{S}^2$ . Finally, we recall that  $\text{SO}(3)$  is topologically real projective 3-space (perhaps by noting that it is double covered by  $\text{SU}(2) \cong \mathbb{S}^3$ ).

hyperbolic plane. For a given ideal point  $r \in \partial_\infty \mathbb{H}^2$ , at each  $z \in \mathbb{H}^2$  we select the unit vector  $v_r \in T_z \mathbb{H}^2$  which points<sup>25</sup> to  $r$ . This mapping  $z \mapsto v_r \in T_z \mathbb{H}^2$  provides one such section, and varying  $r \in \partial_\infty \mathbb{H}^2$  foliates the unit tangent bundle with translates of this. These foliations have direct algebraic interpretations as well.

**Observation 3.18.** *The foliation of  $\text{UTH}_{\text{Roots}}^2$  by circles (the fibers of the bundle) correspond to collections of cubics with a fixed complex root, as the real root varies. Conversely, the foliation by hyperbolic planes corresponds to fixing the real root and letting the complex conjugate roots vary over  $\mathbb{C} \setminus \mathbb{R}$ .*

Together, these foliations provide a *trivialization* of the unit tangent bundle: an explicit choice of homeomorphism  $\text{UTH}^2 \rightarrow \mathbb{H}^2 \times \mathbb{S}^1$ , sending each  $v \in \text{UTH}^2$  to its basepoint  $z \in \mathbb{H}^2$ , and the angle  $\theta$  that  $v$  makes with respect to the direction field associated with some fixed ideal point. Working in the upper half plane model, it is easiest to choose this as the direction field associated to  $\infty$ ; as in the euclidean coordinates  $z = x + iy$  this is simply the direction made with the vertical at every point. Explicitly, the point  $(z, r)$  in the space of roots, identified with the unit tangent vector  $v \in T_z \mathbb{H}^2$ , is sent to  $(z, \theta)$  for

$$\theta = 2 \arctan \left( \frac{r - x}{y} \right). \quad (8)$$

*Remark 3.19.* Using a Möbius transformation to send the upper half plane to the unit disk, we may represent the space of roots as the interior of a solid torus of revolution in  $\mathbb{R}^3$ , as in Figure 29b. This homeomorphism provides the beautiful pictures visible in Figure 10 produced by David Dumas' wonderful program.

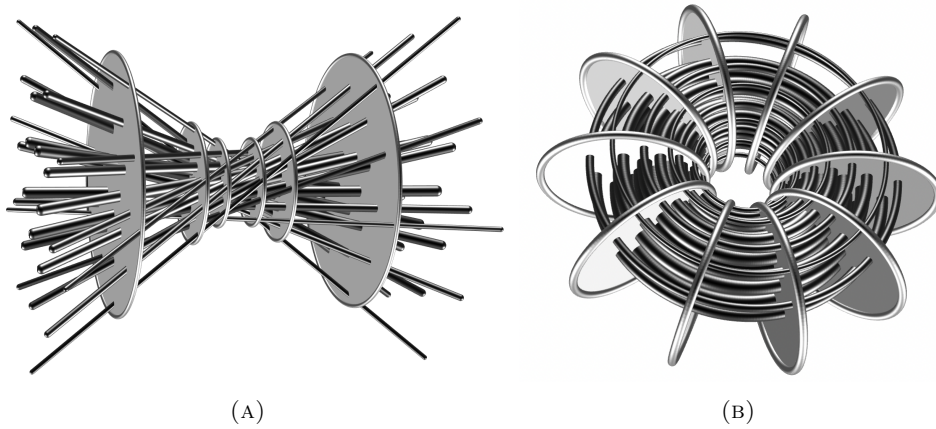


FIGURE 29. Foliation of  $\text{UTH}_{\text{Roots}}^2$  by circles and hyperbolic planes. In (A) we view  $\text{UTH}_{\text{Roots}}^2$  in an affine patch of  $\text{UTC}\mathbb{P}^1 = \mathbb{R}\mathbb{P}^3$ , where the hyperbolic foliation is visible as parallel disks. In (B), it is realized as the interior of a torus of revolution in  $\mathbb{R}^3$  via Remark 3.19.

*Remark 3.20.* This also provides the means to represent cubics literally as unit tangent vectors in  $\mathbb{H}^2$ : As  $\theta$  is measured with respect to geodesics limiting to  $\infty$  in the upper half plane, we may depict the cubic with roots  $\{z, \bar{z}, r\}$  by the unit vector at  $z$  pointed along the geodesic<sup>26</sup> to  $r$ . As this depicts a 3-dimensional space using 2-dimensions, we cannot understand the entire space

<sup>25</sup>That is, choose  $v$  so that the geodesic  $\gamma_v$  with initial tangent  $v$  at  $z$  has  $\lim_{t \rightarrow \infty} \gamma(t) = r$ .

<sup>26</sup>Using the coordinates  $z = x + iy$  on the upper half plane, this vector is in the direction in direction  $(2y(r - x), (r - x)^2 - y^2)$ .

of cubics this way - however it provides a useful means of looking at 2-dimensional families, such as Figure 30.

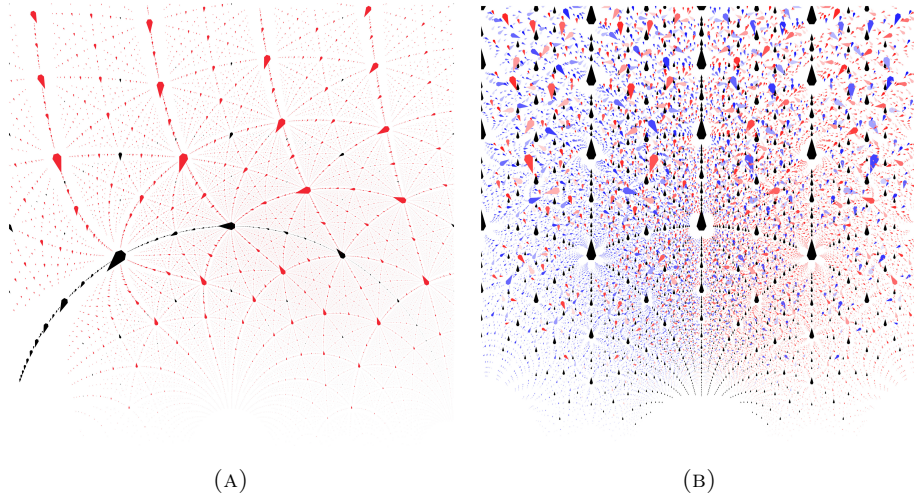


FIGURE 30. Cubic numbers as a vector field, as shown in Figure 28. The roots of the polynomial family  $ax^3 + bx^2 + cx + a$  (30a), and all cubics (30b).

We next turn to the description of this geometry on the space of coefficients, which we likewise denote  $\text{UTH}_{\text{Coefs}}^2$ . Here, the surface cut out by the discriminant represents the ideal boundary of the geometry, whose points correspond to the polynomials with negative discriminant, depicted in Figure 27d. The important geometric information is a description of the  $\mathbb{S}^1$  fibers, which provide the structure of the unit tangent bundle, and a choice of section  $\mathbb{H}^2 \rightarrow \text{UTH}_{\text{Coefs}}^2$  giving a trivialization. Via Observation 3.18, the choice made in the roots model has a convenient description in terms of their corresponding polynomials, which we summarize below.

**Observation 3.21.** *The trivialization in Observation 3.18 is expressed in the space of coefficients as:*

- *Each fiber of the  $\mathbb{S}^1$  foliation passes through a unique cubic with real root at infinity, identified with the quadratic  $ax^2 + bx + c \in \mathbb{H}^2$ . The fiber passing through this point is parameterized by  $[a : b - ra : c - rb : rc]$  in the space of coefficients, for  $r \in \mathbb{RP}^1 = \mathbb{R} \cup \{\infty\}$ .*
- *Each fiber of the  $\mathbb{H}^2$  foliation has constant real root  $r \in \mathbb{RP}^1$ . This fiber is parameterized by  $[1 : -2u - r : 2ru - u^2 - v^2 : -ru^2 - rv^2]$  for  $u, v \in \mathbb{R}, v > 0$  representing the varying complex root  $u + iv \in \mathbb{H}^2$ .*

As in the quadratic case, the natural geometry is more difficult to see at first from the coefficient perspective. However, drawing  $\text{UTH}_{\text{Coefs}}^2$  in the affine patch which puts quadratics at infinity, we see the hyperbolic foliation consists of copies of the now familiar *parabola model* of  $\mathbb{H}^2$ . Choosing other affine patches may render (some of) these as copies of the more familiar Klein disk model. These two foliations of the space of cubics, by hyperbolic planes and by circles, provide convenient means of keeping track of information about cubics. We see some examples of this below as we seek a geometric understanding of the roots map.

**3.3.3. Geometry of the Roots Map.** The roots map  $\mathcal{R}: \mathbb{P}\text{Coefs} \rightarrow \text{Roots}$  restricts to the space of real cubics of negative discriminant to a homeomorphism  $\text{UTH}_{\text{Coefs}}^2 \rightarrow \text{UTH}_{\text{Roots}}^2$  equivariant with respect to the  $\text{PSL}(2; \mathbb{R})$  actions given by equations (6) and (7). Thus  $\mathcal{R}$  is an isomorphism

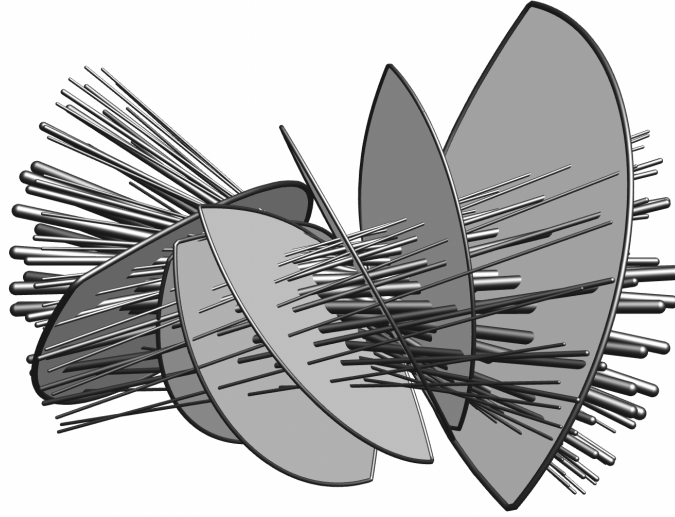


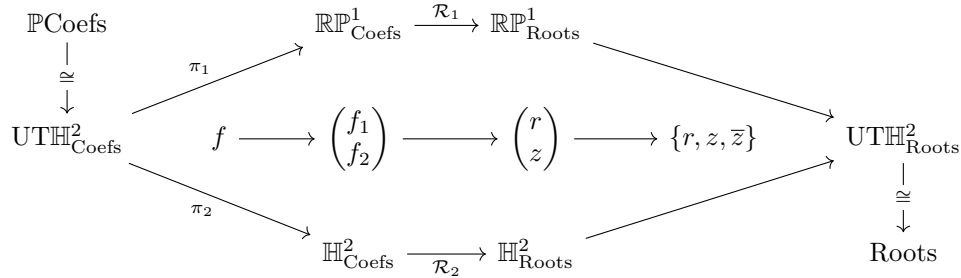
FIGURE 31. Foliation of  $\text{UTH}^2_{\text{Coefs}}$  by hyperbolic planes and circle fibers

of geometries, giving the second half of theorem Theorem 3.14 highlighted at the beginning of this section.

**Proposition 3.22.** *Let  $\text{UTH}^2_{\text{Coefs}}$  be the set of real quadratics with exactly one real root,  $\text{UTH}^2 = \{[a : b : c : d] \mid \Delta_3(a, b, c, d) < 0\}$ , and  $\text{UTH}^2_{\text{Roots}} = \{\{r, z, \bar{z}\} \mid r \in \mathbb{RP}^1, z \in \mathbb{C} \setminus \mathbb{R}\}$  be the set of their root-sets. Equipping each with the  $\text{PSL}(2; \mathbb{R})$  metric identifying them with the unit tangent bundle to the hyperbolic plane, the roots map  $\mathcal{R}: \text{UTH}^2_{\text{Coefs}} \rightarrow \text{UTH}^2_{\text{Roots}}$  is an isometry.*

For the quadratics, the space of roots was already naturally a subset of the complex plane, and the roots map identified as a familiar isometry. Here, while the analogous theorem again follows for free from the  $\text{PSL}(2; \mathbb{R})$  action, we need a more in depth analysis to provide useful information relating metric properties of complex cubic numbers to their minimal polynomials. A first step in this direction is to take a more detailed look at the roots map itself.

**Theorem 3.23.** *The roots map  $\mathcal{R}: \mathbb{PCoefs} \rightarrow \text{Roots}$ , restricted to the space  $\text{UTH}^2_{\text{Coefs}}$  of real cubics with negative discriminant, factors as  $\mathcal{R}_3 = (\mathcal{R}_1, \mathcal{R}_2) \circ (\pi_1, \pi_2)$  where  $\pi = (\pi_1, \pi_2)$  is the trivialization of the unit tangent bundle given by the foliations by circles, hyperbolic planes respectively in Observation 3.21, and  $\mathcal{R}_1, \mathcal{R}_2$  are the root maps for linear and quadratic polynomials. This is best seen diagrammatically, compare the commutative diagram below with Figure 32.*



*Proof.* This is not deep, and follows directly from our geometric interpretations of the space of quadratic and linear polynomials. As isometries of  $\text{UTH}^2$  preserve the fiber bundle structure,

$\mathcal{R}$  preserves the  $\mathbb{R}P^1$  foliation, and similarly the  $\mathbb{H}^2$  foliation described in Observations 3.18 and 3.21. By Observation 3.18, we may identify these foliations with the preimages of projections  $\pi_1, \pi_2$  onto the linear and irreducible quadratic factors respectively. As these are preserved by the roots map,  $\mathcal{R}_3$  factors through the trivialization  $\pi$  to a pair of maps sending these factors to their roots. But these are already familiar: they are just the lower dimensional roots maps  $\mathcal{R}_1$  and  $\mathcal{R}_2$ . □

The bottom row of this diagram gives the formula for the complex root as in Theorem 3.14; the top row gives the analog returning the real root. Choosing to identify the base  $\mathbb{H}^2_{\text{Coefs}}$  with one of the sections of Observation 3.21, one may see the solution to the cubic as a *process* as follows. (For simplicity of exposition, we identify it with the fiber of cubics with real root zero here.) Starting with a point  $f \in \text{UTH}^2_{\text{Coefs}}$  (recall Figure 31 as a visual aid here), we slide along the fiber through  $f$  until reaching the hyperbolic sheet specified by the section. The real root is given by the distance traveled along this fiber, and the complex root is given by taking the resulting point, which is now a cubic of the form  $(ax^2 + bx + c)x$  and applying the isometry from the parabola model of  $\mathbb{H}^2$  in  $[a : b : c]$  to the upper half plane.

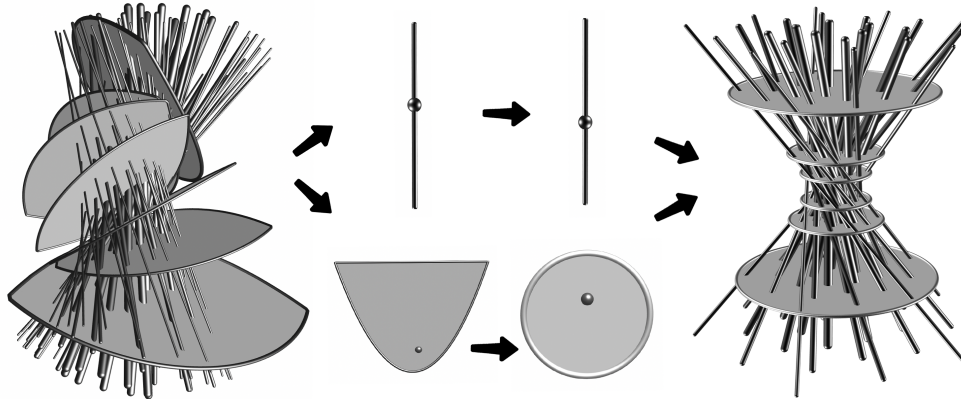


FIGURE 32. Geometric factoring of the roots map  $\mathcal{R}_3: \text{UTH}^2_{\text{Coefs}} \rightarrow \text{UTH}^2_{\text{Roots}}$  of Theorem 3.23, using the root maps  $\mathcal{R}_1, \mathcal{R}_2$  of lower degrees. Compare with the diagram in Theorem 3.23.

*Remark 3.24.* One may derive an expression for the cubic formula from this procedure, similarly to what was done in Remark 3.10, using the parameterization of the  $\mathbb{R}P^1, \mathbb{H}^2$  factors in Observation 3.21 and attempting to invert their dependence of the coefficients  $[a : b : c : d]$  on the parameters  $u, v$ . Of course, the inherent messiness of the cubic formula must make this challenging at some point, which we can now specify: it lies in giving explicit formulas for the projections of  $\text{UTH}^2_{\text{Coefs}}$  onto its foliations<sup>27</sup>.

3.3.4. *Applications to Cubic Numbers.* When reasoning about cubic numbers, we often want to deal just with the points in  $\mathbb{C}$  themselves, and not the abstract space of roots. Thus, from the perspective of polynomials, we are interested in the image of the *projection*  $\text{UTH}^2_{\text{Roots}} \rightarrow \mathbb{H}^2_{\text{Roots}} \subset \mathbb{C}$ , not the space of roots itself. This is yet another place where the circle and

<sup>27</sup>In light of Theorem 3.23 it cannot be anywhere else: as the only remaining portion to the cubic formula from this perspective is to solve the associated quadratic and linear equations: both of which have simple roots maps as we have seen before.

hyperbolic fibrations of the space of cubics are important, as they are respectively the kernel and 1-eigenspaces of the differential of this projection, respectively.

One place this may arise is in trying to bound distances between cubic numbers. Thus, to control distances between cubic numbers in terms of their minimal polynomials, we do not need to use a full expression<sup>28</sup> for the unit tangent bundle metric on  $\text{UTH}_{\text{Coefs}}^2$  but rather just a means of measuring the hyperbolic distance between their projections to the base  $\mathbb{H}^2$ . While abstractly this is given exactly by the pull back of the metric on  $\mathbb{H}_{\text{Coefs}}^2$  by the bundle projection  $\text{UTH}^2 \rightarrow \mathbb{H}^2$ , any sufficiently simple expression for this would hopefully make some of the analysis of Section 5 in the quadratic case extendable to cubics.

Another place this arises is in the study of one and two parameter families of cubics. Let  $F: \mathbb{R}^n \rightarrow \mathbb{P}\text{Coefs}$  be a smooth map for  $n \in \{1, 2\}$  tracing out a submanifold of the space of cubics. A natural question for the production of good images, is when does the result of drawing the complex root of each polynomial in the family produce a coherent image in  $\mathbb{C}$ : that is, when is the composition  $\mathcal{R}_{\mathbb{C}} \circ F$  a homeomorphism onto its image? Given that on the space of roots, the projection onto the complex root is directly collapsing the  $\mathbb{RP}_{\text{Roots}}^1$  factor, we recall  $\mathcal{R}_{\mathbb{C}}$  is the projection along the  $\mathbb{RP}^1$  fibers of Observation 3.21, followed by an isometry. This gives an explicit condition on  $F$ .

**Observation 3.25.** *Let  $F: \mathbb{R}^n \rightarrow \text{UTH}_{\text{Coefs}}^2$  be a family of real cubics in the space of projectivized coefficients, for  $n \in \{1, 2\}$ . Then the map  $\mathcal{R}_{\mathbb{C}} \circ F$  sending a cubic to its complex root is an embedding if  $F$  is everywhere transverse to the  $\mathbb{RP}^1$  fibration of  $\text{UTH}_{\text{Coefs}}^2$ .*

Restricting attention to planar starscapes, the relevant families  $F: \mathbb{R}^2 \rightarrow \mathbb{RP}^3$  are those whose image is some affine plane  $\mathcal{S} \subset \mathbb{RP}^3$  (that is, the projectivization of some  $\mathbb{R}^3$  through the origin) intersected with the space of cubics of negative discriminant, as in Corollary 3.15 highlighted in the introduction to this section. Examples include the accompanying figure (26) as well as the gallery Figures 2a, 2b and 7a-7d. The fiber above any point  $r \in \mathbb{C}$  is a line  $(\mathcal{R}_2\pi_2)^{-1}(r) = L_r$  (parameterized as in Observation 3.21), thus any affine plane  $\mathcal{S} \subset \text{UTH}_{\text{Coefs}}^2$  containing  $L_r$  fails to embed under projection onto the complex root. As we may find an affine plane containing any projective line we like, this can happen at any point in the upper half plane. However, the restriction from general 2-dimensional families to affine planes greatly restricts the prevalence of this behavior. The fibers of  $\text{UTH}_{\text{Coefs}}^2$  are pairwise skew lines in  $\mathbb{RP}^3$ , and thus no two are ever contained in a plane.

**Corollary 3.26.** *Let  $\mathcal{S} \subset \text{UTH}_{\text{Coefs}}^2$  be an affine 2-dimensional projective subspace, and  $\mathcal{R}|_{\mathcal{S}}: \mathcal{S} \rightarrow \mathbb{C}$  be the projection onto the complex root. Then  $\mathcal{R}|_{\mathcal{S}}$  is singular along at most one projective line  $L \subset \mathcal{S}$ . Furthermore, for a planar starscape (i.e.  $\mathcal{S}$  has rational normal vector), this line, if it exists, corresponds to a rational polynomial with a linear factor over  $\mathbb{Q}$  (i.e. a quadratic point in the complex plane). Finally, every such polynomial gives a singularity for  $\mathcal{R}_{\mathcal{S}}$  for some planar starscape  $\mathcal{S}$ .*

To see the statement that the line lies over a quadratic point, suppose the projective line corresponds to roots  $\{r, z, \bar{z}\}$ , where  $r$  is the varying real root, while  $z$  and  $\bar{z}$  are fixed. Then the projective line has an expression as

$$[1 : -z - \bar{z} - r : z\bar{z} + (z + \bar{z})r : -z\bar{z}r]. \quad (9)$$

<sup>28</sup>While the Riemannian metric here is easy to describe by translating the standard euclidean metric on some tangent space to a point  $p \in \text{UTH}_{\text{Coefs}}^2 \subset \mathbb{RP}^3$  around by action given by the representation  $\rho$ , its expression is complicated, making the computation of a distance function unwieldy.

If this lies in a planar starscape, then it lies in a projective plane with rational normal, i.e. there is a rational vector  $[r : s : t : u]$  such that

$$\begin{pmatrix} 1 & -z - \bar{z} & z\bar{z} & 0 \\ 0 & 1 & -z - \bar{z} & z\bar{z} \end{pmatrix} \begin{pmatrix} r \\ s \\ t \\ u \end{pmatrix} = 0.$$

In particular, this implies  $1$ ,  $z + \bar{z}$  and  $z\bar{z}$  are  $\mathbb{Q}$ -linearly dependent. If they have rank two, then this implies that  $[r : s : t] = [s : t : u]$ , which implies  $[r : s : t : u]$  has the form  $[1 : x : x^2 : x^3]$ ; this further implies  $z$  is rational (as the projective line in coefficient space has a fixed rational root  $x$ ). If they have rank one, then  $z$  lies on the intersection of two rational geodesics, i.e. is quadratic (see Observation 3.12).

For the final statement, suppose the projective line  $L$  is as in (9) above. Then it lies on infinitely many rational geodesics; taking any two will span an appropriate  $\mathcal{S}$ .

#### 4. DIOPHANTINE APPROXIMATION

**4.1. Classical Diophantine Approximation.** The study of Diophantine approximation is the study of the relative placement of real or complex numbers with regards to their arithmetic complexity. To illustrate, we consider the unit interval  $[0, 1]$ . We measure the complexity of a rational number  $p/q$  in lowest terms by its denominator, defining its *height* to be  $q$ . Then we observe a fundamental phenomenon one might call **repulsion**: distinct rationals of low height cannot be too close to one other. Explicitly,

$$\left| \frac{p_1}{q_1} - \frac{p_2}{q_2} \right| \geq \frac{1}{q_1 q_2}. \quad (10)$$

This leads one to consider the question of **good approximations**: fix  $\alpha \in [0, 1]$  and ask whether there are rational  $p/q$  which are surprisingly close to  $\alpha$ , in terms of their height. One asks whether there are infinitely or finitely many  $p/q$  such that

$$\left| \alpha - \frac{p}{q} \right| < \frac{1}{q^k}. \quad (11)$$

It turns out that  $k = 2$  is a natural cusp in regards to this behaviour. For  $k < 2$  (a looser condition), there are always infinitely many *good approximations* in the sense of (11). However, there are numbers for which, with  $k = 2$ , there are only finitely many.

**Theorem 4.1** (Dirichlet [18]). *Let  $\alpha \in \mathbb{R}$ . Then  $\alpha$  is irrational if and only if there exist infinitely many distinct  $p/q \in \mathbb{Q}$  such that*

$$|\alpha - p/q| < 1/q^2.$$

In other words, rationals are “poorly approximable” and irrationals are “well approximable.” This can be proven by a simple pigeonhole principle argument, which we include here for the sake of exposition, as later proofs will imitate the method.

*Proof.* Choose an integer  $Q > 1$ . Divide the unit interval  $[0, 1]$  into  $Q$  even subintervals. Then, among the real numbers  $0, \alpha, 2\alpha, \dots, Q\alpha$ , there must be two, say  $i\alpha$  and  $j\alpha$ , where  $0 \leq i < j \leq Q$ , whose fractional parts fall into the same subintervals. Then we have  $|(j-i)\alpha - p| < 1/Q$  for some integer  $p$ . Letting  $q = j - i$ , observe that  $q < Q$ , and we obtain  $|\alpha - p/q| < 1/qQ < 1/q^2$ . As  $\alpha$  is irrational, we may choose  $Q'$  to be such that  $|q\alpha - p| > 1/Q'$ , and run the argument again; by force, we discover a new, distinct rational approximation. In this way, if  $\alpha$  is irrational we discover infinitely many such approximations. By contrast, if  $\alpha$  is rational, then (10) limits the ability to find good approximations.  $\square$

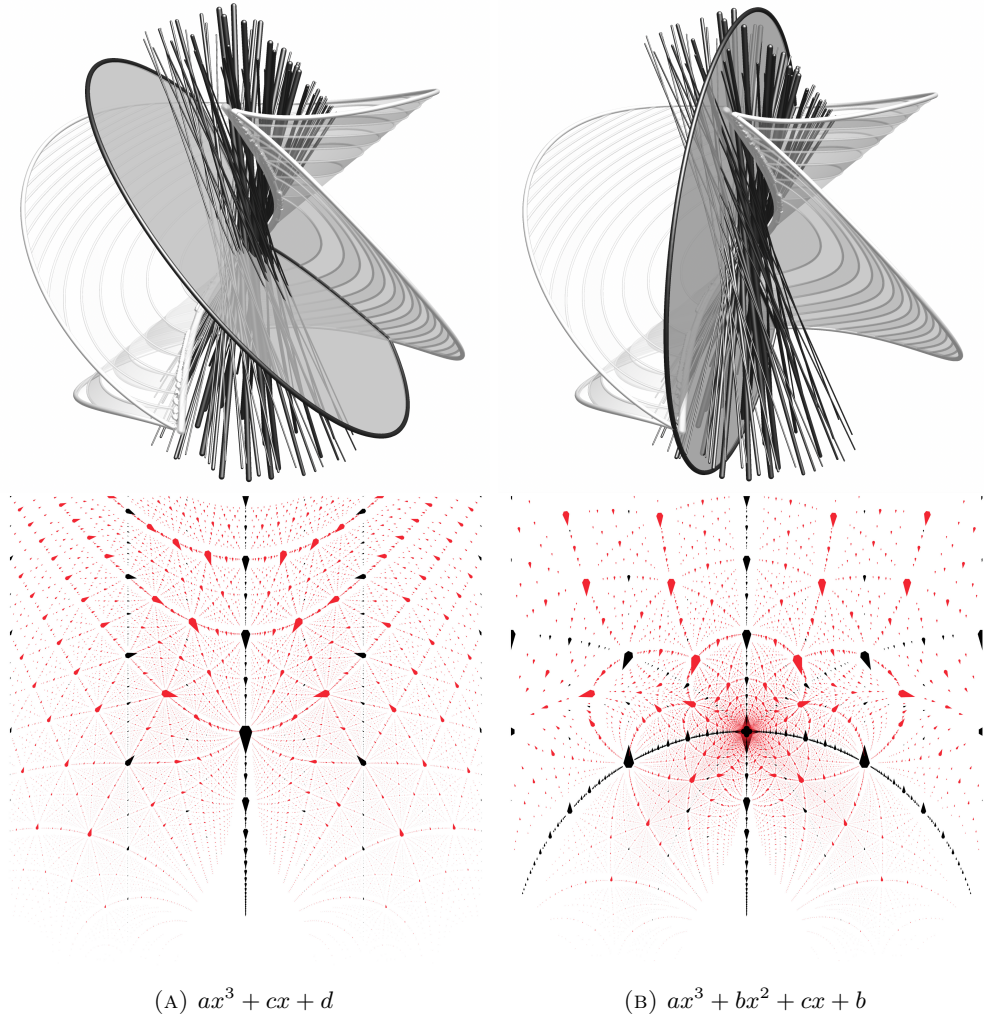


FIGURE 33. 2-parameter projective families of cubics, plotted in coefficient space together with their projection onto their complex root. The family on the left is transverse to the  $\mathbb{S}^1$  fibers of  $\text{UTH}_{\text{Coefs}}^2$ , and so the projection onto roots is an embedding. The family on the right is not transverse to the  $\mathbb{S}^1$  foliation, and contains the fiber  $(x^2 + 1)(px + q)$ . Thus the projection onto the complex root is not an embedding, and collapses an entire curve above  $i$ .

Dirichlet's Theorem is illustrated in Figure 14; if one places disks over each rational  $p/q$  with radius  $1/q^2$ , then the irrationals are covered by infinitely many disks, while rationals by only finitely many. We can create a more starscape-esque version by a constant scaling, in Figure 15. This latter version has a different feel, and more vividly illustrates the mutual repulsion of rational numbers.

The natural accompaniment to Dirichlet's elementary result is a deep one of Roth: if the exponent 2 is strengthened to  $2 + \epsilon$  for any positive  $\epsilon$ , then all *algebraic*  $\alpha$  fail to have infinitely many good approximations [44].

**Theorem 4.2** (Roth [44]). *Let  $\epsilon > 0$ . Let  $\alpha \in \mathbb{R}$  be algebraic of degree  $\geq 2$ . Then there are only finitely many distinct  $p/q \in \mathbb{Q}$  such that*

$$|\alpha - p/q| < 1/q^{2+\epsilon}.$$

This finiteness is in fact true for almost all real numbers  $\alpha$  (in the sense of Lebesgue measure), a result due to Khintchine [30, Theorem 29].

However, one can construct real numbers which are well-approximable to all higher exponents, called *Liouville numbers* after Liouville's famous construction [34]. The key to constructing a Liouville number is to artificially build something incredibly close to a series of rational numbers. The simplest example is  $\sum_{k=0}^{\infty} \frac{1}{10^{k!}}$ : the partial sums form rational approximations that are too good to allow for a finiteness property like Theorem 4.2, even for any fixed positive exponent of  $q$ . These were the first explicit transcendental numbers.

Having studied the exponent  $k$  in approximation within  $1/q^k$ , we can turn to a finer question of constants. For example, does Dirichlet's Theorem hold if  $1/q^2$  is replaced with  $1/Cq^2$  for various increasing values of  $C$ ? The theorem holds until  $C = \sqrt{5}$ , above which the golden ratio and certain of its relatives are no longer approximable by infinitely many rationals. This state of affairs continues until another tipping point,  $C = 2\sqrt{2}$ , above which  $\sqrt{2}$  is poorly approximable, and so on. These tipping points form the beginning of the theory of the *Lagrange spectrum*.

For the rich theory of Diophantine approximation, including further historical context for these results, the reader may begin with [15, 27, 48].

The Diophantine approximation of the complex plane away from the real line is less well-studied. Here we must ask the approximants to come from number fields: in our context, it is natural to stratify these by degree, and ask: how well-approximable is a complex number by algebraic numbers of degree  $\leq d$ ?

In order to do so, we need to generalize the notion of height, to measure the arithmetic complexity of algebraic numbers in general.

**4.2. Measuring arithmetic complexity with the naïve height of a polynomial.** The simplest notion of arithmetic complexity may be with reference to the coefficients of its minimal polynomial. Recall that an algebraic number has a unique *minimal polynomial*, most often taken to be the unique monic irreducible  $f(x) \in \mathbb{Q}[x]$  for which it is a root. We may take this polynomial to be in  $\mathbb{Z}[x]$  by scaling up the denominator, which causes us to lose the monic condition. We will write  $f_\alpha$  for the unique scaling whose coefficients are integral but with no common factor, and refer to this as the *minimal polynomial*, following much of the literature of Diophantine approximation (for example [16]).

Consider any polynomial  $f = a_d x^d + \cdots + a_1 x + a_0 \in \mathbb{Z}[x]$ . Then the *naïve height* of  $f$  is defined as

$$H(f) := \max_{0 \leq i \leq d} |a_i|.$$

This measure has the advantage of simplicity, and a close connection to the linear algebra of the lattice of polynomials of degree  $d$  in the space of coefficients. It is also clear that there are only finitely many polynomials of bounded degree and height.

We will write  $H(f_\alpha)$  for the height of the minimal polynomial  $f_\alpha$  of  $\alpha$ , which measures the arithmetic complexity of  $\alpha$ .

**4.3. Good approximations drawn from fixed degree.** To generalize Dirichlet's Theorem 4.1, one might ask to approximate by algebraic numbers of bounded degree  $d$  (so that Dirichlet's Theorem becomes the case of  $d = 1$ , i.e. approximation by rationals). One can define, following Koksma [31] the quantity  $k_d(\alpha)$  to be the supremum of all  $k$  such that there are infinitely many algebraic numbers  $\beta$  of degree  $\leq d$  satisfying

$$|\alpha - \beta| < \frac{1}{H(f_\beta)^k}.$$

Dirichlet's Theorem 4.1, in this language, states that  $k_1(\alpha) \leq 2$  for  $\alpha$  rational and  $k_1(\alpha) \geq 2$  for  $\alpha$  real and irrational. Roth's Theorem 4.2 is that  $k_1(\alpha) = 2$  for  $\alpha$  real and algebraic.

For general degree, Sprindžuk gave an answer for almost all  $\alpha$  (generalizing Khintchine's statement). We see a qualitative difference between real and non-real  $\alpha$ .

**Theorem 4.3** (Sprindžuk, [51]). *For almost all  $\alpha \in \mathbb{R}$ ,  $k_d(\alpha) = d+1$ . For almost all  $\alpha \in \mathbb{C} \setminus \mathbb{R}$ ,  $k_d(\alpha) = (d+1)/2$ .*

This gives us a better idea of the natural sizing for algebraic points in the complex plane: a sizing of  $1/H(f_\alpha)^{(d+1)/2}$  would be the natural analogue of Figure 15. See Figure 36.

Next, we may consider the generalization of Roth's Theorem 4.2 governing the approximability of algebraic numbers. Schmidt showed that for algebraic  $\alpha \in \mathbb{R}$  of degree at least 2,  $k_d(\alpha) = \min\{\deg(\alpha), d+1\}$  [46]. For complex numbers away from the real line (our concern here), it is slightly more complicated.

**Theorem 4.4** (Bugeaud, Evertse [16], Theorem 2.1, Corollary 2.4). *For algebraic  $\alpha \in \mathbb{C} \setminus \mathbb{R}$ ,*

$$k_d(\alpha) = \min\{\deg(\alpha)/2, (d+1)/2\}$$

*except in the case that  $\deg(\alpha) \geq d+2$  and  $d$  is even. In this case,  $k_d(\alpha) \in \{(d+1)/2, (d+2)/2\}$ .*

*In particular, for  $d = 2$ , we have  $k_2(\alpha) = 2$  if and only if the quantities  $1, \alpha\bar{\alpha}$  and  $\alpha + \bar{\alpha}$  are  $\mathbb{Q}$ -linearly dependent (and  $k_2(\alpha) = 3/2$  otherwise).*

In degree  $d > 2$ , Bugeaud and Evertse give precise conditions for determining which of the two possibilities for  $k_d(\alpha)$  is correct in most cases, but were not able to compute it in all cases.

Let us consider the dichotomy given for  $d = 2$ , where Theorem 4.4 says that some  $\alpha$  are much more approximable than others, based on whether  $1, \alpha\bar{\alpha}$  and  $\alpha + \bar{\alpha}$  are  $\mathbb{Q}$ -linearly dependent. To see why this is, we recast this characterization more geometrically: such  $\alpha$  have the property that they lie on rational hyperbolic geodesics, i.e. those geodesics corresponding to rational planes in coefficient space. These are exactly the *rational geodesics* discussed in Observation 3.12.

This dichotomy is illustrated in Figure 34. In fact, we will show in Section 5 that this dichotomy holds even for non-algebraic  $\alpha$ . Note that the  $\deg(\alpha) \geq d+2$  condition is not needed for  $d = 2$ , since cubics cannot lie on rational geodesics<sup>29</sup>, an effect which is quite prominent in Figure 1c.

Based on this geometric interpretation of the  $d = 2$  case of Bugeaud and Evertse, one wonders if the exceptional cases all have similar geometric interpretations. We muse on this briefly in Section 6.

**4.4. The importance of  $\mathrm{PSL}(2; \mathbb{Z})$  and the hyperbolic metric.** There is a natural symmetry of the algebraic numbers in the upper half plane: the action of  $\mathrm{PSL}(2; \mathbb{Z})$ . That is, the equivariant action of  $\mathrm{PSL}(2; \mathbb{C})$  on coefficient and root space, restricted to those elements which preserve the lattice  $\mathbb{Z}^3$  in the space  $\mathbb{R}^3$  of coefficients (see Section 3.2.5). In this work, we extol the philosophy that, for Diophantine approximation away from the real line, this action should be built into our definitions. Hyperbolic distance and complex distance are conformally equivalent<sup>30</sup>, and this symmetry respects the former. Therefore the relative hyperbolic positions of the algebraic numbers are preserved under  $\mathrm{PSL}(2; \mathbb{Z})$ . Several of the notions of arithmetic complexity in the literature partially respect this symmetry. If they do not, then, given any complex Diophantine approximation statement (such as those of Bugeaud and Evertse), it seems natural to translate by  $\mathrm{PSL}(2; \mathbb{Z})$  until the statement is strongest (by which we mean, translate by  $\mathrm{PSL}(2; \mathbb{Z})$ , find the best approximations according to the theorem, and

<sup>29</sup>One way to see this is to reduce to the unit circle; cubics cannot lie on the unit circle  $\alpha\bar{\alpha} = 1$  unless their real root  $r$  is rational, since the constant coefficient of the minimal polynomial  $\alpha\bar{\alpha}r$  is rational.

<sup>30</sup>That is, locally the hyperbolic metric and the Euclidean metric are very nearly multiples of each other. This becomes exact at the level of tangent spaces for the Riemannian metric, where  $ds_{\mathrm{Hyp}}^2 = \frac{1}{\mathrm{Im}(z)} ds_{\mathrm{Euc}}^2$ .

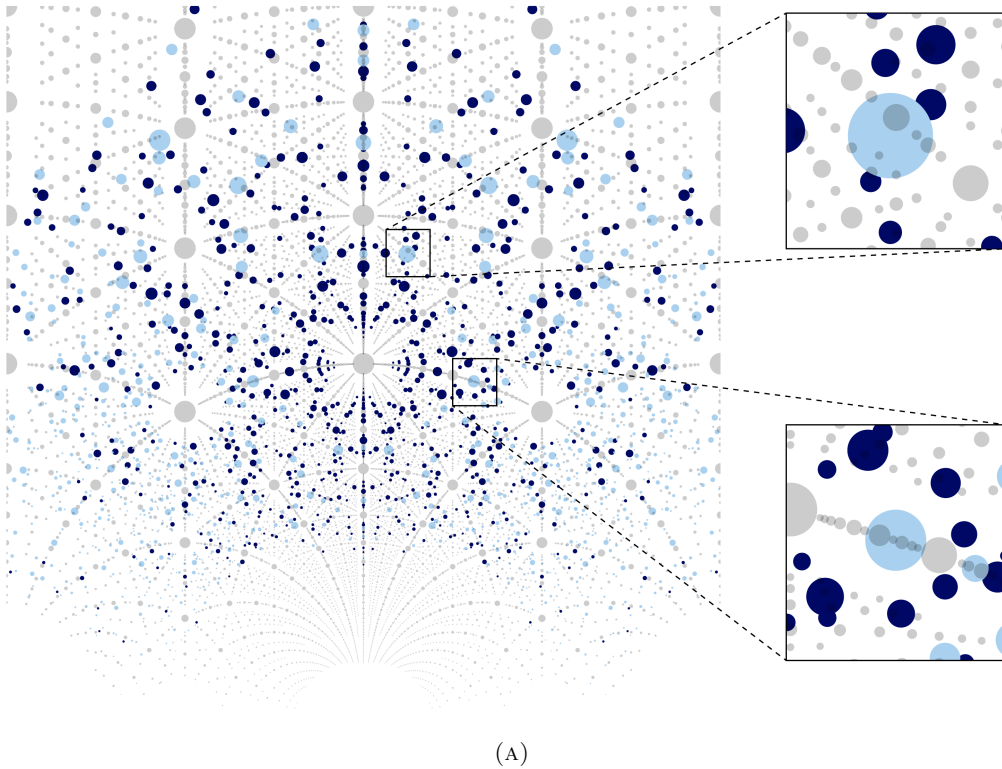


FIGURE 34. Quadratics shown in gray, quartics shown in light blue (if they have no real conjugates) and dark blue (if they do). The quartics which lie off such geodesics (such as the one highlighted in the top right) are approximated only by quadratics at some distance on these geodesics. In contrast quartics on a geodesic such as the unit circle have more quadratics near them as shown in the lower highlight.

then transport the constellation back to the original region of interest, where perhaps a priori only worse approximations were guaranteed).

Perhaps our position is most simply stated in terms of our visualizations: the positions of the dots are periodic under  $\mathrm{PSL}(2; \mathbb{Z})$  and therefore we argue the sizings of them should be too<sup>31</sup>. We illustrate this in Figure 35, showing the transport of a constellation of algebraic numbers under  $\mathrm{PSL}(2; \mathbb{Z})$ , but shown in the euclidean metric and the height sizing. The varying sizes and distances of the dots illustrate the changing levels of approximation from the classical perspective.

While  $H(f_\alpha) = H(f_{1/\alpha})$ , unfortunately  $H(f_\alpha) \neq H(f_{\alpha+1})$ . Consequently, the naïve height is not invariant under the action of  $\mathrm{PSL}(2; \mathbb{Z})$  on  $\alpha$ . For non-real numbers, the height does, however, attain a minimum on its full  $\mathrm{PSL}(2; \mathbb{Z})$  orbit. Therefore we define

$$H_{\mathrm{PSL}}(f) = \min\{H(f \circ A) : A \in \mathrm{PSL}(2; \mathbb{Z})\}.$$

To compute this minimum, there is a recent algorithm due to Stoll-Cremona and Hutz-Stoll which generalizes the reduction theory of binary quadratic forms with respect to  $\mathrm{PSL}(2; \mathbb{Z})$  to general binary forms [28, 52]. It is not known how small a height one is guaranteed under their algorithm, nor where the minimum is attained.

<sup>31</sup>Of course, this argument applies only away from the real line: in  $\mathbb{R}$ , all of  $\mathbb{Q}$  falls into a single orbit, and no metric is preserved: such invariance would lose too much information.

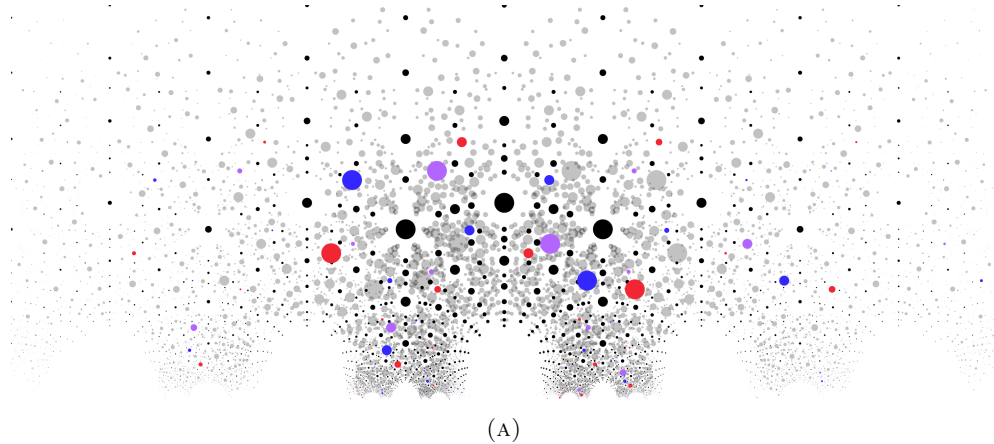


FIGURE 35. Cubic algebraic numbers in the naïve height, using the maximum coefficient, plotted in the euclidean metric.  $\mathrm{PSL}(2; \mathbb{Z})$  orbits are shown for the complex roots of  $x^3 + x - 1$  (red),  $x^3 + x^2 - 1$  (purple) and  $x^3 + x^2 + x - 1$  (blue).

**4.5. Weil height.** A more nuanced generalization of the notion of height is the Weil height, defined in terms of the absolute values of an ambient number field. For an algebraic number  $\alpha$  contained in a number field  $K$  of degree  $d$ , the Weil height is defined<sup>32</sup> as

$$H(\alpha) = \left( \prod_{v \in M_K} \max\{1, |\alpha|_v\} \right)^{1/d}, \quad (12)$$

where the product is over the set  $M_K$  of all absolute values on  $K$ . This is actually independent of the choice of  $K$  containing  $\alpha$ . This definition is a generalization of the case  $K = \mathbb{Q}$ , namely

$$H(p/q) = \prod_{v \in M_{\mathbb{Q}}} \max\{1, |p/q|_v\},$$

where  $|\cdot|_v$  ranges over all  $p$ -adic absolute values, as well as the archimedean one. This case can be more simply and intuitively rewritten as

$$H(p/q) = \max\{|p|, |q|\},$$

if  $p$  and  $q$  are taken to be coprime and integral. However, in a general number field,  $\alpha$  doesn't have a canonical representation as a quotient. The Weil height as defined in (12) is insensitive to the various representations, thanks to the product rule

$$\prod_{v \in M_K} |\alpha|_v = 1.$$

Fortunately, the Weil height and naïve height of its minimal polynomial are closely related by a well known relationship in terms of the degree  $d$  [15, Lemma A.2]:

$$\left( \frac{d}{\lfloor d/2 \rfloor} \right)^{-1} H(f_\alpha) \leq H(\alpha)^d \leq \sqrt{d+1} H(f_\alpha). \quad (13)$$

Here it is important that  $f_\alpha$  is minimal in the sense of coprime integer coefficients.

<sup>32</sup>We beg the reader's forgiveness for the use of  $H$  for both naïve height of a polynomial and Weil height of a number; they do *not* satisfy  $H(f_\alpha) = H(\alpha)$ , but the notation is standard in the literature.

Note that  $H(\alpha) = H(1/\alpha)$ . For the same reasons discussed in the previous section, it is natural to define

$$H_{\text{PSL}}(\alpha) = \min\{H(A.\alpha) : A \in \text{PSL}(2; \mathbb{Z})\}.$$

**4.6. Repulsion in the complex plane in terms of Weil height.** Now we can state a generalization of the repulsion statement (10) which is particularly natural with regards to the Weil height. Let  $\alpha \neq 0$  be algebraic. Then

$$H(\alpha) = H(1/\alpha) = \prod_v \max\left\{\left|\frac{1}{\alpha}\right|_v, 1\right\} \geq \left|\frac{1}{\alpha}\right|.$$

Therefore,

$$|\alpha| \geq \frac{1}{H(\alpha)}.$$

(This takes the place of the observation that  $1/q \geq 1/q$  in the rational case! However, here it is potentially a considerable loss, if a number of absolute values are involved in the computation.) Then, replacing  $\alpha$  with a difference  $\alpha - \beta$ , and using the fact that  $H(\alpha - \beta) \leq 2H(\alpha)H(\beta)$  (which follows easily from the definition), we have repulsion of algebraic numbers:

$$|\alpha - \beta| \geq \frac{1}{2H(\alpha)H(\beta)}. \quad (14)$$

**4.7. Discriminant as a measure of arithmetic complexity.** From the perspective of the geometry discussed in the previous section, and the images we've drawn, one might consider the measure of arithmetic complexity given by the discriminant.

For a polynomial  $f = a_d x^d + \cdots + a_1 x + a_0 = a_d \prod_{i=1}^d (x - \alpha_i) \in \mathbb{Z}[x]$ , let  $\Delta_f$  denote the discriminant of  $f$ . Recall that the discriminant is a measure of the differences between the roots:

$$\Delta_f = a_d^{2d-2} \prod_{i < j} (\alpha_i - \alpha_j)^2.$$

We will refer to an algebraic number as having a discriminant, namely the discriminant of its minimal polynomial, and write  $\Delta_\alpha := \Delta_{f_\alpha}$ . This has the particular advantage of being invariant under  $\text{PSL}(2; \mathbb{Z})$ .

How do the previously defined heights and the discriminant relate? Mahler proved a relationship in one direction [36], namely:

$$|\Delta_\alpha| \leq d^d H(\alpha)^{d(2d-2)}. \quad (15)$$

By using (13), we obtain the related inequality:

$$|\Delta_\alpha| \leq d^d (d+1)^{d-1} H(f_\alpha)^{2d-2}. \quad (16)$$

In general one doesn't expect a converse inequality, since the discriminant is invariant under  $f(x) \mapsto f(x+1)$ , while the Weil height would be expected to grow. Even within one fundamental region of the upper half plane, one doesn't expect a tight relationship. For example, it is possible to define a family of quadratic irrationalities such that  $H(\alpha)^4/|\Delta_\alpha| \rightarrow \infty$ . Namely, the polynomials  $x^2 + n$  have roots approaching  $\infty$  along the imaginary axis, and  $4H(\alpha)^4/|\Delta_\alpha| = 4n^2/4n = n \rightarrow \infty$ .

**4.8. Sizing in starscape images.** In light of the comparisons (13), (15), and (16), as well as Theorems 4.3 and 4.4, one might compare the naive sizings in Figures 12 and 13 with slightly more nuanced versions given in Figure 36. These latter sizings are all chosen to match Theorem 4.3 just as Figure 15 matches Dirichlet's Theorem 4.1.

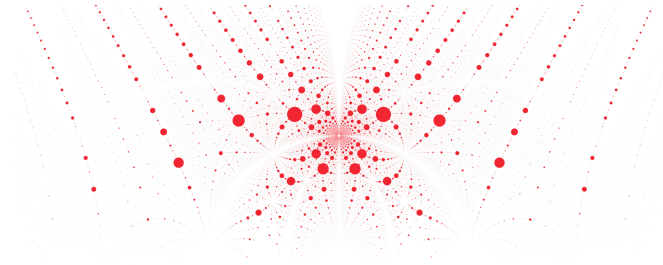
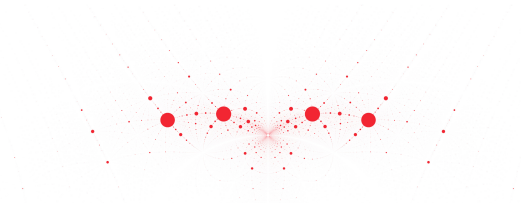
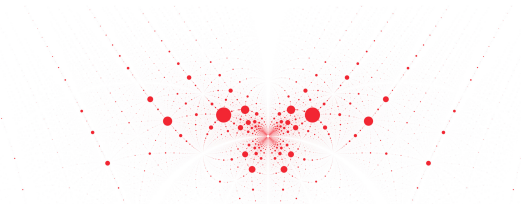
(A) Discriminant:  $|\Delta_\alpha|^{(d+1)/(4d-4)}$ (B) Naïve height:  $H(f_\alpha)^{(d+1)/2}$ (C) Weil height or Mahler measure:  $H(\alpha)^{d(d+1)/2} = M(f)^{(d+1)/2}$ 

FIGURE 36. Several natural choices of sizing by arithmetic complexity of the roots of to match Theorem 4.3, scaled so that the complex root of  $x^3 + x - 1$  is the same size. The roots plotted are the family  $ax^3 + cx^2 + bx + c$ . Compare with Figures 12 and 13.

## 5. DIOPHANTINE APPROXIMATION IN THE QUADRATICS

We now revisit the basic theory of Diophantine approximation by complex quadratic irrationalities, from the starscapes perspective: we use the *hyperbolic distance* to measure distance and the *discriminant* to measure arithmetic complexity. We generalize repulsion (as in (10) and (14)), Dirichlet's Theorem 4.1 guaranteeing infinitely many approximations, and Roth's Theorem 4.2 on the approximation of algebraic numbers, in this new situation. In this way, we recover the  $d = 2$  case of Theorem 4.4, with some additional geometric nuance (we distinguish between approximations coming from different rational geodesics). The proofs are elementary

(with the exception that they depend on Schmidt's Subspace Theorem), and are based in the geometry of Section 3. We work in the coefficient space and transport the results to the complex plane afterward.

This perspective offers a few benefits. First, it respects the natural  $\mathrm{PSL}(2; \mathbb{Z})$  symmetry. Second, the geometry nicely explains the special cases that arise in Theorem 4.4, and we can now observe that the same dichotomy holds for non-algebraic complex numbers: those on rational geodesics are better approximable. In particular, Theorem 5.3 implies that  $k_2(\alpha) \geq 2$  for any complex number on a rational geodesic, whereas Theorem 4.3 says we have  $k_2(\alpha) = 3/2$  for almost all complex non-real numbers. Also, our method discriminates between approximations taken from fixed rational geodesics. The relationship between our hyperbolic/discriminant statements and the classical exponents  $k_2(\alpha)$  is explained in Section 5.7.

Throughout this section, it will be convenient to use Vinogradov notation: that is,  $f \ll_\alpha g$  denotes that  $f$  is bounded above by a constant multiple of  $g$ , where the constant may depend on  $\alpha$ .

**5.1. Repulsion amongst imaginary quadratics.** Recall that with the Weil height function we have a simple repulsion principle, (14):

$$|\alpha - \beta| > \frac{1}{2H(\alpha)H(\beta)}.$$

Using the hyperbolic metric (denoted  $d_{hyp}$ ) and the discriminant, we obtain the following version of repulsion.

**Theorem 5.1.** *Let  $\alpha \neq \beta$  be two non-real quadratic irrationalities, of discriminants  $\Delta_\alpha$  and  $\Delta_\beta$  respectively. Then the hyperbolic distance between  $\alpha$  and  $\beta$ , considered in the upper half plane, is at least*

$$d_{hyp}(\alpha, \beta) \geq \mathrm{acosh} \left( 1 + \frac{\sqrt{2} - 1}{\sqrt{|\Delta_\alpha \Delta_\beta|}} \right).$$

If  $\Delta_\alpha = \Delta_\beta$ , then

$$d_{hyp}(\alpha, \beta) \geq \mathrm{acosh} \left( 1 + \frac{1}{|\Delta_\alpha|} \right).$$

*Proof.* Suppose  $\alpha$  and  $\beta$  are associated to some vectors  $f_\alpha, f_\beta$  in coefficient space. By (5), the distance between them is

$$d_{\mathrm{Cofes}}(f_\alpha, f_\beta) = \mathrm{acosh} \left( \frac{-\langle f_\alpha, f_\beta \rangle}{\sqrt{|\Delta_\alpha \Delta_\beta|}} \right).$$

Since  $\alpha \neq \beta$ , this distance is greater than 0. However, it lies in

$$\mathrm{acosh} \left( \frac{\mathbb{Z}}{\sqrt{|\Delta_\alpha \Delta_\beta|}} \right),$$

which is a discrete set of values whose smallest positive value is

$$\mathrm{acosh} \left( \frac{n}{\sqrt{|\Delta_\alpha \Delta_\beta|}} \right),$$

where  $n$  is the smallest integer greater than  $\sqrt{|\Delta_\alpha \Delta_\beta|}$ . In particular,  $n^2 - \Delta_\alpha \Delta_\beta \geq 1$ . This implies that

$$\frac{n}{\sqrt{|\Delta_\alpha \Delta_\beta|}} \geq 1 + \frac{\sqrt{2} - 1}{\sqrt{|\Delta_\alpha \Delta_\beta|}}.$$

The special case is the case that  $n = |\Delta_\alpha| + 1$ . □

**5.2. Fundamental geometric lemma.** Fix  $\alpha \in \mathbb{C} \setminus \mathbb{R}$ , not quadratic. We will consider approximations by quadratic irrational  $\beta$ . We can give corresponding vectors in coefficient space:

$$f_\alpha = [\alpha_1 : 1 : \alpha_2], \quad f_\beta = [p_1 : n : p_2]$$

where  $p_1, n, p_2 \in \mathbb{Z}$  and  $\alpha_1, \alpha_2$  are not both rational. More precisely, we have  $\alpha_1 = 1/(\alpha + \bar{\alpha})$  and  $\alpha_2 = (\alpha\bar{\alpha})/(\alpha + \bar{\alpha})$ .

We wish to compute the hyperbolic distance between  $f_\alpha$  and  $f_\beta$ . Our proofs will rely on a fundamental lemma which relates this distance to linear forms, with coefficients depending on  $\alpha$ , in  $f_\beta$ 's coordinates.<sup>33</sup>

**Lemma 5.2.** *Suppose  $\alpha \in \mathbb{C} \setminus \mathbb{R}$  is a fixed non-quadratic, with  $f_\alpha = [\alpha_1 : 1 : \alpha_2]$ .*

*Let  $\beta$  be quadratic, with  $f_\beta = [p_1 : n : p_2]$ , where  $n, p_1, p_2 \in \mathbb{Z}$ .*

*Define the linear forms:*

$$\begin{aligned} L_1 &:= L_1(p_1, n, p_2) = n\alpha_1 - p_1, \\ L_2 &:= L_2(p_1, n, p_2) = -n\alpha_2 + p_2, \\ L_3 &:= L_3(p_1, n, p_2) = \alpha_1 p_2 - \alpha_2 p_1. \end{aligned}$$

(1) *We have*

$$d_{hyp}(\alpha, \beta) \leq \operatorname{acosh} \left( 1 + \frac{\max\{|L_1 L_2|, L_3^2\}}{|\Delta_\beta|} \right).$$

(2) *Suppose  $\beta$  is sufficiently close to  $\alpha$ , namely  $d_{hyp}(\alpha, \beta) < \operatorname{acosh} 2$ . Then*

$$d_{hyp}(\alpha, \beta) \geq \operatorname{acosh} \left( 1 + \frac{m_\alpha |L_1 L_2|}{|\Delta_\beta|} \right),$$

*for some constant  $m_\alpha > 0$  depending only on  $\alpha$ .*

*Proof.* Recall that the distance is invariant under scaling, so we will temporarily replace  $f_\alpha$  with  $f'_\alpha = n f_\alpha$ , so the middle coordinates of the two vectors agree. We have

$$\begin{aligned} & \frac{\langle f'_\alpha, f_\beta \rangle^2}{\|f'_\alpha\|^2 \|f_\beta\|^2} - 1 \\ &= \frac{(n^2 - 2n\alpha_1 p_2 - 2n\alpha_2 p_1)^2 - (n^2 - 4n^2 \alpha_1 \alpha_2)(n^2 - 4p_1 p_2)}{\|f'_\alpha\|^2 \|f_\beta\|^2} \\ &= 4n^2 \frac{(\alpha_1 p_2 - \alpha_2 p_1)^2 + (n\alpha_1 - p_1)(n\alpha_2 - p_2)}{\|f'_\alpha\|^2 \|f_\beta\|^2} \\ &= 4 \frac{L_3^2 - L_1 L_2}{\|f_\alpha\|^2 \|f_\beta\|^2} \end{aligned}$$

Evidently,

$$L_3^2 - L_1 L_2 \leq 2 \max\{|L_1 L_2|, L_3^2\}.$$

Therefore

$$\frac{\langle f_\alpha, f_\beta \rangle^2}{\|f_\alpha\|^2 \|f_\beta\|^2} \leq 1 + \frac{2 \max\{|L_1 L_2|, L_3^2\}}{\|f_\beta\|^2}.$$

Hence,

$$\frac{-\langle f_\alpha, f_\beta \rangle}{\|f_\alpha\| \|f_\beta\|} \leq 1 + \frac{\max\{|L_1 L_2|, L_3^2\}}{\|f_\beta\|^2}.$$

<sup>33</sup>This generalizes the rational approximation case, since there the angle  $\theta$  between the projective lines  $[\alpha : 1]$  and  $[p : q]$  satisfies

$$\cos \theta = \frac{\langle (\alpha, 1), (p, q) \rangle}{\|(p, q)\| \|(\alpha, 1)\|} = \frac{|q\alpha - p|}{\|(p, q)\| \|(\alpha, 1)\|}.$$

Next we show

$$L_3^2 - L_1L_2 \gg_\alpha \min\{|L_1L_2|, L_3^2\}.$$

By the definitions of the  $L_i$ , we have

$$L_1\alpha_2 + L_2\alpha_1 = L_3.$$

In particular,

$$L_3^2 - L_1L_2 = (L_1\alpha_2 + L_2\alpha_1)^2 - L_1L_2 \geq (4\alpha_1\alpha_2 - 1)L_1L_2$$

by the arithmetic-geometric mean inequality. Note that  $K_\alpha := 4\alpha_1\alpha_2 - 1 > 0$  since  $\alpha$  is not real. Thus if  $L_1L_2$  is positive, we are done. On the other hand, if it is negative, then

$$L_3^2 - L_1L_2 = L_3^2 + |L_1L_2| \geq |L_1L_2|.$$

We have shown that, for some constant  $m'_\alpha > 0$  depending only on  $\alpha$ ,

$$\frac{\langle f_\alpha, f_\beta \rangle^2}{\|f_\alpha\|^2 \|f_\beta\|^2} \geq 1 + \frac{m'_\alpha |L_1L_2|}{\|f_\beta\|^2}.$$

Therefore, for  $\beta$  sufficiently close to  $\alpha$  (i.e., so that  $\frac{\langle f_\alpha, f_\beta \rangle^2}{\|f_\alpha\|^2 \|f_\beta\|^2} < 2$ ), this implies (taking  $m_\alpha = (\sqrt{2} - 1)m'_\alpha$ ) that

$$\frac{-\langle f_\alpha, f_\beta \rangle}{\|f_\alpha\| \|f_\beta\|} \geq 1 + \frac{m_\alpha |L_1L_2|}{\|f_\beta\|^2}.$$

□

**5.3. Quadratic Dirichlet's Theorem on a rational geodesic.** We first consider the question of Diophantine approximation on a single *rational geodesic*, i.e. the image of a rational plane in coefficient space (see Section 3.2.5). This is motivated by the observation that each such geodesic looks, in Figure 1a, like a copy of Figure 15, so we expect it to have Diophantine approximation properties similar to the rationals. It will turn out that points lying on such geodesics are better approximable than points elsewhere in  $\mathbb{C}$ : see Figure 34. Recall that, given  $\alpha \in \mathbb{C} \setminus \mathbb{R}$ ,  $\alpha$  lies on a rational geodesic if and only if  $1$ ,  $\alpha + \bar{\alpha}$  and  $\alpha\bar{\alpha}$  are  $\mathbb{Q}$ -linearly dependent (Observation 3.12).

We begin with an analogue to Dirichlet's Theorem 4.1, asserting the existence of infinitely many good approximations on a rational geodesic.

**Theorem 5.3.** *Let  $\alpha \in \mathbb{C} \setminus \mathbb{R}$  not be quadratic irrational, but lying on a rational geodesic. Then there exists a constant  $K_\alpha > 0$ , depending only on the  $\mathrm{PSL}(2; \mathbb{Z})$  orbit of  $\alpha$ , such that there are infinitely many quadratic irrational  $\beta$  lying on that rational geodesic, with*

$$d_{hyp}(\alpha, \beta) \leq \operatorname{arcosh} \left( 1 + \frac{K_\alpha}{|\Delta_\beta|^2} \right).$$

*Proof.* Suppose  $\alpha \in \mathbb{C} \setminus \mathbb{R}$  is a fixed non-quadratic, with  $f_\alpha = [\alpha_1 : 1 : \alpha_2]$ . The theorem statement is invariant under  $\mathrm{PSL}(2; \mathbb{Z})$  (i.e. replacing  $\alpha$  and all candidate  $\beta$  with their images under the action of some element of  $\mathrm{PSL}(2; \mathbb{Z})$ , we preserve  $\Delta_\beta$  and the hyperbolic distances). We assume  $\alpha$  is on a rational geodesic, so  $a\alpha_1 + b + c\alpha_2 = 0$ . We may translate by  $\mathrm{PSL}(2; \mathbb{Z})$  until  $\max\{|a|, |b|, |c|\}$  is minimal; this is a constant depending only on the  $\mathrm{PSL}(2; \mathbb{Z})$  orbit of  $\alpha$ . We can actually choose a canonical geodesic amongst these finitely many in any way we wish; say the one of smallest radius, and amongst those, center nearest the origin but to its right. We set some such convention.

Let  $Q > 0$  be an integer.

We use the classical method of proof of Dirichlet's Theorem 4.1 to find a solution  $(n_0, q_0) \in \mathbb{Z}^2$  to

$$|n_0\alpha_1 - q_0| \leq 1/Q, \quad n_0 \leq Q.$$

Namely, we divide the unit interval into  $Q$  even subintervals, and the box principle guarantees some  $i\alpha_1$  and  $j\alpha_1$ , for some  $0 \leq i < j \leq Q$ , lie in the same interval modulo  $\mathbb{Z}$ ; we let  $n_0 = j - i$ . We have  $an_0\alpha_1 = -bn_0 - cn_0\alpha_2$ , so that

$$|cn_0\alpha_1 - cq_0| \leq |c|/Q, \quad |cn_0\alpha_2 + bn_0 + aq_0| = |-an_0\alpha_1 + aq_0| \leq |a|/Q.$$

We let  $f_\beta = [p : n : q] = [cq_0 : cn_0 : -bn_0 - aq_0]$ . The corresponding  $\beta \in \mathbb{C}$  is a candidate good quadratic irrational approximation to  $\alpha$ .

Increasing  $Q$  and finding a new approximation, we can in fact produce infinitely many such  $f_\beta$  which are linearly independent, and such that the resulting infinite sequence of distinct  $\beta$  approach  $\alpha$ .

It remains to show that these  $\beta$  are indeed good approximations. We have the following observations:

$$\begin{aligned} n &\ll_\alpha Q, \quad |L_1 L_2| \ll_\alpha 1/Q^2, \\ L_3^2 &= |L_1\alpha_2 + L_2\alpha_1|^2 \ll_\alpha \max\{|L_1|^2, |L_2|^2\} \ll_\alpha 1/Q^2. \end{aligned}$$

Here and for the entire proof, the constants in the Vinogradov notation depend on  $\alpha$ , but this in the canonical choice of  $\alpha$  within its  $\mathrm{PSL}(2; \mathbb{Z})$  orbit, so the constants actually only depend on the orbit.

Combining these with Lemma 5.2,

$$\cosh d_{\mathrm{Coefs}}(f_n, f_\beta) - 1 \ll_\alpha \frac{1}{n^2 |\Delta_\beta|}.$$

Let  $C_\alpha = |\Re(\alpha)|/2|\Im(\alpha)|$ . This is a positive constant depending only on  $\alpha$ . Then for all  $\beta$  sufficiently close to  $\alpha$ ,  $|\Re(\beta)| > C_\alpha |\Im(\beta)|$ . We consider only those solutions  $\beta$  which are at least that close. Then  $n/2p > C_\alpha |\Delta_\beta|^{1/2}/2p$ , hence  $n > C_\alpha |\Delta_\beta|^{1/2}$ . Using this fact, we obtain

$$\cosh d_{\mathrm{Coefs}}(f_n, f_\beta) - 1 \ll_\alpha \frac{1}{|\Delta_\beta|^2}.$$

This proves the theorem.  $\square$

It is interesting to note that the constant  $K_\alpha$  depends on a particular ideal class of a real quadratic field, since by Observation 3.12, it can only lie on one rational geodesic and that geodesic is associated to such an ideal class. In the proof, the constant  $K_\alpha$  directly depends on the class. It is natural to wonder about a Lagrange spectrum for  $\alpha$  on rational geodesics.

Also interesting is that all  $\alpha$  lying on rational geodesics are exceptions to Sprindžuk's Theorem 4.3. It is likely possible to prove using Khintchine's classic methods, that, within a single geodesic, almost all  $\alpha$  have  $k_2(\alpha) = 2$ .

**5.4. Quadratic Dirichlet's Theorem in general.** In the general case, where  $\alpha$  may not lie on a geodesic, we have weaker approximation guarantee, with a similar proof.

**Theorem 5.4.** *Let  $\alpha \in \mathbb{C} \setminus \mathbb{R}$  not be a quadratic irrational. Let  $K > 0$  be any constant. Then, there are infinitely many quadratic irrationalities  $\beta$  with*

$$d_{\mathrm{hyp}}(\alpha, \beta) \leq \operatorname{acosh} \left( 1 + \frac{K}{|\Delta_\beta|^{3/2}} \right).$$

*Proof.* Let  $Q > 1$  be an integer.

Let  $f_i = [i\alpha_1 : i : i\alpha_2] = if_\alpha$  for positive integers  $i$ . Divide the unit interval into  $Q$  equal subintervals, and consider the vectors  $f_i$  modulo  $[\mathbb{Z} : \mathbb{Z} : \mathbb{Z}]$ . Then, by the pigeonhole principle, there are some  $0 \leq i < j \leq Q^2$  such that  $f_i$  and  $f_j$  have first and third coordinates lying in the same pair of subintervals modulo  $\mathbb{Z}$ . Let  $n := j - i$ . Note that  $0 < n \leq Q^2$ .

By construction, we have  $|n\alpha_1 - p_1| < 1/Q$  and  $|n\alpha_2 - p_2| < 1/Q$  for some integers  $p_1$  and  $p_2$ . Defining  $f_\beta = [p_1 : n : p_2]$ , we have a corresponding  $\beta \in \mathbb{C}$ : this is the candidate good approximation we seek.

Choose  $Q'$  large enough such that  $|n\alpha_1 - p_1|, |n\alpha_2 - p_2| > 1/Q'$  for all  $n < Q^2$ ,  $p_1, p_2 \in \mathbb{Z}$ . Then, running this argument again with  $Q = Q'$ , we obtain a new solution  $f'_\beta$  that is linearly independent of  $f_\beta$ . By this method, there are infinitely many such solutions, with  $\beta$  approaching  $\alpha$ .

It remains to show that these  $\beta$  are indeed good approximations. We have the following:

$$n \leq Q^2, \quad |L_1 L_2| \leq 1/Q^2, \quad L_3^2 = |L_1 \alpha_2 + L_2 \alpha_1|^2 \ll_\alpha \max\{|L_1|^2, |L_2|^2\} \leq 1/Q^2.$$

Combining these with Lemma 5.2,

$$\cosh d_{\text{Coefs}}(f_n, f_\beta) - 1 \ll_\alpha \frac{1}{n|\Delta_\beta|}.$$

Note that the theorem statement is invariant under the action of  $\text{PSL}(2; \mathbb{Z})$ . Therefore, we may assume without loss of generality that  $\Re(\alpha) > C\Im(\alpha)$  for any positive constant  $C$ , by translation by  $\mathbb{Z}$ . This implies the same fact about all  $\beta$  sufficiently close to  $\alpha$ : that for any fixed positive  $C$ , we can guarantee  $n/2p > C|\Delta_\beta|^{1/2}/2p$ , hence  $n > C|\Delta_\beta|^{1/2}$ . Using this fact, we obtain

$$\cosh d_{\text{Coefs}}(f_n, f_\beta) - 1 \ll_\alpha \frac{1}{C|\Delta_\beta|^{3/2}}.$$

This proves the theorem.  $\square$

**5.5. Poor approximation of algebraic numbers by quadratics.** In this section, we will give a complementary result to Theorems 5.3 and 5.4, showing that algebraic numbers are not any better approximable than those theorems guarantee.

Most of the deep results in the Diophantine approximation of algebraic numbers, including Roth's Theorem 4.2 and Theorem 4.4 of Bugeaud and Evertse, are applications of the following far-reaching result.

**Theorem 5.5** (Schmidt's Subspace Theorem [47, 48]). *Let  $n \geq 2$ , and let  $L_1, \dots, L_n$  be linearly independent linear forms in  $n$  variables, with real algebraic coefficients. Let  $\epsilon > 0$  be real. Then the solutions  $\mathbf{x} \in \mathbb{Z}^n$  to*

$$|L_1(\mathbf{x})L_2(\mathbf{x}) \cdots L_n(\mathbf{x})| < \frac{1}{(\max\{1, |x_1|, \dots, |x_n|\})^\epsilon}$$

*lie in finitely many proper subspaces of  $\mathbb{Q}^n$ .*

As an example, if one takes  $\alpha \in \mathbb{R}$  to be algebraic, Roth's Theorem 4.2 can be reformulated as the statement that there are only finitely many solutions to

$$|q||q\alpha - p| < \frac{1}{q^\epsilon} \tag{17}$$

i.e.  $L_1(p, q) = q$  and  $L_2(p, q) = q\alpha - p$ .

Theorem 4.4 of Bugeaud and Evertse uses Schmidt's Subspace Theorem on the space of coefficients. To approximate an algebraic number  $\alpha$ , the coefficient vector  $f$  is subject to a linear form given by  $|f(\alpha)|$  (so the coefficients of the linear form are the powers of  $\alpha$ ). In our case, the application is different: we work again on the space of coefficient vectors, but our linear form is given in terms of  $1, \alpha + \bar{\alpha}$  and  $\alpha\bar{\alpha}$ . That is, in terms of the coefficient vector associated to  $\alpha$ , instead of a vector of its powers. We are, in effect, searching for approximations to the coefficient vector  $f_\alpha$  of  $\alpha$  within the coefficient space. It is interesting to ask whether this method extends to higher degree.

We will now use Schmidt's Subspace Theorem 5.5 to imply the main result of this section.

**Theorem 5.6.** *Suppose that  $\alpha \in \mathbb{C} \setminus \mathbb{R}$  is algebraic and non-quadratic. Let  $\eta > 0$ . If  $\alpha$  lies on a rational geodesic, then there are only finitely many quadratic irrationals  $\beta$  on that geodesic such that*

$$d_{\text{hyp}}(\alpha, \beta) \leq \text{acosh} \left( 1 + \frac{1}{|\Delta_\beta|^{2+\eta}} \right). \tag{18}$$

Amongst quadratic irrationals  $\beta$  not sharing a rational geodesic with  $\alpha$ , there are only finitely many such that

$$d_{hyp}(\alpha, \beta) \leq \operatorname{acosh} \left( 1 + \frac{1}{|\Delta_\beta|^{3/2+\eta}} \right). \quad (19)$$

In particular, if  $\alpha$  is not on any rational geodesic, then there are only finitely many quadratic irrational  $\beta$  satisfying (19) at all.

*Proof.* Note that, by Theorem 5.1, at most one  $\beta$  having  $\Delta_\beta = \Delta$  can satisfy (18) or (19), for each  $\Delta$ . Therefore, by throwing away at most finitely many approximations  $\beta$ , we can reduce to considering  $\beta$  having discriminant  $|\Delta_\beta|$  exceeding any fixed bound, or, consequently, to considering  $\beta$  sufficiently close to  $\alpha$ .

First, we will show that there are only finitely many  $\beta$  which are not on the same rational geodesic as  $\alpha$  (where  $\alpha$  may or may not be on any rational geodesic), and which satisfy

$$d_{\text{Coefs}}(f_\alpha, f_\beta) \leq \operatorname{acosh} \left( 1 + \frac{1}{|\Delta_\beta|^{3/2+\eta}} \right).$$

For  $\beta$  sufficiently close to  $\alpha$ , Lemma 5.2 implies that any such solution  $\beta$  satisfies

$$|L_1 L_2| \ll_\alpha 1/|\Delta_\beta|^{1/2+\eta}.$$

For  $\beta$  sufficiently close to  $\alpha$ , we also have

$$|\Re(\beta)| \gg_\alpha |\Im(\beta)|. \quad (20)$$

In particular,

$$n \gg_\alpha |\Delta_\beta|^{1/2}.$$

Therefore (altering  $\eta$ ),

$$|n||L_1(p_1, n, p_2)||L_2(p_1, n, p_2)| \ll_\alpha \frac{1}{|n|^\eta}.$$

These three linear forms are independent. So by Schmidt's Subspace Theorem 5.5, these solutions lie on finitely many proper subspaces, i.e. rational geodesics. Note that this finite collection of orbits depends only on  $\alpha$ . Choose any one geodesic. In particular, assume that  $ap_1 + bn + cp_2 = 0$ . In particular,  $|a|$ ,  $|b|$ ,  $|c|$  are bounded above by a constant depending only on  $\alpha$ .

Then, what we have is actually

$$|n\alpha_1 - p_1||cn\alpha_2 + ap_1 + bn| = |n\alpha_1 - p_1||n\alpha_2 - p_2||c| \ll_\alpha \frac{1}{|n|^{1+\eta}} < \frac{1}{|n|^\eta}.$$

Since  $\alpha$  is not on the geodesic,  $a\alpha_1 + b + c\alpha_2 \neq 0$ , which implies these are independent linear forms in two variables  $n$  and  $p_1$ . Again by Schmidt's Subspace Theorem 5.5, the solutions lie on finitely many lines in (non-projectivized) coefficient space. Hence there are finitely many solutions.

Next, we show that there are only finitely many solutions  $\beta$  which are on the same rational geodesic as  $\alpha$  (thus we are in the case that  $\alpha$  is on a rational geodesic), and which satisfy

$$d_{hyp}(\alpha, \beta) \leq \operatorname{acosh} \left( 1 + \frac{1}{|\Delta_\beta|^{2+\eta}} \right).$$

For such  $\beta$  sufficiently close to  $\alpha$ , by Lemma 5.2,

$$|L_1 L_2| |\Delta_\beta| \ll_\alpha 1/|\Delta_\beta|^\eta.$$

By the same argument surrounding (20) (altering  $\eta$ ),

$$|n|^2 |n\alpha_1 - p_1||n\alpha_2 - p_2| \ll_\alpha \frac{1}{|n|^\eta}.$$

Assume that this geodesic is characterised by  $ap_1 + b + cp_2 = 0$ , and therefore  $a\alpha_1 + b + c\alpha_2 = 0$ . Therefore  $|n\alpha_2 - p_2| = |a/c||n\alpha_1 - p_1|$  and so this becomes (altering  $\eta$ ):

$$|n||n\alpha_1 - p_1| \ll_\alpha \frac{1}{|n|\eta}.$$

These are independent linear forms in two variables, so by Schmidt's Subspace Theorem 5.5 on the two-dimensional space in  $n$  and  $p_1$ , we have solutions on only finitely many lines in coefficient space. This means there are only finitely many  $\beta$ .  $\square$

**5.6. Complex Liouville numbers.** We demonstrate that there are non-quadratic complex numbers which are extremely well-approximable by quadratic irrationals (in particular, so as to be necessarily non-algebraic, as a result of Theorem 5.6).

In analogy with the classical case, we will call  $\alpha \in \mathbb{C}$  a *complex quadratic Liouville number* if, for every positive integer  $m$ , there are infinitely many quadratic irrational  $\beta$  such that

$$d_{hyp}(\alpha, \beta) \leq \text{acosh} \left( 1 + \frac{1}{|\Delta_\beta|^m} \right). \quad (21)$$

To accomplish this, we will construct a Cauchy sequence of quadratic irrationals  $\beta_k$ . Calling the limit  $\alpha$ , we will show that the hyperbolic distance between  $\alpha$  and  $\beta_k$  satisfies (21). The construction is simple: we only require at each stage that

$$d_{hyp}(\beta_k, \beta_{k+1}) < \text{acosh} \left( 1 + \frac{1}{|\Delta_{\beta_k}|^k} \right), \quad |\Delta_{\beta_k}| \geq 2. \quad (22)$$

As the quadratic irrationals of absolute discriminant  $\geq 2$  are dense, this is possible. To see that the sequence is Cauchy and the limit satisfies (21), we can compute, for  $M > m$ ,

$$\begin{aligned} d_{hyp}(\beta_M, \beta_m) &\leq \sum_{k=m}^{M-1} d_{hyp}(\beta_k, \beta_{k+1}) \\ &\leq d_{hyp}(\beta_m, \beta_{m+1}) \sum_{k=m}^{M-1} \frac{d_{hyp}(\beta_k, \beta_{k+1})}{d_{hyp}(\beta_m, \beta_{m+1})} \\ &\ll d_{hyp}(\beta_m, \beta_{m+1}) \\ &\leq \text{acosh} \left( 1 + \frac{1}{|\Delta_{\beta_m}|^m} \right). \end{aligned}$$

Note that the step in which the sum symbol disappears follows from (22) and (27) in the next section. This implies (21).

As this construction has a great deal of freedom, we can construct quadratic Liouville numbers on any fixed rational geodesic, for example. The countability of the rational geodesics also implies we can construct quadratic Liouville numbers not lying on any rational geodesic.<sup>34</sup>

**5.7. Comparison with classical results.** We wish to compare Theorems 5.4 and 5.6 with Theorem 4.4. In other words, to compare the classical approach to Diophantine approximation in the complex plane with the approach we consider here, using hyperbolic metric and discriminant sizing.

We begin with a lemma relating the naïve height and the discriminant as measures of arithmetic complexity. In the case of quadratics, and taking into account  $\text{PSL}(2; \mathbb{Z})$  invariance, (16) becomes

$$|\Delta_\alpha| \leq 12H_{\text{PSL}}(f_\alpha)^2. \quad (23)$$

<sup>34</sup>To see this, count the geodesics and assign a tubular neighbourhood of width  $1/n$  to the  $n$ -th such geodesic; require all terms  $\beta_k$  past the  $n$ -th to avoid the the first  $n$  tubular neighbourhoods; each term has finitely many restrictions placed upon it. (To make this work, the geodesics must be ordered as the terms are created, i.e. the  $n$ -th geodesic is always chosen so that the closure of its neighbourhood does not include  $\beta_n$ .)

As discussed above, we don't expect an inequality in the other direction in general. However, if we take into account the  $\mathrm{PSL}(2; \mathbb{Z})$  action, and loosen the exponents, then we can prove such a thing in the quadratic case.

**Proposition 5.7.** *Suppose  $\beta$  is of degree 2. Then*

$$|\Delta_\beta| \geq 3H_{\mathrm{PSL}}(f_\beta), \quad (24)$$

and alternately,

$$|\Delta_\beta| \geq \frac{3H_{\mathrm{PSL}}(f_\beta)^2}{N_{\mathrm{PSL}}(\beta)}, \quad (25)$$

where  $N_{\mathrm{PSL}}$  denotes the norm of the element of its  $\mathrm{PSL}(2; \mathbb{Z})$  orbit which lies in the standard fundamental region.

*Proof.* The quantities involved are all invariant under the action of  $\mathrm{PSL}(2; \mathbb{Z})$ , so it suffices to assume  $\beta$  lies in the usual  $\mathrm{PSL}(2; \mathbb{Z})$  fundamental region. For  $\beta$  an imaginary quadratic irrationality satisfying  $ax^2 + bx + c = 0$ , lying in the usual fundamental region,

$$H(f_\beta) = \max\{|a|, |b|, |c|\}, \quad N(\beta) = |c/a| \geq 1, \quad |\Re(\beta)| = |b/2a| \leq 1/2.$$

From this we conclude that  $|b| \leq |a| \leq |c|$  hence  $H(f_\beta) = |c|$  and  $b^2 < |ac|$ . Then we have

$$|\Delta_\beta| = 4|ac| - b^2 \geq 3|ac| \geq 3|c| = 3H(f_\beta).$$

Alternately, we use  $N(\beta) = |c/a|$  for the second inequality.  $\square$

Next, we recall that the hyperbolic metric and euclidean metric are locally conformally equivalent. More precisely, for  $\beta$  sufficiently close to  $\alpha$  in either metric,

$$(1 - \epsilon)\Im(\alpha)d_{hyp}(\alpha, \beta) < |\alpha - \beta| < (1 + \epsilon)\Im(\alpha)d_{hyp}(\alpha, \beta). \quad (26)$$

Finally, we need a series expansion as  $x \rightarrow \infty$  for the inverse hyperbolic cosine:

$$\mathrm{acosh}(1 + 1/x^2) = \frac{\sqrt{2}}{x} - \frac{1}{6\sqrt{2}x^3} + \frac{3}{80\sqrt{2}x^5} + \dots \quad (27)$$

Collecting the above relationships, it is a simple computation to derive the following:

**Lemma 5.8.** (1) *Suppose*

$$d_{hyp}(\alpha, \beta) < \mathrm{acosh}\left(1 + \frac{C}{|\Delta_\beta|^k}\right).$$

*Then*

$$|\alpha - \beta| < \frac{(1 + \epsilon)\Im(\alpha)N_{\mathrm{PSL}}(\beta)^{k/2}\sqrt{2C}}{3^{k/2}H_{\mathrm{PSL}}(f_\beta)^k}.$$

(2) *Suppose*

$$d_{hyp}(\alpha, \beta) > \mathrm{acosh}\left(1 + \frac{C}{|\Delta_\beta|^k}\right).$$

*Then for  $|\Delta_\beta|$  sufficiently large,*

$$|\alpha - \beta| > \frac{(1 - \epsilon)\Im(\alpha)\sqrt{2C}}{12^{k/2}H_{\mathrm{PSL}}(f_\beta)^k}.$$

In particular, Theorems 5.1, 5.3, 5.4, and 5.6 imply statements in the euclidean metric and naïve height, which we collect here for completeness.

**Theorem 5.9.** (1) Let  $\alpha \neq \beta$  be two non-real quadratic irrationalities. Then for  $|\Delta_\beta|$  sufficiently large,

$$|\alpha - \beta| \geq \frac{(1 - \epsilon)\Im(\alpha)(2 - \sqrt{2})}{2\sqrt{3}H_{\text{PSL}}(f_\beta)^{1/2}H_{\text{PSL}}(f_\alpha)^{1/2}}.$$

If  $\Delta_\alpha = \Delta_\beta$  is sufficiently large in absolute value, then

$$|\alpha - \beta| \geq \frac{(1 - \epsilon)\Im(\alpha)\sqrt{2}}{2\sqrt{3}\min\{H_{\text{PSL}}(f_\beta), H_{\text{PSL}}(f_\alpha)\}}.$$

(2) Let  $\alpha \in \mathbb{C} \setminus \mathbb{R}$  not be quadratic irrational, but lying on a rational geodesic. Then there exists a constant  $K_\alpha > 0$ , depending only on the  $\text{PSL}(2; \mathbb{Z})$  orbit of  $\alpha$ , such that there are infinitely many quadratic irrational  $\beta$  lying on that rational geodesic, with

$$|\alpha - \beta| < \frac{K_\alpha}{H_{\text{PSL}}(f_\beta)^2}.$$

(3) Let  $\alpha \in \mathbb{C} \setminus \mathbb{R}$  not be a quadratic irrational. Let  $K > 0$  be any constant. Then, there are infinitely many quadratic irrationalities  $\beta$  with

$$|\alpha - \beta| < \frac{K}{H_{\text{PSL}}(f_\beta)^{3/2}}.$$

(4) Suppose that  $\alpha \in \mathbb{C} \setminus \mathbb{R}$  is algebraic and non-quadratic. Let  $\eta > 0$ . If  $\alpha$  lies on a rational geodesic, then there are only finitely many quadratic irrationals  $\beta$  on that geodesic such that

$$|\alpha - \beta| < \frac{1}{H_{\text{PSL}}(f_\beta)^{2+\eta}}. \tag{28}$$

Amongst quadratic irrationals  $\beta$  not sharing a rational geodesic with  $\alpha$ , there are only finitely many such that

$$|\alpha - \beta| < \frac{1}{H_{\text{PSL}}(f_\beta)^{3/2+\eta}}. \tag{29}$$

In particular, if  $\alpha$  is not on any rational geodesic, then there are only finitely many quadratic irrational  $\beta$  satisfying (19) at all. Note that in (18) and (19),  $H_{\text{PSL}}$  can be weakened to  $H$ .

In particular, up to constants depending on  $\alpha$ , our theorems recover the computation of  $k_2(\alpha)$  given by Theorem 4.4 of Bugeaud and Evertse for the quadratic case.<sup>35</sup> Theorem 5.9 offers some refinement in terms of drawing a distinction between approximations on a geodesic containing  $\alpha$  or not.

However, the constants are different. As the imaginary part of  $\alpha$  approaches  $\infty$ , the constant  $K_\alpha$  of item (2) of Theorem 5.9 weakens. By contrast item (1) of Theorem 5.9 becomes a stronger statement as  $\alpha \rightarrow \infty$ . It is natural to ask whether there is an analogue to the Lagrange spectrum for approximation by quadratic irrationals, at least for those lying on a geodesic. The preceding discussion demonstrates that knowledge of the spectrum in one of the classical or hyperbolic/discriminant settings would not imply the other, although there would be some relationships.

## 6. TO BOLDLY GO

The investigation of algebraic starscapes raises a wide variety of possible future research directions, many of which we intend to continue to investigate. We invite you to join us.

---

<sup>35</sup>To see this for items (2) and (3) in Theorem 5.9 requires some consideration of the relationship between  $H_{\text{PSL}}(f_\alpha)$  and  $H(f_\alpha)$ ; we need to know the quotient is bounded in terms of the height of the relevant element of  $\text{PSL}(2; \mathbb{Z})$ , which is a constant in terms of  $\alpha$ .

**The homogeneous geometry of higher degrees.** For higher degree polynomials, the beginnings of the geometric story remain relatively unchanged, but strong conclusions such as Theorems 3.3 and 3.23 become more complicated to draw, as the dimension of the space of polynomials grows.

In particular, fixing a degree  $n \geq 1$ , we have that  $\mathbb{P}\text{Coefs}_n \cong \mathbb{C}\mathbb{P}^n$  identifies with complex projective space, and  $\text{Roots}_n \cong \text{SP}^n(\mathbb{C}\mathbb{P}^1)$  is the set of unordered  $n$ -tuples in the Riemann sphere. The roots map  $\mathcal{R}_n: \mathbb{C}\mathbb{P}^n \rightarrow \text{SP}^n(\mathbb{C}\mathbb{P}^1)$  is a homeomorphism, and is equivariant with respect to the natural  $\text{PSL}(2; \mathbb{C})$  actions on each side: given on the space of roots by precomposition with a Möbius transformation, and on the space of coefficients by the action of the unique irreducible representation  $\text{PSL}(2; \mathbb{C}) \rightarrow \text{PSL}(n; \mathbb{C})$ .

Restricting to real coefficients, the fact that  $\mathcal{R}$  is a homeomorphism implies  $\mathcal{R}_n: \mathbb{R}\mathbb{P}^n \rightarrow \text{SP}^n(\mathbb{C}\mathbb{P}^1)$  is an embedding, equivariant with respect to the restricted  $\text{PSL}(2; \mathbb{R})$  action on each side. The orbits of this action decompose the space of degree  $n$  polynomials, whose nature depends on the degree. For  $n \leq 3$ , each component of the complement of the discriminant locus comprises an entire orbit itself, and thus comes equipped with the structure of a homogeneous geometry for  $\text{PSL}(2; \mathbb{R})$ . For  $n > 3$ , the  $\text{PSL}(2; \mathbb{R})$  orbits foliate each component. Consider as an example the space of quartics. The complement of the discriminant locus has two components; those with two pairs of complex conjugate roots, and those with a pair of complex conjugate roots and two real roots. The  $\text{PSL}(2; \mathbb{R})$  action decomposes the latter into a family of codimension-1 hypersurfaces, which are generically<sup>36</sup> diffeomorphic to  $\text{PSL}(2; \mathbb{R})$  itself. This complicates the overall picture, and suggests generalizations of Theorems 3.3 and 3.23 will involve fiber bundles of homogeneous spaces, rather than just the spaces themselves.

Building a more robust geometric toolkit would not only allow the extension of these ideas to higher degree polynomials, but strong enough tools may provide a window into exploring their solvability. In particular, while the next case of interest, quartics, admits a solution by radicals, the quintics and beyond do not. It is an exciting prospect to try and understand this dichotomy geometrically along our journey.

**Starscape curves.** Revisit Figure 26. The images of rational planes (projective rational lines) in the coefficient space form delicate beaded necklaces (linear starscapes). Any two algebraic numbers lie on at least one common curve (more if the point has the non-transversal property discussed in Corollary 3.26). It is possible to give algebraic equations for these curves in general dimension, in terms of the two associated minimal polynomials  $f_1$  and  $f_2$ , namely, viewing the complex plane as  $\mathbb{R}^2$ , the curve is  $\Re(f_1(x + iy))\Im(f_2(x + iy)) = \Re(f_2(x + iy))\Im(f_1(x + iy))$ . We will call these *starscape curves*. The intricacies of some of these curves suggest that the projective geometry of coefficient space is quite disguised by projecting onto complex roots. Determining whether these starscape curves are related to any natural geometric structures on the complex plane may allow us to develop further extensions of the material in Section 3 to higher degree.

Furthermore, starscape curves appear to have a repulsion effect all their own (see the white-space surrounding geodesics in Figure 1a, for example). Is it possible to quantify how well approximable some complex number  $\alpha$  is by these curves? We might measure the distance between  $\alpha$  and a curve. What is the *height* of a starscape curve?

**Planar starscapes.** The planar starscapes we have studied provide a two dimensional analogue to the curves described above, with the complex quadratics (Figure 1a) providing a primary example. As the degree of polynomials increases these families can get more complicated, but the projection to the upper half-plane by complex roots is always available (although

<sup>36</sup>Indeed, by the action of  $\text{PSL}(2; \mathbb{R})$ , the pair of complex roots can be moved to any point in  $\mathbb{H}^2$ . Fixing this point, the remaining degree of freedom of the  $\text{PSL}(2; \mathbb{R})$  action acts by rotation on the ideal boundary  $\partial_\infty \mathbb{H}^2 = \mathbb{R}\mathbb{P}^1$ , and each  $\text{PSL}(2; \mathbb{R})$  orbit is determined by the *angle* between these two points, measured between the tangent vectors at the complex root pointing to the real roots, as in Equation 8.

each polynomial might be represented by increasing numbers of individual roots). Even in the cubic case where there is at most one complex pair we start to see new behaviour with the “blackhole”-like phenomena seen in Figure 30a, where a quadratic point is the complex root of many polynomials. The starscapes shown in Figures 2d, 2e, and 2f show further intriguing behaviours that might be studied, such as seemingly denser regions and the isolated quadratic and cubic points at the top middle of Figure 2f.

**Algorithms to draw starscapes and Farey Structure.** Some of the images here have taken minutes or even hours to compute. Can we develop faster, more intelligent algorithms? The current images are made using a brute force approach: generate a large number of polynomials, solve them, and then plot the results which fit into a desired region. The code is short and many of the hard subproblems, like solving polynomials, are already implemented in computer algebra environments. However, it is very inefficient: we don’t effectively sieve for points which will end up in the desired region, and work is repeated for every point.

The geometry discussed above provides a path to improvements. Can we efficiently predict which polynomials need to be solved for a given region? Along each curve we see a recursive pattern resembling the rational numbers in Figure 15. An efficient way to generate rational numbers is to use the Farey (or Stern-Brocot) tree structure, discussed in Section 3.1.2 and shown in Figure 18: in essence, use the mediant operation to fill in gaps, recursively. A variation on this can be achieved by the naïve addition of polynomials as coefficient vectors. This produces a new polynomial with a root “between” the original two along the curve. In effect, we are asking about higher dimensional Stern-Brocot trees [32]. It should also be possible to make use of the  $\mathrm{PSL}(2; \mathbb{Z})$  symmetry, at least in large-scale pictures.

**Continued Fractions.** Do there exist continued fraction algorithms for approximation by algebraic numbers of fixed or bounded degree? The Farey structure of the rationals is, in some sense, the source of the continued fraction algorithm for real numbers approximated by rationals (the continued fraction algorithm can be viewed both as a traversal of a Cayley graph for  $\mathrm{PSL}(2; \mathbb{Z})$  and as a geometric process of repeated mediants). Figure 1a wonders aloud, might it be possible to extend the continued fraction method to approximate complex numbers by quadratic irrationals? It is possible that existing multidimensional continued fraction algorithms, which have a long history, may provide hints; a recent article from which to enter the literature is [39].

**Higher degree and geometry-sensitive Diophantine approximation.** We have seen that the geometry of the roots map naturally classifies certain types of approximations. Our example is quadratic approximations from one rational geodesic, where we saw that approximations from a geodesic containing  $\alpha$  can be better than approximations not on the geodesic. Moving to the cubic case, one might ask how well a quadratic is approximated by cubics from a particular planar starscape. If the quadratic is a singular point in the sense of Corollary 3.26 and Figure 33, then we conjecture the cubics from that planar starscape are better approximations of the quadratic than those from starscapes not having the property.

More generally, to what extent can the results of Section 5 be extended to higher degree? Could such an extension settle the outstanding cases in the work of Bugeaud and Evertse? In higher degree, are the exceptionally well-approximable algebraic numbers all living on starscape curves, or are there other reasons to be well-approximable? The work of Bugeaud and Evertse also indicates a difference in approximability based on how many real conjugates an algebraic number has. What pictures would one draw to see this effect?

**Mahler measure and Lehmer’s Conjecture.** Lehmer’s famous conjecture is related to another important measure of arithmetic complexity, namely the *Mahler measure* (which is not technically any type of measure). A polynomial  $f = a_d x^d + \cdots + a_1 x + a_0 = a_d \prod_{i=1}^d (x - \alpha_i) \in \mathbb{Z}[x]$

has Mahler measure

$$M(f) = |a_d| \prod_{i=0}^d \max\{1, |\alpha_i|\}.$$

The Weil height of an algebraic number is exactly related to the Mahler measure of its minimal polynomial:  $M(f_\alpha) = H(\alpha)^d$ .

Lehmer's conjecture states that there is a lower bound to  $M(f)$  away from polynomials whose roots are roots of unity. The smallest known Mahler measure of a non-root-of-unity is called *Salem's number*, 1.176280818... associated to the roots of the *Lehmer polynomial*  $x^{10} + x^9 - x^7 - x^6 - x^5 - x^4 - x^3 + x + 1$ .<sup>37</sup> Lehmer's Conjecture is known to hold for non-reciprocal polynomials (those whose coefficients are not palindromic) [50], and Voutier [54] gives an explicit lower bound in terms of the degree, implying the conjecture is true if fields are restricted by degree. Therefore to properly visualize Lehmer's conjecture would require a starscape in increasing degree, and some understanding of the real roots accompanying the complex roots.

For these various reasons, there is a sense in which Lehmer's conjecture does not properly belong to the complex plane and the algebraic starscapes, although it is natural to wonder if it gives rise to any interesting images. One related image which is particularly stunning is the reciprocal polynomials, shown in Figure 37. The image itself asks a variety of interesting questions.

#### REFERENCES

- [1] Dan Anderson. <https://twitter.com/dandersod/status/1264918722155876353>, May 2020. Accessed: 2020-08-09.
- [2] Dan Anderson. <https://twitter.com/dandersod/status/1265007977964228609>, May 2020. Accessed: 2020-08-09.
- [3] J.W. Anderson. *Hyperbolic Geometry*. Springer undergraduate mathematics series. Springer, 1999.
- [4] John Baez. Algebraic Numbers. <https://blogs.ams.org/visualinsight/2013/09/01/algebraic-numbers/>, September 2013. Accessed: 2020-08-09.
- [5] John Carlos Baez. The Beauty of Roots. <https://johncarlosbaez.wordpress.com/2011/12/11/the-beauty-of-roots/>. Accessed: 2020-08-09.
- [6] John Carlos Baez. The Beauty of Roots (Part 2). <https://johncarlosbaez.wordpress.com/2012/01/07/the-beauty-of-roots-part-2/>. Accessed: 2020-08-09.
- [7] David H. Bailey, Jonathan M. Borwein, Neil J. Calkin, Roland Girgensohn, D. Russell Luke, and Victor H. Moll. *Experimental mathematics in action*. A K Peters, Ltd., Wellesley, MA, 2007.
- [8] Andrej Bauer. TedEx "Zeroes". <http://math.andrej.com/2014/10/16/tedx-zeroes/>. Accessed: 2020-08-09.
- [9] Jwalin Bhatt. Field of Algebraic numbers in C. <https://www.youtube.com/watch?v=8NDfMxw49co>, July 2018. Accessed: 2020-08-09.
- [10] Peter Borwein. *Computational excursions in analysis and number theory*, volume 10 of *CMS Books in Mathematics/Ouvrages de Mathématiques de la SMC*. Springer-Verlag, New York, 2002.
- [11] Peter Borwein, Tamás Erdélyi, and Friedrich Littmann. Polynomials with coefficients from a finite set. *Transactions of the American Mathematical Society*, 360:5145–5154, 2008.
- [12] Peter Borwein and Loki Jörgenson. Visible structures in number theory. *Amer. Math. Monthly*, 108(10):897–910, 2001.
- [13] Harrison Bray, Diana Davis, Kathryn Lindsey, and Chenxi Wu. The shape of thurston's master teapot, 2019.
- [14] Stephen Brooks. Visualisation of the (countable) field of algebraic numbers in the complex plane. <https://en.wikipedia.org/wiki/File:Leadingcoeff.png>, March 2010. Accessed: 2020-08-09.
- [15] Yann Bugeaud. *Approximation by algebraic numbers*, volume 160 of *Cambridge Tracts in Mathematics*. Cambridge University Press, Cambridge, 2004.
- [16] Yann Bugeaud and Jan-Hendrik Evertse. Approximation of complex algebraic numbers by algebraic numbers of bounded degree. *Ann. Sc. Norm. Super. Pisa Cl. Sci. (5)*, 8(2):333–368, 2009.

---

<sup>37</sup>The complex roots of Lehmer's polynomial all lie on the unit circle, and its Mahler measure is a function of its real roots.

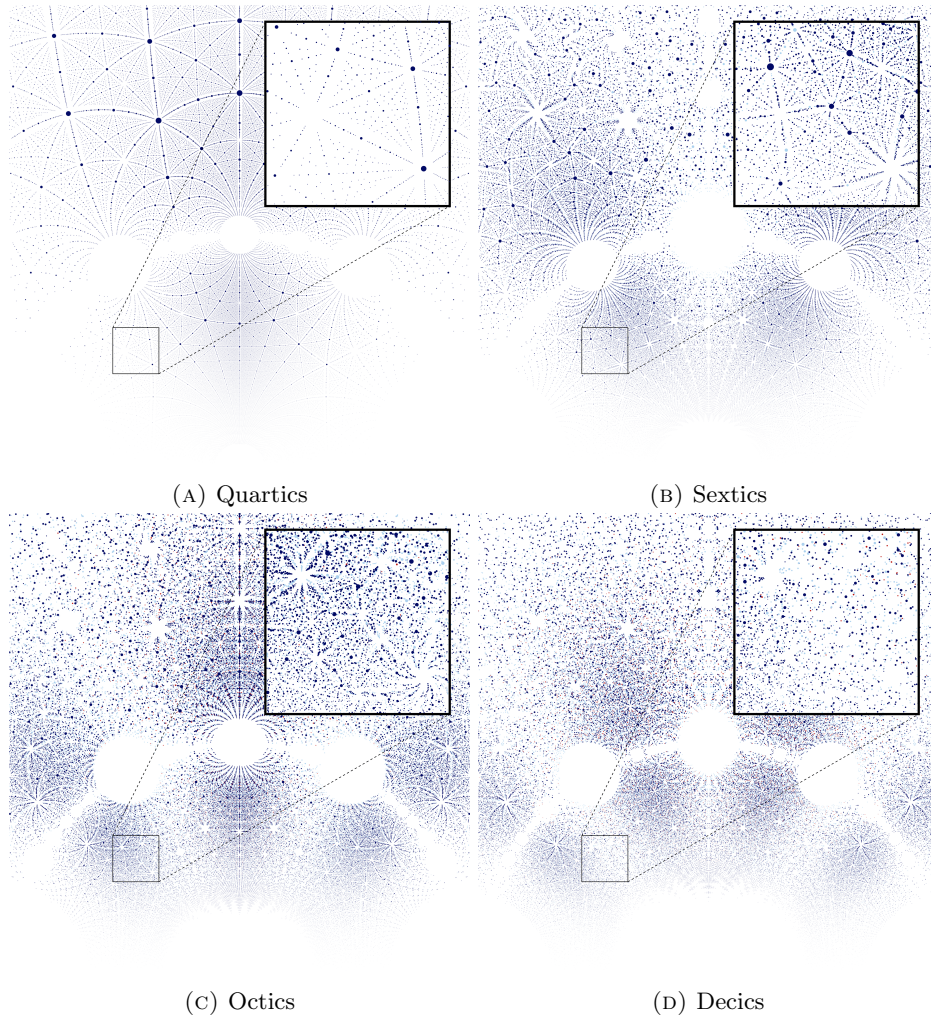


FIGURE 37. Pictures of roots of reciprocal polynomials off the unit circle (the many roots on the unit circle are not plotted). For odd degrees the reciprocal polynomials always have the root  $-1$ . The points are coloured by the number of conjugate real roots with dark blue for 0, light blue for 2, dark red for 4 and light red for 6 (dark and light blue are swapped from Figure 34 to make the image clearer). Note the strong repulsion of the unit circle in all cases, especially close to  $i$  and third/sixth roots of unity. There are also denser regions in the direction of the  $d$ -th roots of unity for degree  $d$ .

- [17] Dan Christiansen. Plots of roots of polynomials with integer coefficients. <http://jdc.math.uwo.ca/roots/>. Accessed: 2020-08-09.
- [18] L. G. P. Dirichlet. Verallgemeinerung eines satzes aus der lehre von den kettenbrüchen nebst einige anwendungen auf die theorie der zahlen. *S.-B. Preuss. Akad. Wiss.*, pages 93–95, 1842.
- [19] David Dumas. *SL(View)*, 2020. <https://dumas.io/slview/>.
- [20] Greg Egan. Littlewood applet. <http://www.gregegan.net/SCIENCE/Littlewood/Littlewood.html>. Accessed: 2020-08-09.
- [21] Jordan S. Ellenberg. What do roots of random polynomials look like? <https://quomodocumque.wordpress.com/2010/01/09/what-do-roots-of-random-polynomials-look-like/>. Accessed: 2020-08-09.
- [22] Bernat Espigulé. The beauty of roots. <http://gallery.bridgesmathart.org/exhibitions/2019-icerm-illustrating-mathematics/geonat>. Accessed: 2020-08-09.

- [23] Fauxtographique. Algebraic Numbers of Degree 2. <https://www.deviantart.com/fauxtographique/art/Algebraic-Numbers-of-Degree-2-384042962>. Accessed: 2020-08-09.
- [24] Matt (<https://mathematica.stackexchange.com/users/1735/matt-groff>) Groff. What methods are known to visualize patterns in the set of real roots of quadratic equations? Mathematica & Wolfram Language Stack Exchange. URL:<https://mathematica.stackexchange.com/questions/63028/how-can-we-plot-the-complex-roots-of-an-equation/63064#63064> (version: 2020-06-12).
- [25] Edmund Harriss. <https://twitter.com/Gelada/status/1263599901784621056>, May 2020. Accessed: 2020-08-09.
- [26] Edmund Harriss, Pierre Arnoux, Kate Stange, and Steve Trettel. Algebraic starscapes. Art Exhibit at Gaukurinn, Reykjavik, Iceland, February 2020.
- [27] Marc Hindry and Joseph H. Silverman. *Diophantine geometry*, volume 201 of *Graduate Texts in Mathematics*. Springer-Verlag, New York, 2000. An introduction.
- [28] Benjamin Hutz and Michael Stoll. Smallest representatives of  $SL(2, \mathbb{Z})$ -orbits of binary forms and endomorphisms of  $\mathbb{P}^1$ . *Acta Arith.*, 189(3):283–308, 2019.
- [29] iadvd (<https://math.stackexchange.com/users/189215/iadvd>). What methods are known to visualize patterns in the set of real roots of quadratic equations? Mathematics Stack Exchange. URL:<https://math.stackexchange.com/q/1412264> (version: 2020-06-12).
- [30] A. Ya. Khintchine. *Continued fractions*. Translated by Peter Wynn. P. Noordhoff, Ltd., Groningen, 1963.
- [31] J. F. Koksma. Über die Mahlersche Klasseneinteilung der transzendenten Zahlen und die Approximation komplexer Zahlen durch algebraische Zahlen. *Monatsh. Math. Phys.*, 48:176–189, 1939.
- [32] Hakan Lernerstad. The  $n$ -dimensional Stern-Brocot tree. *Int. J. Number Theory*, 15(6):1219–1236, 2019.
- [33] Jonathan Lidbeck. Complex polynomial roots. <https://www.flickr.com/photos/jondissed/37297981445>. Accessed: 2020-08-09.
- [34] Joseph Liouville. Remarques relatives à des classes très-étendues de quantités dont la valeur n'est ni algébrique, ni même réductible à des irrationnelles algébriques. *C. R. Acad. Sci. Paris*, 18:883–885, 1844.
- [35] John E. Littlewood. *Some problems in real and complex analysis*. D. C. Heath and Co. Raytheon Education Co., Lexington, Mass., 1968.
- [36] K. Mahler. An inequality for the discriminant of a polynomial. *Michigan Math. J.*, 11:257–262, 1964.
- [37] David M. Marciel. Visualizing the patterns in the sets of complex and real roots of quadratic and cubic equations. <http://hobymaths.blogspot.com/2015/09/visualizing-patterns-in-sets-of-complex.html>. Accessed: 2020-08-09.
- [38] John Matson. Polynomial Plot: Simple Math Expressions Yield Intricate Visual Patterns [Slide Show]. <https://www.scientificamerican.com/article/math-polynomial-roots/>, December 2009. Accessed: 2020-08-09.
- [39] Nadir Murru. Linear recurrence sequences and periodicity of multidimensional continued fractions. *Ramanujan J.*, 44(1):115–124, 2017.
- [40] Paul Nylander. polynomial roots. <https://nylander.wordpress.com/2008/12/29/polynomial-roots/>. Accessed: 2020-08-09.
- [41] A. M. Odlyzko and B. Poonen. Zeros of polynomials with 0, 1 coefficients. *Enseign. Math. (2)*, 39(3-4):317–348, 1993.
- [42] Michael Pershan. <https://twitter.com/mpershan/status/1264931366275293190>, May 2020. Accessed: 2020-08-09.
- [43] Clifford A. Pickover. *The mathematics of Oz*. Cambridge University Press, Cambridge, 2002. Mental gymnastics from beyond the edge.
- [44] K. F. Roth. Rational approximations to algebraic numbers. *Mathematika*, 2:1–20; corrigendum, 168, 1955.
- [45] M. S. cubics lead coef 3 more. <https://www.flickr.com/photos/104348204@N05/11557321664/>. Accessed: 2020-08-09.
- [46] Wolfgang M. Schmidt. Simultaneous approximation to algebraic numbers by rationals. *Acta Math.*, 125:189–201, 1970.
- [47] Wolfgang M. Schmidt. Norm form equations. *Ann. of Math. (2)*, 96:526–551, 1972.
- [48] Wolfgang M. Schmidt. *Diophantine approximation*, volume 785 of *Lecture Notes in Mathematics*. Springer, Berlin, 1980.
- [49] Pablo Shmerkin and Boris Solomyak. Zeros of  $\{-1, 0, 1\}$  power series and connectedness loci for self-affine sets. *Experimental Mathematics*, 15:499 – 511, 2006.
- [50] C. J. Smyth. On the product of the conjugates outside the unit circle of an algebraic integer. *Bull. London Math. Soc.*, 3:169–175, 1971.
- [51] V. G. Sprindžuk. *Mahler's problem in metric number theory*. Translated from the Russian by B. Volkmann. Translations of Mathematical Monographs, Vol. 25. American Mathematical Society, Providence, R.I., 1969.
- [52] Michael Stoll and John E. Cremona. On the reduction theory of binary forms. *J. Reine Angew. Math.*, 565:79–99, 2003.

- [53] The Sage Developers. *SageMath, the Sage Mathematics Software System (Version 9.1)*, 2020. <https://www.sagemath.org>.
- [54] Paul Voutier. An effective lower bound for the height of algebraic numbers. *Acta Arith.*, 74(1):81–95, 1996.
- [55] Daniel Wiegrefe. Fractals from complex roots of polynomials. <https://wiegrefe.info/home/fractals-from-complex-roots-of-polynomials>. Accessed: 2020-08-09.
- [56] Enrique Zeleny. Algebraic Numbers In The Complex Plane. <https://demonstrations.wolfram.com/AlgebraicNumbersInTheComplexPlane/>. Accessed: 2020-08-09.

DEPARTMENT OF MATHEMATICS, UNIVERSITY OF COLORADO, CAMPUS BOX 395, BOULDER, COLORADO 80309-0395